UNIVERSIDADE FEDERAL DO PAMPA

ÁLVARO SOSA MACHADO

FADIGA ACUMULADA PELO EXERCÍCIO E USO DO EXTRATO DE CHÁ VERDE (*Camellia sinensis*) NA PREVENÇÃO DE SEUS EFEITOS

Uruguaiana

2022

ÁLVARO SOSA MACHADO

FADIGA ACUMULADA PELO EXERCÍCIO E USO DO EXTRATO DE CHÁ VERDE (Camellia sinensis) NA PREVENÇÃO DE SEUS EFEITOS

Tese apresentada no Programa de Pós-Graduação em Bioquímica da Universidade Federal do Pampa, como requisito parcial para obtenção do Título de **Doutor em Bioquímica**.

Orientador:

Prof. Dr. Felipe Pivetta Carpes

Coorientadora:

Profa. Dra. Mauren Assis de Souza

Uruguaiana

2022

M149e Machado, Álvaro Sosa

FADIGA ACUMULADA PELO EXERCÍCIO E USO DO EXTRATO DE CHÁ VERDE (Camellia sinensis) NA PREVENÇÃO DE SEUS EFEITOS.

231 p.

Tese (Doutorado)-- Universidade Federal do Pampa, DOUTORADO EM BIOQUÍMICA, 2022.

"Orientação: Felipe Pivetta Carpes".

1. bioquímica. 2. biomecânica. 3. fadiga muscular. 4. dano muscular. 5. estresse oxidativo. I. Título.

ÁLVARO SOSA MACHADO

EXTRATO DE CHÁ VERDE (*Camellia sinensis*) NA PREVENÇÃO DE FADIGA ACUMULADA

Tese apresentada no Programa de Pós-Graduação em Bioquímica da Universidade Federal do Pampa, como requisito parcial para obtenção do Título de **Doutor em Bioquímica**.

Tese defendida e aprovada em: 24 de novembro de 2022.

Banca examinadora:

_____
Prof. Dr. Felipe Pivetta Carpes
Orientador / UNIPAMPA

_____
Profa. Dra. Mauren Assis de Souza
Co-orientadora / UNIPAMPA, RS, Brasil

_____
Prof. Dr. Alberto Encarnación Martínez
Universitat de València, Espanha

_____
Profa. Dra. Heiliane de Brito Fontana
UFSC, SC, Brasil

_____
Prof. Dr. Jeam Maciel Geremia
UFRGS, RS, Brasil

_____
Prof. Dr. Leonardo Magno Rambo
UNIPAMPA, RS, Brasil

página reservada para a inclusão das assinaturas digitais

AGRADECIMENTOS

Eu só posso iniciar meus agradecimentos mencionando aqueles que são a pedra fundamental da minha formação. Quando uma família da classe trabalhadora decide apoiar os estudos dos filhos, decide também aceitar uma série de sacrifícios e privações. Nunca esqueço quem somos e de onde viemos. Agradeço aos meus pais **Nilvo Machado** e **Jacqueline Sosa** pela oportunidade que me deram e pelo amor que me transmitem. Esse caminho fizemos juntos e o mérito é nosso.

Agradeço aos meus irmãos **Mathias** e **Mayara** por sermos tão unidos. Toda decisão tomada sempre teve como crivo dar orgulho a vocês. Que Oxalá nos permita muito tempo juntos, com alegria e prosperidade.

Nenhum caminho é difícil desde que tenho o carinho da minha companheira de todas as horas **Verônica**. Sou feliz pela nossa história e espero conquistar muitas vitórias ao teu lado.

Essa tese é resultado de uma ampla rede de colaboração, mas também de apoio mútuo e solidariedade. Nesse sentido tive muita sorte. Desde 2011 estive em um ambiente muito frutífero e de muitas amizades junto ao **Grupo de Pesquisa em Neuromecânica Aplicada**.

Agradeço ao professor Dr. **Felipe Carpes** por ter respondido meu e-mail nas férias de 2010 e ter construído minha formação desde então. Espero poder sempre retribuir passando adiante tudo o que aprendi. Obrigado pela nossa relação tão franca e amistosa. Tua dedicação e sensibilidade junto aos alunos é uma inspiração.

Agradeço a minha co-orientadora Dra **Mauren Souza**, cuja contribuição nesta tese é central. Tenho orgulho de dizer que minha co-orientadora é uma mulher negra que fez valer os direitos pelos quais lutamos e hoje se mostra uma profissional tão competente.

Para não ser injusto, agradeço a todos amigos de GNAP que fiz nessa trajetória na pessoa de um companheiro muito especial, meu querido amigo e sempre minha dupla **Willian da Silva**, a quem eu devo muito do que pude conquistar até aqui. Agradeço também ao TAE Dr. **Marcos Kunzler** pelo suporte técnico e pela boa amizade, e à professora Dra **Pâmela Mello Carpes** pela estrutura que nos disponibilizou.

Agradeço à **Universitat de València** onde estive para realizar meu período de período de doutorado sanduíche sob supervisão do prof. Dr. **Jose Priego**, a quem também sou muito grato pela recepção, por ser tão atencioso e por agregar parte fundamental da minha tese. Estendo esse agradecimento ao prof. Dr. **Pedro Pérez-Soriano** e aos demais membros do **Grupo de Investigación en Biomecánica Deportiva** que tão bem me acolheram.

Agradeço a **Universidade Federal do Pampa** e seu quadro de funcionários que me permitiram sonhar. A UNIPAMPA é um orgulho que eu vou carregar para sempre, e é a instituição que envaidecido posso afirmar que ajudei a construir como graduado, pós-graduado e militante do movimento estudantil.

Ao **Programa de Pós-Graduação em Bioquímica** e ao qualificado quadro de professores pelas lições. Foi um desafio conciliar a biomecânica e a bioquímica, mas tenho a expectativa de ter contribuído para a consolidação do programa. Torço e luto para que o ensino superior público continue sendo gratuito e de qualidade para mudar vidas e desenvolver o país.

Agradeço à **CAPES** pela bolsa de estudos concedida durante o doutorado e pela bolsa sanduíche no exterior (PDSE).

RESUMO

A fadiga muscular é um fenômeno fisiológico e transitório que gera perda de força e resistência, tendo como consequências o dano muscular, estresse oxidativo e inflamação. Para a recuperação do músculo envolvido na fadiga, é preciso permitir que o processo de reparação de homeostase ocorra, o que pode demandar até 96 h. Existem situações, como na reabilitação acelerada de lesões ou em competições esportivas, em que é imposto ao músculo um processo de fadiga por dias consecutivos de exercícios, sem permitir o adequado tempo para recuperação, o que pode acarretar uma condição de fadiga acumulada. É do interesse de terapeutas, treinadores e atletas melhor compreender como quantificar essa condição, e fim de evitar ou reduzir os efeitos da fadiga acumulada. Contudo, tanto a quantificação da fadiga acumulada (como por meio de marcadores de desempenho e estresse durante o exercício), quanto as estratégias para sua prevenção e tratamento (como intervenções nutricionais com o extrato de chá verde, encontrado na *Camellia sinensis*) , são desafiadoras. Com uma combinação de experimentos realizados durante o período da pandemia de coronavírus (2020-2023), o objetivo desta tese foi investigar indicadores de fadiga acumulada e seus efeitos no desempenho em competições esportivas de alto nível, determinar a fiabilidade de técnicas para monitorar a fadiga muscular, e avaliar o potencial do extrato de chá verde como uma intervenção de baixo custo para minimizar efeitos da fadiga acumulada. Interpretamos nossos principais resultados como indicadores de que (1) competições envolvendo muitos dias consecutivos de exercício acarretam fadiga acumulada; (2) a fadiga acumulada pode ser identificada a partir de informações de volume e intensidade monitoradas durante o exercício; (3) as perda de desempenho em função do acúmulo de fadiga são influenciadas pela escolha dos dias de descanso ao longo da competição; (4) medidas de temperatura da pele empregando termografia infravermelha podem ajudar na identificação da marcadores de fadiga acumulada em testes realizados em laboratório; (5) a administração de extrato de chá verde antes da exposição à condição de fadiga acumulada é associada com redução em marcadores de dano muscular e estresse oxidativo; (6) a administração de extrato de chá verde antes da exposição à condição de fadiga acumulada minimiza reduções em variáveis

neuromecânicas associadas com a produção de força em condição de fadiga acumulada. Consideramos que as informações incluídas nesta tese contribuem para o avanço do conhecimento sobre o tema, com uma abordagem integrativa de conceitos e ferramentas de diferentes áreas, auxiliando na melhor compreensão dos processos envolvidos no mecanismo de fadiga acumulada, sua melhor quantificação e monitoramento, e formas de prevenção.

Palavras chaves: antioxidantes; dano muscular; eletromiografia; estresse oxidativo; exaustão; exercício físico; neuromecânica; recuperação; termografia infravermelha.

ABSTRACT

Muscle fatigue is a physiological and transient phenomenon that generates loss of strength and endurance, with consequences for muscle damage, oxidative stress and inflammation. For the recovery of the muscle involved in fatigue, it is necessary to allow the homeostasis repair process to occur, which can take up to 96 h. There are situations, such as in the accelerated rehabilitation of injuries or in sports competitions, in which a process of fatigue is imposed on the muscle for consecutive days of exercises, without allowing adequate time for recovery, which can lead to a condition of cumulative fatigue. It is in the interest of therapists, coaches and athletes to better understand how to quantify this condition in order to avoid or reduce the effects of cumulative fatigue. However, both the quantification of cumulative fatigue (such as through markers of performance and stress during exercise) and strategies for its prevention and treatment (such as nutritional interventions with green tea extract, found in Camellia sinensis), are challenging. With a combination of experiments carried out during the period of the coronavirus pandemic (2020-2023), the objective of this thesis was to investigate indicators of cumulative fatigue and its effects on performance in high-level sports competitions, to determine the reliability of techniques to monitor muscle fatigue, and to evaluate the potential of green tea extract as a low-cost intervention to minimize the effects of cumulative fatigue. We interpret our main results as indicating that (1) competitions involving many consecutive days of exercise lead to cumulative fatigue; (2) cumulative fatigue can be identified from volume and intensity information monitored during exercise; (3) performance losses due to fatigue accumulation are influenced by the choice of rest days throughout the competition; (4) skin temperature measurements using infrared thermography can help identify markers of cumulative fatigue in laboratory tests; (5) administration of green tea extract prior to exposure to the condition of cumulative fatigue is associated with a reduction in markers of muscle damage and oxidative stress; (6) administration of green tea extract prior to exposure to the cumulative fatigue condition minimizes reductions in neuromechanical variables associated with force production in the cumulative fatigue condition. We consider that the information included in this thesis contributes to the advancement of knowledge on the subject, with an

integrative approach to concepts and tools from different areas, helping to better understand the processes involved in the mechanism of cumulative fatigue, its better quantification and monitoring, and ways of prevention.

Keywords: antioxidants; muscle damage; electromyography; oxidative stress; exhaustion; physical exercise; neuromechanics; recovery; infrared thermography.

LISTA DE FIGURAS

CAPÍTULO I

Figure 1. A: Power vs stage time for intensity zones entitled Z1 to Z7 during two editions of the Giro d' Italia. The power was measured in Watts and the stage time was measured in seconds. The figure shows the non-linear association between power and time during two editions of the Giro d' Italia. The highest intensity zones were predominant in stages of shorter duration requesting athletes to develop higher average power, while the lower intensity zones were predominant in longer stages requiring lower average power. Note the double distribution of Z1 and Z2 that suggest the lowest race period predominantly involve time in Z1 and Z2 intensity zones. **B:** Total volume time vs stage time for intensity zone Z1 to Z7 during two editions of the Giro d' Italia. The intensity zones are entitled Z1, Z2, Z3, Z4, Z5, Z6, and Z7, and each slope is entitled Yz1, Yz2, Yz3, Yz4, Yz5, Yz6, and Yz7, respectively. The total volume time was measured in seconds, and each stage duration was measured in seconds. **C:** Normalized time volume by time stage during the Giro d' Italia. The intensity zones are entitled Z0, Z1, Z2, Z3, Z4, Z5, Z6, and Z7. The mean and standard deviation are shown with black lines and gray shadows, respectively. The thick lines show the higher decrease of time volume tracked in Z1, the intensity zone with the most dispersion. The rest days occurred between stages 9 and 10, and stages 14 and 15. The first rest day of 2016 edition was not considered. **D:** The posterior probability of cluster pertinence of the main Gaussian cluster (cluster 1) in the principal component space explained 86% of the total data variance. Four clusters were identified in the principal component space from the Akaike information criterion [AIC = $2k - 2\ln(L)$ with k equal to the number of clusters and L equal to the maximum value of the likelihood function for the Gaussian model] 73

CAPÍTULO III

CAPÍTULO IV

CAPÍTULO V

CAPÍTULO VI

LISTA DE TABELAS

LISTA DE ABREVIATURAS

ECV - extrato de chá verde

IF - impact factor

EMG - eletromiografia

RMS - raiz quadrada média

IRT - termografia infravermelha

ATP - adenosina trifosfato

ADP - adenosina difosfato

ERO - espécies reativas de oxigênio

O^{-}_{2} – radical superóxido

H_2O_2 - peróxido de hidrogênio

O_2 - oxigênio

H_2O - água

GSSH - glutationa dissulfeto

GSH - sulfidril

Ca^{2+} - íon cálcio

CK - creatina quinase

Pcr - fosfocreatina

Il-1 - interleucina 1

Il-6 - interleucina 6

TNF-α - fator de necrose tumoral-alfa

NF-κB - factor nuclear kappa B

PO - radicais aroxila

O_2^- - superóxido

OH^- - radical hidroxila

RO_2^- - radical peroxil

RO^- - radical alcóxido

HO_2^- - hidroperoxil

SUMÁRIO

PREÂMBULO

Esta tese faz parte de estudos desenvolvidos no Grupo de Pesquisa em Neuromecânica Aplicada desde o ano de 2012 junto a linha de pesquisa em "Química e Bioquímica de Produtos Biologicamente Ativos" junto ao Programa de Pós-Graduação em Bioquímica da Universidade Federal do Pampa. Naquela altura, nosso grupo explorava os efeitos do exercício físico combinado ou não com a suplementação com extrato de chá verde (ECV, oriundo das folhas da *Camellia sinensis*) sobre diversos aspectos da memória em modelo animal, sobretudo pela via da defesa antioxidante (Flôres et al., 2014; Schimidt et al., 2014, 2017). À medida que avançávamos na compreensão dos mecanismos de atuação do ECV nas defesas antioxidantes a nível de sistema nervoso central, ampliávamos nossa revisão bibliográfica para compreender os benefícios no desempenho durante o exercício físico. Vimos que em modelo animal, a suplementação com ECV gerava ganho de resistência à fadiga (Murase et al., 2005, 2006), sugerindo um potencial de aplicabilidade no contexto do exercício físico em humanos.

Mas ao contrário do que presumíamos, os estudos publicados até aquele momento indicavam que em humanos os efeitos positivos do ECV não se repetiam em termos de ganho de força ou resistência durante a prática de exercícios extenuantes (Jówko, 2015). Chegamos à conclusão que poderia ser útil deslocar nosso olhar sobre a fadiga muscular para melhor ajustar a aplicabilidade dessa intervenção. A fadiga muscular é a perda de desempenho que ocorre ao longo de uma prática de exercício físico extenuante, e depende de um período de descanso para recaptar e metabolizar produtos da fadiga, bem

como reduzir o estresse oxidativo e reconduzir a musculatura exercitada a uma situação de homeostase. Nesse sentido, entendemos que a suplementação com ECV poderia atuar evitando o dano das fibras ou acelerando a recuperação dos músculos exercitados devido a suas propriedades antioxidantes. Vimos que os estudos geralmente testavam os efeitos da fadiga enquanto ela era desenvolvida ou imediatamente após, mas que uma situação muito comum no esporte era negligenciada: a fadiga acumulada. Entendemos a fadiga acumulada como o resultado da interrupção de um período de recuperação pós-fadiga por um novo exercício extenuante, que gera persistência do dano muscular e do estresse oxidativo (Machado et al., 2018). Esse tema foi abordado em minha dissertação de mestrado, defendida no mesmo programa de pós-graduação, e concluindo que a suplementação com ECV é capaz de reduzir estresse oxidativo e preservar a contratilidade muscular em ciclistas treinados.

Ao observarmos que um produto natural, seguro e de fácil acesso promoveu as defesas antioxidantes em ratos e camundongos, decidimos investigar sua aplicabilidade em humanos, na tentativa de defender a musculatura envolvida em exercícios realizados em dias consecutivos do estresse oxidativo, que além de causar perda de desempenho, fragiliza a integridade do tecido.

O planejamento inicial para o projeto foi significativamente comprometido pela condição de saúde pública estabelecida no mundo todo em decorrência da pandemia de coronavírus, mas ao final da jornada, buscamos deixar evidente que apesar as limitações, conseguimos atingir o objetivo inicialmente proposto, com alguns ajustes ao longo do caminho.

APRESENTAÇÃO

Organizamos este documento em cinco capítulos, conforme o detalhamento a seguir. Os capítulos redigidos especificamente para a composição da tese estão no idioma Português. Os artigos originais, que foram publicados ou que estão em avaliação pelas revistas científicas, estão redigidos no idioma Inglês, e estão apresentados conforme a formatação indicada pela revista destino, salvo o posicionamento das tabelas e figuras, as quais optamos por apresentar já no corpo do texto.

No primeiro capítulo apresentamos o estado da arte com uma revisão narrativa da literatura sobre os temas fadiga muscular, suas causas, efeitos e possíveis intervenções. Nesse capítulo, damos especial destaque ao extrato de chá verde. Finalmente, encerramos a introdução com a justificativa do trabalho e os objetivos da pesquisa.

No segundo capítulo, apresentamos o artigo original entitulado *"Exploratory analysis of cumulative fatigue in stage races of professional cycling derived from volume and intensity indicators"*, submetido à revista *International Journal of Sports Physiology and Performance* (IF: 4,211).

O terceiro capítulo é composto pelo artigo original *"Distance and camera features measurements affect detection of temperature asymmetries using infrared thermography"*, submetido a revista *Quantitative InfraRed Thermography Journal* (IF: 1,57).

A seguir, apresentamos o artigo original com título de *"Influence of infrared camera model and evaluator reliability in the assessment of skin temperature*

responses to physical exercise", publicado na revista *Journal of Thermal Biology* (IF: 2,902)

No quinto capítulo, apresentamos o artigo original *"Can infrared thermography serve as an alternative to assess cumulative fatigue?"*, submetido a revista *Journal of Thermal Biology* (IF: 2,90).

O sexto capítulo é composto pelo artigo original *"Green tea supplementation favors exercise volume in untrained men under cumulative fatigue*", aceito para publicação na revista *Science & Sports* (IF: 0,987).

Ao final do documento adicionamos uma discussão e conclusão geral dos resultados, bem como percepções sobre potenciais aplicações práticas e perspectivas futuras.

CAPÍTULO I

1. INTRODUÇÃO

1.1 Fadiga muscular

1.1.1 Definição

Nas ciências do esporte e da saúde, o termo “fadiga” é utilizado para descrever diferentes contextos da perda de força, energia, motivação ou ânimo (Allen & Westerblad, 2001; Greenberg, 2002). É possível subdividir a fadiga em central, referente a uma cadeia de eventos ocorridos no sistema nervoso central (Rosenthal et al., 2008), e periférica, referente a perda de desempenho ou falha na capacidade de funções neuromusculares (Cè et al., 2020). Essa divisão ocorre sobretudo para fins didáticos e exploração de diferentes mecanismos e tratamentos, mas sabe-se que existe uma interdependência entre esses domínios (Bigland-Ritchie et al., 1978; Taylor et al., 2016). No contexto do desempenho atlético, a perda de magnitude ou capacidade de sustentar força por origem periférica é chamada de fadiga muscular (Enoka & Duchateau, 2008).

As primeiras descrições acadêmicas disponíveis do fenômeno de fadiga muscular no contexto da prática de exercícios datam do início do século XX, sendo boa parte desses trabalhos acessíveis por meio da revisão de Karlsson (1979). Este autor atribui pioneirismo à descoberta feita por Setchenov em 1903, em que “atividades divertidas” prolongavam o tempo de duração em tarefas extenuantes. Essas atividades divertidas seriam traduzidas contemporaneamente como treinamento físico, e da percepção de que elas melhoravam o desempenho emergiu o campo de estudo da fadiga muscular e suas condicionantes.

Naquele momento, o principal mecanismo considerado como desencadeador da fadiga era a produção de ácido lático, “na fibra ou em algum lugar próximo”, e que seria responsável por gerar calor no músculo exercitado experimentalmente, reduzindo sua capacidade contrátil (Peters, 1913). Mais tarde, o aumento da produção e o acúmulo de metabólitos da contração muscular passaram a ser considerados como partes constituintes do desenvolvimento da fadiga, tanto do músculo exercitado quanto de músculos não envolvidos no exercício, bem como no SNC (Marx, 1933). Ainda, a depleção de substratos necessários para a contração muscular e para a reconversão de metabólitos em estoques de energia passaram a ser consideradas como principais fatores desencadeantes do processo de redução da força e resistência localizada (Karlsson, 1979).

A partir dos anos 70, o número de estudos sobre fadiga muscular aumentou expressivamente, o que foi positivo porque permitiu a colaboração internacional no entorno do tema e ampliou a capacidade de compreender a totalidade do assunto. Mas trouxe a expansão trouxe um problema: a heterogeneidade das definições. Por esse motivo, Enoka *et. al.* (2008) se propuseram a revisar a literatura sobre o estudo da fadiga para propor a padronização de termos, conceitos, e traçar diretrizes para protocolos de avaliação, impactando assim na melhor definição do conceito e facilitando o delineamento de estudos. Eles concluem que a definição mais adequada para fadiga muscular seria “diminuição gradual na capacidade de força do músculo ou o ponto final de uma atividade sustentada”.

Quanto às consequências práticas da fadiga muscular, sabe-se que ela prejudica o desempenho esportivo e as tarefas de vida diária (Hunter, 2018). Se

trata de um processo fisiológico e transitório, em que o organismo saudável encontra meios para recuperar a homeostase e preparar os músculos para retornarem a seu potencial máximo (J. Fernandes et al., 2019; Peake et al., 2017). Ainda que o treinamento físico possa minimizar ou retardar a fadiga muscular (Ribeiro et al., 2014; Sundstrup et al., 2016), e que existam diversas propostas de intervenções para mitigar seus efeitos (Hou et al., 2021), ela é inerente ao funcionamento do sistema neuromuscular, visto que este dispõe de recursos energéticos limitados. Desta forma, desde um sujeito sedentário até um atleta de elite, todos estão sujeitos aos efeitos limitantes da fadiga muscular.

Para entender o desempenho sob fadiga em esportes cuja prática demanda grandes deslocamentos, movimentos amplos e recrutamento simultâneo de músculos para movimentação vários segmentos corporais, é possível produzir uma situação de fadiga mais global e observar seus efeitos em músculos de interesse (Goodall et al., 2015, 2017; P. W. M. Marshall et al., 2018). Por outro lado, a fadiga muscular, além de ser causada pela escassez de nutrientes, é também causada pela produção de metabólitos (Ørtenblad et al., 2013). Portanto, para alguns estudos é necessário reduzir o número de músculos exercitados para evitar um efeito chamado “fadiga muscular não local”, em que os metabólitos de um músculo circulam pela corrente sanguínea e afetam o desempenho de outro (Halperin et al., 2015). Por isso, é importante a possibilidade de simular situações causadoras de fadiga no ambiente e sob os protocolos controlados de um laboratório.

Uma vez que esse conceito é compreendido minimamente pela comunidade científica e suas relações com o desempenho motor são descritas, surge o interesse em a) compreender melhor os mecanismos envolvidos e b)

descrever comportamentos associados com a fadiga muscular. Isso acarreta uma série de protocolos e medidas que se prestam a auxiliar na compreensão do fenômeno da fadiga, desde seus mecanismos, até seus efeitos agudos, de médio, e de longo prazo.

1.1.2 Eventos biomecânicos da fadiga muscular

Ao simular a fadiga muscular com experimentos realizados em laboratório, usando modelos de músculos isolados em vez de corpos inteiros, amplia-se a oportunidade de utilizar e otimizar medidas biomecânicas para descrever em maior detalhe seu desenvolvimento. Em laboratório podemos avaliar o músculo antes, imediatamente após e durante a fadiga. Também, é possível utilizar equipamentos sensíveis a perturbações externas ou aqueles cuja instalação é fixa, como por exemplo, plataformas de força, dinamômetro isocinético, câmeras termográficas, eletromiografia, etc.

Por meio da dinamometria é possível verificar que a fadiga muscular gera redução transitória da força (Bigland-Ritchie et al., 1978; Clarke et al., 1955), além de afetar negativamente a taxa de desenvolvimento de força (D'Emanuele et al., 2021) e a capacidade de sustentar a forças máximas e sub-máximas ao longo do tempo (Hunter et al., 2005). Sumarizamos esses eventos na figura 1. Também podemos observar que a fadiga muscular tem efeitos relativamente persistentes, cuja recuperação demanda horas ou até mesmo dias, dependendo da intensidade do protocolo (J. Fernandes et al., 2019; Linnamo et al., 1997).

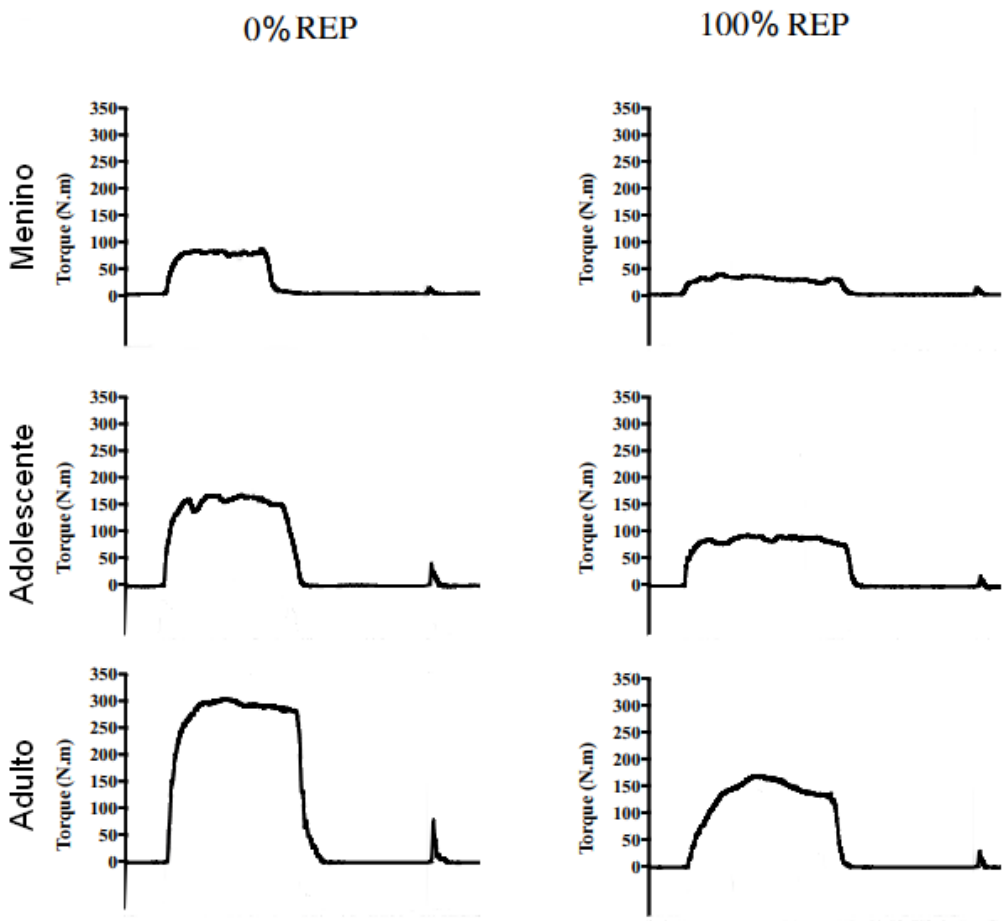

Figura 1. Exemplo de avaliação da fadiga muscular. Nesse estudo foi avaliada força máxima ao longo do tempo de vasto lateral durante tarefas de contração isométrica voluntária máxima nas situações antes (0% de repetições máximas, 0% REP) e depois (100% de repetições máximas, 100% REP) de um protocolo de indução de fadiga. É possível notar redução da magnitude da força muscular após a indução de fadiga. Adaptado de (Piponnier et al., 2019).

Por meio da eletromiografia (EMG), sabe-se que em exercício sub-máximo a fadiga muscular demanda aumento da amplitude do sinal elétrico para permitir maior recrutamento de fibras, bem como desloca à esquerda os componentes do sinal elétrico no domínio da frequência (Cifrek et al., 2009).

Em um primeiro momento, a amplitude de ativação elétrica estimada pela raiz quadrada média (RMS) tem uma relação direta com a intensidade de ativação muscular (Boe et al., 2008). À medida que uma tarefa fatigante progride, o aumento da magnitude da atividade elétrica é interpretado como uma perda de eficiência, típica de uma musculatura que encontra estagnação na capacidade de contrair e perda de eficiência de suas unidades motoras, exigindo recrutamento adicional de unidades motoras para realizar a mesma tarefa (Cifrek et al., 2009). Dessa forma, a EMG pode variar em intensidade e indicar fadiga muscular. Porém, os estudos têm demonstrado que a relação entre fadiga e ativação elétrica não é linear. A primeira alteração na ativação elétrica tende a ser um incremento conforme a fadiga muscular se desenvolve (Bilodeau et al., 2003), mas vez que não existe mais a possibilidade de incrementar a ativação ou em situações em que a musculatura não parte de uma condição de homeostase, a ativação elétrica pode decair com a intensificação da fadiga (Mendez-Villanueva et al., 2012).

Da mesma forma, podem ocorrer mudanças no domínio da frequência, sendo a variação no espaçamento entre os potenciais de ação de recrutamento muscular um indicador de redução de desempenho durante uma tarefa extenuante, e uma mudança no tipo de fibra predominante durante a contração (Bilodeau et al., 2003; Cifrek et al., 2009). Algumas das possíveis observações da frequência da EMG como indicadores de fadiga são o deslocamento da média, da mediana (González-Izal et al., 2012) e do pico de frequência, bem como da razão entre altas e baixas frequências (Karthick & Ramakrishnan, 2016). Por fim, uma análise alternativa ad EMG é a entropia, uma forma de calcular a complexidade dos disparos dos potenciais de ação ao longo do tempo,

em que quanto menor a possibilidade de variação do sinal, pior é a condição fisiológica da musculatura avaliada, indicando fadiga muscular (Zhang & Zhou, 2012).

Devido a EMG demonstrar essa relação não-linear com a fadiga muscular e ao fato de as medidas no domínio do tempo serem muito sensíveis a fatores extrínsecos, demandando especial cuidado na coleta e processamento de sinais em testes em diferentes dias (Albertus-Kajee et al., 2010), os pesquisadores têm procurado e desenvolvido técnicas alternativas para atestar a presença e a intensidade da fadiga muscular.

Uma medida indireta da fadiga que pode funcionar como alternativa é a termografia infravermelha (IRT), que recentemente vem sendo utilizada para tentar descrever a relação entre a fadiga resultante do exercício físico e variações da temperatura da pele (Priego Quesada et al., 2015). A IRT é medida por meio de câmeras termográficas, que possuem sensores

Termografia infravermelha é uma técnica de imagem usada pra registrar radiação infravermelha, e a partir dela estimar as temperaturas de uma superfície (Priego Quesada, 2017). Os raios infravermelhos não estão no espectro visível, mas são emitidos por todo corpo que apresenta calor (Ring, 2006). Existem diferenças entre alguns corpos em função de suas propriedades físicas, o que impacta na capacidade de detecção da temperatura por meio da câmera termográfica. Algumas das propriedades que impactam na capacidade de a câmera termográfica medir calor são a absorbância, a emissividade, a refletividade e a transmissividade. Dessas, destacamos a emissividade como variável mais importante para o tipo de medida realizada na biomecânica, que indica a capacidade de um corpo emitir raios infravermelhos, ou seja, de mostrar

à câmera sua temperatura. A pele humana tem a emissividade quase perfeita, variando entre 0,97 e 0,99, em uma escala que vai até 1 (Priego Quesada, 2017).

Existem pelo menos duas hipóteses que sustentam o uso da IRT nos estudos da fadiga. A primeira é que o exercício físico gera demanda de sangue nas regiões exercitadas, o que aumenta a irrigação não somente nos músculos, mas também nos capilares mais externos, aquecendo a pele. Após uma vasoconstrição periférica inicial, o aumento da temperatura central demanda vasodilatação para eliminação de calor (Simmons et al., 2011). Por outro lado, entre os mecanismos de termorregulação que são disparados pelo exercício sustentado está a sudorese, que gera dissipação de calor por meio da evaporação e levando a uma manutenção ou resfriamento na pele avaliada (A. de A. Fernandes et al., 2014; Formenti et al., 2013). A segunda, é que o exercício físico gera dano muscular (J. Fernandes et al., 2019). Esse dano muscular é resolvido por meio de um processo inflamatório, que gera um aquecimento local ao longo de até 4 dias (Peake et al., 2017). Esse calor produzido nos músculos seria transmitido por indução aos tecidos mais superficiais até o ponto de aquecer a pele, e esta emitir radiação correspondente ao calor até a detecção da câmera termográfica. Até o momento, não há um consenso sobre a aplicabilidade e a melhor forma de avaliar a IRT no contexto da fadiga muscular (Hadžić et al., 2019), portanto estudos mais aprofundados são necessários.

1.1.3 Eventos bioquímicos relacionados com a fadiga muscular

A contração muscular pode ser descrita como uma cadeia de eventos bioquímicos que acontecem em paralelo a eventos mecânicos, frequentemente os influenciando. O modelo das pontes cruzadas é atualmente o mais aceito para

explicar a contração muscular e, consequentemente, a produção de movimento e força (Karp, 2010). Esse modelo indica de forma esquemática que o músculo é composto por uma série de miofibrilas, que por sua vez são compostas por um incontável número de pares de proteínas que interagem: a actina, que pode ser indicada como uma estrutura longa e estática, que se projeta e se liga a uma base que ancora nas linhas Z o esquema em dois sentidos; e a miosina, que é uma proteína longa e fina que se insere entre as actinas e possui braços com a propriedade de se ligar à actina e curvar-se, puxando as actinas, encurtando a distância entre as linhas Z e realizando movimento (figura 2).

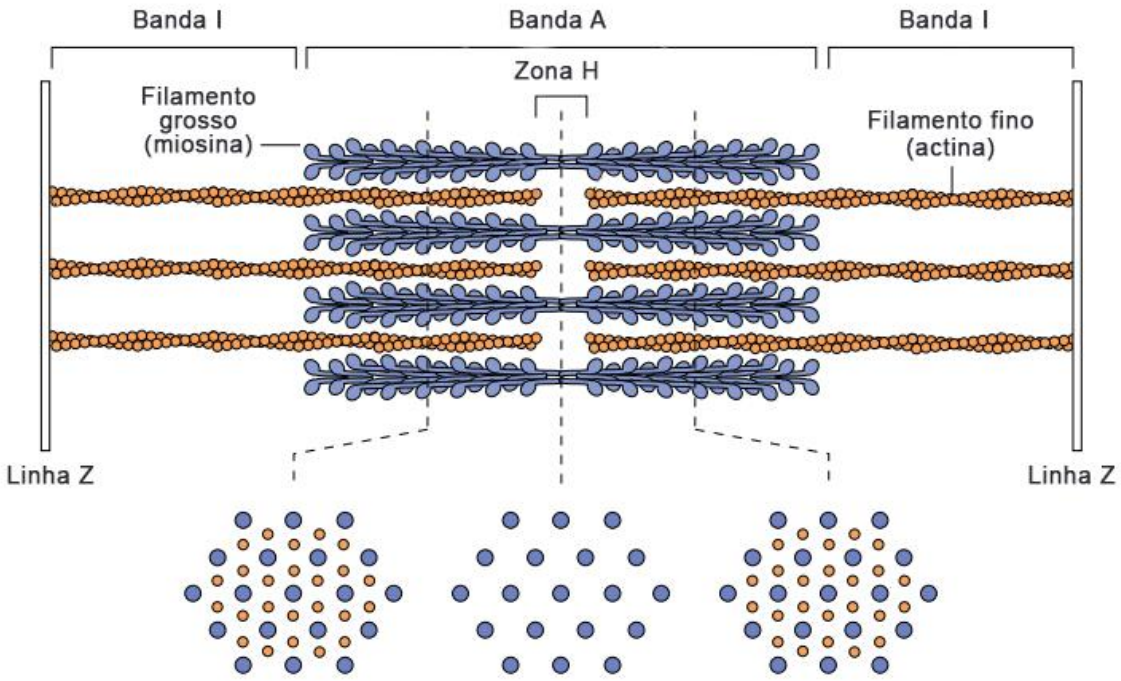

Figura 2. Diagrama do modelo de pontes cruzadas dos sarcômeros, apresentando a matriz de filamentos sobreposta. Adaptado e traduzido de Karp (2010).

Para acontecer a contração muscular, esse sistema precisa de nutrientes, o que converte energia química em energia mecânica e calor. Disso, se conclui

que a fadiga muscular pode ocorrer por diminuição dos estoques nutricionais (Ørtenblad et al., 2013). A base nutricional da contração muscular é o aporte de glicogênio, que é substrato para produção de adenosina trifosfato (ATP) no ciclo de Krebs e, principalmente, na cadeia transportadora de elétrons (Hargreaves & Spriet, 2020). O ATP é uma molécula utilizada como forma de armazenar e transferir a energia nas ligações de fosfatos, necessária para realizar o ciclo de contração muscular, uma vez que se liga no complexo actina-miosina e o desfaz, possibilitando uma nova ligação e nova contração (Lai et al., 2008). Dessa forma, não é possível realizar contração muscular sem ATP, e, portanto, tanto o ciclo de Krebs quanto a cadeia transportadora de elétron são fundamentais para essa ação.

O aumento da atividade da cadeia transportadora de elétrons para produzir energia, principalmente nos complexos I e III, gera como consequência altos níveis de espécies reativas de oxigênio (ERO), como superóxido, o peróxido, os radicais de hidroxila, etc. (Steinbacher & Eckl, 2015). Estes elementos altamente instáveis são necessários em processos como ação imunológica e indiretamente à hipertrofia (Barbieri & Sestili, 2012; Powers & Jackson, 2008). Por outro lado, as ERO prejudicam a dinâmica da contração muscular ao afetarem negativamente a dinâmica de acoplamento e movimentação entre actina e miosina. Prochniewicz *et. al.* (2008) indicam que as ERO causam uma desorganização da transição entre a ligação fraca e a ligação forte entre actina e miosina, justamente o momento em que atualmente se considera como sendo a fase de maior produção de força no modelo de pontes cruzadas. Além de afetar a contratilidade, as ERO podem causam dano oxidativo em outras moléculas, sendo capazes de corromper e até degradá-las

(Steinbacher & Eckl, 2015), o que no contexto do exercício pode significar a geração de dano muscular, do qual falaremos a seguir.

O organismo possui meios de equilibrar a produção e neutralização de ERO com algumas enzimas endógenas e pelo consumo de produtos antioxidantes a fim de manter os processos fisiológicos (Dekkers et al., 1996; Lamprecht, 2015). Citamos aqui alguns exemplos: a superóxido dismutase é uma enzima que reduz o radical superóxido (O^{-}_{2}) em peróxido de hidrogênio (H_2O_2) e oxigênio (O_2) (Fukai & Ushio-Fukai, 2011); a glutationa peroxidase reduz o peróxido de hidrogênio (H_2O_2) a água (H_2O) (Lubos et al., 2011); a glutationa redutase é a enzima responsável por gerar a redução da glutationa dissulfeto (GSSG) a forma sulfidril (GSH), que por sua vez tem propriedade antioxidante (Couto et al., 2016); e por fim, a catalase com função de decompor o peróxido em H_2O e O_2 (Goyal & Basak, 2010).

Por outro lado, quando a produção de ERO é exacerbada e as defesas antioxidantes se tornam insuficientes para equilibrar o sistema, ocorre a situação de estresse oxidativo, que consiste em a sobreposição da quantidade de ERO sobre as defesas antioxidantes ser tamanha ao ponto de as ERO reagirem com diversas moléculas celulares (Birben et al., 2012). No contexto da fadiga muscular, tanto a respiração celular quanto o recrutamento de células inflamatórias em resposta ao dano muscular podem gerar estresse oxidativo, que por sua vez não só retarda a resolução do dano muscular como o intensifica, contribuindo para a perda de força (Accattato et al., 2017).

Além da já relatada depleção de nutrientes e do estresse oxidativo, as análises bioquímicas indicam que a fadiga muscular ocorre por consequência do dano muscular, definido como a ruptura e desorganização dos sarcômeros em

decorrência de contrações intensas, geralmente excêntricas e às quais o sujeito não está habituado (Clarkson & Hubal, 2002). A princípio, o dano muscular é causado quando a tensão mecânica promovida pela contração é maior do que a capacidade de as unidades contráteis resistirem (Kuipers, 1994), mas o dano muscular persiste e até aumenta mesmo após encerrada a tensão mecânica (da Silva, Machado, Souza, Mello-Carpes, et al., 2018). O dano muscular também se retro-alimenta toda vez que a desorganização e ruptura de sarcômeros libera o íon cálcio (Ca^{2+}) do retículo sarcoplasmático ao citoplasma, estimulando enzimas proteolíticas a degradar novas porções do músculo. Esse dano continuado pode durar de 1 a 3 dias após o exercício excêntrico (Fatouros & Jamurtas, 2016)

Uma vez que o estímulo mecânico gera dano muscular, o sistema biológico recruta o processo inflamatório como estratégia para conter a piora do estado do tecido e promover a regeneração (Peake et al., 2017). O processo inflamatório se utiliza das ERO como sinalizador para recrutar mais células do complexo inflamatório, bem como para degradar parte dos metabólitos. Por outro lado, a inflamação tende a produzir níveis de ERO que por um período intensificam o dano muscular pela agressão química ao músculo uma vez que agem oxidando moléculas diversas, o que retroalimenta o próprio dano (Mittal et al., 2014). O dano muscular, portanto, é um evento que gera perda de eficiência muscular, contribuindo para a perda de força e resistência que caracteriza a fadiga muscular (Khaitin et al., 2021). Concomitante ao dano muscular, o músculo experimenta a liberação de altos níveis de creatina quinase (CK) que, além de ser um importante marcador do dano, é por si só um fator intensificador da fadiga uma vez que afeta a concentração de fosfato inorgânico no sistema

(Dahlstedt et al., 2000). A CK é uma enzima responsável pela refosforilação da creatina na mitocôndria, produzindo fosfocreatina (Pcr), que atua como um reservatório para rápida disponibilização de energia em diversos tecidos ao manter o equilíbrio entre moléculas de adenosina trifosfato (ATP) e adenosina difosifato (ATP) (Wallimann et al., 1992), conforme esquematizado na figura 3. À medida em que o exercício vigoroso promove danos às fibras musculares, ocorre o extravasamento de proteínas intracelulares à corrente sanguínea, dentre eles a CK que se torna um importante marcador de dano muscular (Baird et al., 2012).

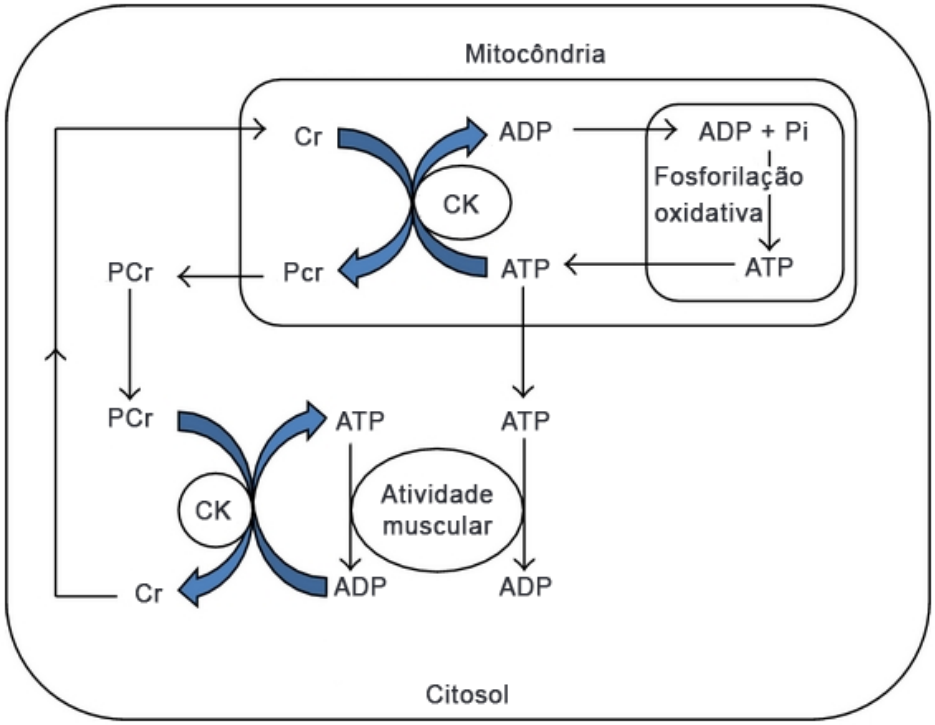

Figura 3. Circuito da fosfocreatina (Pcr) com especial destaque a participação da creatina quinase (CK) no equilíbrio ATP (adenosina trifosfato)/ADP (adenosina difosfato) durante o exercício físico. Traduzido de Baird (2012).

Vimos anteriormente que a fadiga muscular é responsável pelo desenvolvimento de processos inflamatórios locais, principalmente quando a fadiga é acompanhada de dano muscular. A inflamação é um processo fisiológico responsável pelas defesas imunológicas a estímulos ameaçadores, como patógenos, agentes químicos, radiações ou tecidos orgânicos danificados (Chen et al., 2018). O último caso é o que desencadeia a inflamação decorrente da fadiga muscular. Sempre que o dano muscular é induzido, ocorre uma produção de metabólitos que englobam os produtos das reações químicas responsáveis pela contração, e também fragmentos das proteínas dos sarcômeros que foram rompidas pela tensão mecânica, bem como seu conteúdo intracelular (Fatouros & Jamurtas, 2016). Logo, o dano muscular desencadeia o aumento de proteína c-reativa, interleucinas 1 e 6 (il-1, il-6), fator de necrose tumoral-alfa (TNF-α) e factor nuclear kappa B (NF-κB) como sinalizadores inflamatórios (Fernández-Lázaro et al., 2020). Essa sinalização recruta agentes imunológicos como células inflamatórias (neutrófilos, macrófagos, linfócitos T e mastócitos), células-tronco musculares, células vasculares, etc. com o objetivo de remover dejetos e remodelar o músculo danificado (Peake et al., 2017).

1.2 Recuperação da fadiga

Após o fim de um exercício vigoroso que foi capaz de induzir dano muscular, inicia-se um período de recuperação muscular. Essa recuperação consiste em devolver ao músculo a sua homeostase, em que sua capacidade contrátil e, consequentemente, de produzir força, esteja íntegra. Além disso, o músculo regenerado deverá estar livre de qualquer tipo de infiltrado inflamatório, metabólitos e produção exacerbada de ERO. Em resumo, igual à situação em

que se encontrava em um momento pré fadiga muscular (Armstrong et al., 1991). Para alcançar essa regeneração, o músculo deve respeitar uma temporalidade, que é o ciclo de recrutamento e ação dos elementos inflamatórios. Peake *et. al.* (2017) demonstraram que levando em conta o surgimento, ação e remoção dos diferentes tipos de células inflamatórias, o músculo estará alterado desde o início até 7 dias após o dano muscular induzido pelo exercício.

É importante destacar que a temporalidade e intensidade da perda de força, bem como dos demais efeitos da fadiga, não necessariamente será congruente à do processo inflamatório. A recuperação da força máxima depende do tipo e intensidade do exercício (Häkkinen, 1995), da musculatura envolvida, idade, sexo ou nível de treinamento do participante (Enoka & Duchateau, 2008). Para ilustrar a dependência da recuperação da fadiga em relação ao tipo de exercício e as características dos participantes, citamos um estudo que observou que mulheres demoram mais pra recuperar a força máxima isométrica pós fadiga (Albert et al., 2006), enquanto que outro demonstra que homens e mulheres não diferem na recuperação quando o teste de força máxima é feito envolvendo contração isocinética (Gomes et al., 2021).

Por fim, mesmo que a força máxima ou a resistência estejam recuperadas antes do fim do processo inflamatório, outros componentes da fadiga ainda podem estar presentes, como o acúmulo de metabólitos e perda de contratilidade que, se por um lado, é contornada pelo sistema neuromuscular para produzir força máxima, pode estar rebaixado na tarefa de absorver energia mecânica, expondo o músculo ao risco de lesão (Mair et al., 1996).

1.3 Fadiga acumulada

Chamamos de “fadiga acumulada” ou “fadiga cumulativa”, aquela condição em que uma pessoa é submetida a dias consecutivos de esforço físico capaz de gerar fadiga muscular, sem disponibilização de tempo suficiente para recuperação entre as sessões (P. W. Marshall et al., 2021; Montgomery et al., 2008; Stewart et al., 2008). Essa organização espacial do esforço extenuante em dias sucessivos é comum em alguns esportes coletivos, tais como o basquete, ciclismo e até mesmo no treinamento de força (El Helou et al., 2010; Montgomery et al., 2008; Yang et al., 2018). Também pessoas pouco treinadas ou sedentárias podem experimentar essa situação, desde que seu planejamento de ingresso a um ciclo de atividade envolva dias repetidos de exercícios. Por fim, é importante entender os mecanismos envolvidos na fadiga acumulada decorrente da ausência de descanso apropriado para melhor planejar programas de reabilitação fisioterapêutica, mesmo que a intensidade da fadiga desenvolvida possa ser menor.

É importante destacar que nenhuma medida ou marcador é por si só capaz de descrever ou atestar a fadiga acumulada (Kataoka et al., 2022). Sua manifestação depende da combinação entre as características e o histórico das pessoas testadas, os músculos envolvidos, os exercícios executados e a forma de avaliar fadiga. Portanto, é interessante entender a fadiga acumulada como uma categoria derivada de múltiplas observações, a qual deve ser compreendida nas suas características gerais e não como alguma medida específica.

Os efeitos da fadiga acumulada são conflitantes na literatura. Por um lado, para atletas bem treinados e submetidos a uma fadiga de corpo inteiro, o período de descanso de um dia para o outro de exercício parece ser suficiente para

recuperar a condição de produzir força e a contratilidade muscular (P. W. Marshall et al., 2021). Aparentemente, pessoas muito treinadas se beneficiam da sua alta capacidade de recuperação. Porém, como bem indicam os autores, esse estudo tem limitações que impedem a generalização dos achados para outras populações.

Outros estudos vão no sentido oposto, indicando que dias consecutivos de exercícios geram perda de desempenho muscular. Sánchez-Migallón (2022) demonstraram que jogadoras profissionais submetidas a dois dias consecutivos de partidas de hockey apresentaram perda de força em abdutores e adutores do quadril, principalmente no membro não-preferido. No mesmo sentido, homens sedentários submetidos a três dias consecutivos de exercício máximo mostraram perda de força que persistiu por até 3 dias (Stewart et al., 2008). Além de reduzir a força, a fadiga acumulada causa redução na velocidade de contração, perda de resistência e alteração no sinal mecanomiográfico em homens bem treinados (Tosovic et al., 2016).

A fadiga acumulada também afeta negativamente marcadores bioquímicos da fadiga e do status muscular, por exemplo alterando a presença de citocinas pró e anti-inflamatórias após dois dias de exercícios de Crossfit (Tibana et al., 2016), aumentando dano muscular em ciclistas submetidos a exaustão de extensores (da Silva, Machado, Souza, Mello-Carpes, et al., 2018) e gerando aumento de marcadores de estresse oxidativo em ciclistas submetidos a pedaladas em dias consecutivos (Shing et al., 2007).

1.4 Intervenções de combate à fadiga

Como vimos na contextualização histórica do conceito de fadiga, sua descoberta se dá justamente pela observação das “atividades divertidas” como uma intervenção. Dessa forma, notamos que os estudos da fadiga muscular ocorrem justamente com o objetivo final de reduzir, evitar, ou compensar seus efeitos. A fadiga muscular é um problema tanto para o desempenho esportivo, quando para o tratamento fisioterapêutico. No primeiro caso, pode-se dizer que obterão os melhores resultados esportivos aqueles que melhor mitigarem os efeitos da fadiga. No segundo caso, é possível pensar na fadiga como um limitante temporal dos protocolos de reabilitação, impedindo a antecipação do momento de alta dos pacientes. A seguir, comentamos as intervenções de combate à fadiga sob as perspectivas ativa e passiva.

1.4.1 Intervenções ativas

Chamamos de intervenções ativas aquelas que não somente são realizadas voluntariamente pelo participante, mas que impõem movimentação ou ação mecânica aos músculos.

A mais consolidada intervenção voltada a reduzir os efeitos da fadiga é o treinamento de força com emprego de pesos externos, isto é, a imposição de cargas por um determinado conjunto de séries e repetições e cujas sessões estão dispostas ao longo de vários dias, consecutivos ou não, para promover adaptações positivas em termos de força e/ou resistência (P. W. Marshall et al., 2021; Schoenfeld et al., 2016). Essa abordagem é amplamente estudada, o que significa que a margem de ganhos com novas técnicas é cada vez menor. Outra limitação é o fato que seus benefícios demandam grande tempo de adaptação,

sendo os ganhos nos primeiros meses de treinamento advindos principalmente de adaptação neural, sem necessariamente garantir ao músculo o ganho estrutural que repercute em força ou resistência (Folland & Williams, 2007).

Também em forma de exercício, é comum atletas procurarem a recuperação ativa da fadiga pela prática do mesmo exercício que a causou, só que realizado em intensidade baixa. A hipótese que sustenta essa intervenção é que a manutenção do fluxo sanguíneo em alta intensidade acelera a remoção de metabólitos do dano muscular decorrende da fadiga, mas sua adesão encontra como empecilho a falta de estudos que indiquem a intensidade adequada, bem como o fato de serem beneficiados atletas com um nível de treinamento elevado (Ortiz et al., 2019).

1.4.2 Intervenções passivas

Outras intervenções são aplicadas de forma passiva aos sujeitos submetidos a fadiga, ou seja, sem a participação ativa do participante e sem ter a movimentação ou a ação mecânica sobre as musculaturas como principal mecanismo de ação da terapia.

Nessa categoria de intervenções também observamos uma muito utilizada: a crioterapia, crioestimulação ou imersão em água e gelo. Essa técnica também tem como princípio a constrição vasoperiférica, mas por meio da resposta ao estímulo térmico (Charkoudian, 2003), visando reduzir a permeabilidade dos capilares e combatendo o edema periférico, inflamação e dor tardia (Banfi et al., 2009). Essa técnica é relativamente barata e fácil de executar, mas Bouzigon *et. al.* (2021) argumentam que são necessários estudos

que possam consolidar protocolos de tempo/dosagem. Além disso, não se sabe sua eficácia para recuperação da fadiga acumulada.

A seguir, citamos a utilização de recursos eletrotermofototerapêuticos na tentativa de evitar ou reduzir os efeitos da fadiga muscular. A fototerapia tem como objetivo promover modificações estruturais e bioquímicas nos músculos irradiados, com o objetivo de melhorar o padrão de consumo de energia, conforme observado em modelo animal (Vieira et al., 2006). Um estudo recente indica que a laser terapia de baixa intensidade (sobretudo a 135J/músculo) aumenta o tempo de tolerância a pedaladas em atletas treinados, mas também na qualidade da contratilidade (Lanferdini et al., 2018), mas uma meta-análise indica mais uma vez a falta de padronização para determinar a efetividade da técnica (Wang & Wang, 2019). De qualquer forma, essa terapia não é tão acessível, uma vez que depende de equipamentos de alto custo e não são conhecidos seus benefícios na fadiga para dias consecutivos de exercício.

A eletroterapia também tem restrições à generalização de sua aplicação na população interessada em combater a fadiga muscular devido aos custos e a relativa complexidade da execução. Sob a hipótese de melhorar o fluxo sanguíneo pela diminuição da resistência periférica (Miller et al., 2000) ou de aumentar a tolerância ao exercício pela via do alívio de sensações desagradáveis geradas pela fadiga (Astokorki & Mauger, 2017), alguns estudos buscaram avaliar a efetividade da eletroterapia na recuperação pós exercício, mas os resultados foram conflitantes (Lattier et al., 2004; Zarrouk et al., 2011). Além disso, mais uma vez não sabemos seus efeitos na fadiga acumulada na comparação com outras técnicas.

Outra intervenção passiva envolve recursos terapêuticos manuais, como massoterapia, que visam gerar relaxamento muscular no pós-exercício e favorecer o fluxo sanguíneo, além de buscar reduzir edema e promover regeneração de tecidos (Weerapong et al., 2005). A massoterapia pode ser aplicada por um profissional ou feita pelo próprio sujeito por meio de recursos como o *foam roller*, em que o participante utiliza a própria massa corporal contra uma esponja texturizada para produzir a massagem (Jo et al., 2018). Porém, uma análise sistemática com meta-análise sobre o efeito da massoterapia na recuperaçao de força pós-fadiga indicou que a massagem não tem efeito sobre a força (Davis et al., 2020).

1.4.3 Suplementações, como as com extrato de chá verde

Por fim, dentre as estratégias de prevenção ou recuperação da fadiga muscular existe a suplementação com produtos antioxidantes naturais (Jówko, 2015). Os antioxidantes são elementos estáveis o suficiente para doarem um elétron a raciais livres, sendo capazes de minimizar danos oxidativos em biomoléculas (Lobo et al., 2010). No contexto do exercício físico, como já mencionado, as principais fontes de radicais livres, notadamente as espécies reativas de oxigênio (ERO), são os processos bioquímicos da produção de energia (principalmente na cadeia transportadora de elétrons (Steinbacher & Eckl, 2015) e mais tardiamente os processos inflamatórios resultantes do dano muscular (Wadley et al., 2013).

As ERO são moléculas reativas derivadas da redução de moléculas de oxigênio, dentre elas encontram-se: superóxido (O_2^-), radical hidroxila (OH^-), radical peroxil (RO_2^-), radical alcóxido (RO^-) e hidroperoxil (HO_2^-). Essas ERO são

mediadoras de diversos processos fisiológicos (Beckhauser et al., 2016; Rahman et al., 2012), mas são causadoras de danos em estruturas e moléculas uma vez que sua ocorrência se dá em quantidade maior do que as capacidades defensivas do organismo. Nesta revisão já citamos as ações das enzimas antioxidantes como forma de proteção contra o estresse oxidativo (ver seção 1.1.3).

Adicionalmente às defesas endógenas, podemos incrementar as defesas ao estresse oxidativo por meio do consumo de produtos dietéticos. Eles atuam sendo oxidados em substituição a outras potenciais estruturas biológicas (Seifried et al., 2007). Produtos como a vitamina C e os flavonoides presentes em diversas partes de um amplo grupo de plantas são amplamente utilizados e estudados devido ao seu papel no combate a diversas doenças (Panche et al., 2016; Seifried et al., 2007).

Por causa da sua aplicabilidade no contexto clínico, os produtos antioxidantes passaram a ser testados e utilizados na tentativa de retardar ou combater a fadiga muscular (Jówko, 2015), principalmente as folhas da *Camellia sinensis*, uma planta rica em catequinas, sobretudo na forma de extrato de chá verde (ECV) (Schimidt et al., 2017). A escolha do ECV como intervenção dietética se deve ao fato de essa ser a segunda bebida mais consumida no mundo, atrás apenas da água (Khan & Mukhtar, 2013), e sendo considerada, além de acessível, uma suplementação segura para diversos públicos, com baixas possibilidades de toxicidade nos níveis utilizados em estudos com humanos no contexto do exercício físico (Bedrood et al., 2018; Jówko, 2015).

As catequinas são compostos polifenóicos da família dos flavonoides, cuja constituição básica é baseada na presença de dois ou mais anéis aromáticos

(chamados anéis A e B), cada um com pelo menos uma hidroxila aromática conectada com uma ponte de carbono e um heterociclo diidropirano (o anel C) com um grupo hidroxila no carbono 3 (Braicu et al., 2013) (figura 4). As catequinas atuam como antioxidantes por meio de dois mecanismos de ação principais: neutralização de radicais livres (direta) por meio de doação de um elétron do grupo fenólico OH ou estabilização por ressonância dos radicais aroxila (PO) (Fraga et al., 2010); e estímulo à produção de enzimas antioxidantes (indireta) (Bernatoniene & Kopustinskiene, 2018).

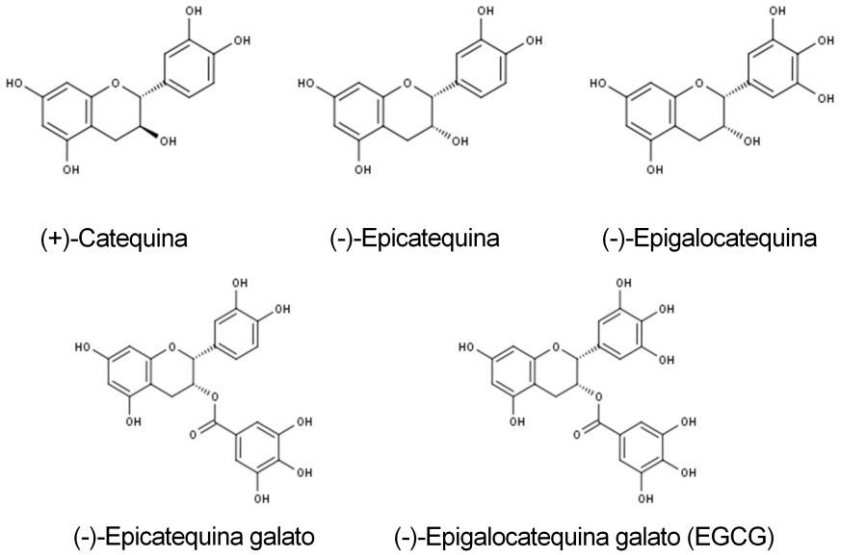

Figura 4. Estruturas químicas das principais catequinas presentes no chá verde. Adaptado de Suzuki et. al. (2016).

A suplementação ECV foi capaz de melhorar a resistência física em camundongos submetidos a exercício de corrida (Murase et al., 2006) e nado até a exaustão (Murase et al., 2005). Ou seja, para esse modelo experimental, o ECV atuou retardando a fadiga aguda, aquela desenvolvida ao longo da prática

de um exercício. A partir disso, diversos autores tentaram encontrar uma aplicabilidade para humanos, mas diversas revisões indicam que não foi possível transpor esse benefício (Hernández et al., 2012; Jówko, 2015).

Se a suplementação com ECV não aumenta o desempenho atlético e tampouco retarda a fadiga muscular em humanos, talvez a sua aplicabilidade deva ser investigada em outro contexto. Tendo em vista que não é somente no momento da realização do exercício, mas também no período entre os insultos promovidos em dias consecutivos que ocorrem eventos bioquímicos prejudiciais ao desempenho, tais quais o estresse oxidativo e o dano muscular, chegamos à conclusão de que a suplementação com ECV pode ter aplicabilidade como estratégia para preservar o desempenho neuromuscular na situação de fadiga acumulada.

1.5 JUSTIFICATIVA

A fadiga muscular é um fenômeno fisiológico, portanto esperado, que em condições típicas é resolvido pelo organismo sem maiores problemas (Enoka & Duchateau, 2008; P. W. Marshall et al., 2021). O sistema imunológico é capaz de remover os metabólitos da fadiga muscular, bem como remodelar o músculo que sofreu dano muscular (Accattato et al., 2017; Fernández-Lázaro et al., 2020).

Em termos de produção de força, a recuperação da fadiga muscular depende de várias características do participantes (Baumert et al., 2021) e dos parâmetros do momento de sua indução (Morán-Navarro et al., 2017), podendo a força voltar a níveis basais no dia seguinte ou permanecer abaixo do normal por alguns dias (Linnamo et al., 1997; P. W. Marshall et al., 2021). Apesar de a força e a resistência serem os parâmetros de onde se constrói o conceito de fadiga, é possível que a força retorne ao normal e outras variáveis biomecânicas permaneçam prejudicadas, o que indica por um lado que o sistema neuromuscular tem mecanismos redundantes que se compensam entre si para executar uma tarefa (P. W. Marshall et al., 2021), mas também que o músculo pode estar produzindo força numa situação de fragilidade, aumentando o risco de lesão.

A variabilidade da presença de marcadores bioquímicos da fadiga muscular também depende do protocolo como um todo, mas podemos tomar o comportamento da CK como um bom descritor do status muscular. Esse marcador de dano geralmente estará muito perto dos valores basais no imediato pós-exercício, mas apresentará um pico no momento 48 horas após. Por fim, sua normalização é esperada 4 dias após o exercício (Baird et al., 2012).

Em resumo, uma vez que a fadiga muscular ocorre, é necessário respeitar uma certa temporalidade para que o músculo se encontre mais uma vez em sua situação de normalidade. Porém, nem sempre esse período pode ser respeitado, seja pela necessidade de acelerar um protocolo de reabilitação, seja pela inviabilidade de um planejamento de exercícios suficientemente espaçado, seja pela necessidade de competir em alta performance por dias consecutivos.

1.6 OBJETIVOS

1.6.1. Objetivo geral

Descrever o fenômeno da fadiga acumulada e propor formas de avaliação e intervenção para minimizar seus efeitos sobre o funcionamento do sistema neuromuscular.

1.6.2 Objetivos específicos

I. Realizar uma análise exploratória do curso temporal dos efeitos cumulativos da fadiga no volume e na potência de ciclistas profissionais durante duas edições de um grand tour. Além disso, analisar como os dias de descanso impactam os indicadores de fadiga cumulativa.

II. Determinar se as especificações de distância e câmera afetam a detecção de assimetrias térmicas, método comumente utilizado na avaliação de membros sob efeito de fadiga muscular.

III. Avaliar a confiabilidade intercâmeras e interexaminadores entre três câmeras termográficas comerciais com diferentes resoluções espaciais considerando medidas realizadas antes e após o exercício físico.

IV. Reproduzir uma situação de fadiga acumulada e determinar se a termografia infravermelha pode avaliar seus efeitos servindo como ferramenta de monitoramento.

V. Determinar se a suplementação de extrato de chá verde pode minimizar os efeitos da fadiga acumulada em marcadores bioquímicos e desempenho neuromecânico.

CAPÍTULO II

ARTIGO ORIGINAL

Exploratory analysis of cumulative fatigue derived from volume and intensity indicators in stage races of professional cycling

Álvaro Sosa Machado[1], Carlos De la Fuente[1,2,3], Alejandro Javaloyes[4], Manuel Moya-Ramón [4,5], Manuel Mateo-March[4,6] & Felipe P Carpes[1]

[1] Applied Neuromechanics Research Group, Multicenter Graduate Program in Physiological Sciences, Federal University of Pampa, Uruguaiana, RS, Brazil

[2] Carrera de Kinesiología, Dpto. de Ciencias de la Salud, Facultad de Medicina, Pontificia Universidad Católica de Chile, Santiago, Chile.

[3] Centro de Innovación, Clínica MEDS, Santiago, Chile.

[4] Sport Sciences Department, Universidad Miguel Hernández de Elche, 03202 Elche, Spain.

[5] Sport Sciences Department, University Miguel Hernandez, Alicante Institute for Health and Biomedical Research (ISABIAL-FISABIO Foundation), Alicante, Spain

[6] Faculty of Sport Sciences, Universidad Europea de Madrid, 28670 Madrid, Spain.

2.1 Abstract

Here we discuss cumulative fatigue based on volume and power output from 12 professional male cyclists during two consecutive editions of the Giro d'Italia. Volume and power output were recorded and described according to time at different intensity zones based on power output (Z0 lower to Z7 higher). Correlations, principal component analysis (PCA), Gaussian clustering, and two-way ANOVA were performed (type error I of 5%). The higher intensity zones elicited higher power output in those shorter stages (R^2 = 0.54). In contrast, the lower intensity zones were predominant in longer stages. The time spent in Z1 to Z3 (r = 0.67, 0.84, and 0.73) correlated more with stage's volume duration than time in Z4 to Z7 (r = 0.48, 0.44, and 0.51, and 0.38). The normalized volume declined between stages 2 to 4, 8 to 10, 13 to 15, and 18 to 19. Negative slopes of time spent in Z4 and Z6 occurred one or two stages before Z1 presented negative slopes. In contrast, positive slopes of higher intensity zones were observed with a negative slope of Z1. Different clusters distributions of time volume to complete the grand tour were found ($p<0.05$). Finally, average power in Z1, Z2, Z3, Z4, Z5, Z6, and Z7 explained 63.62%, 18.20%, 8.12%, 5.84%, 2.98%, 1.20%, and 0.02% of the total variance in the normalized time volume, respectively. Volume and power zone data can recognize cumulative fatigue and performance recovery during a grand tour. Rest days favored the performance recovery, mostly the second rest day.

Keywords: exhaustion; recovery; muscle damage; sports performance; endurance.

2.2 Bullet points

- Markers of cumulative fatigue can be identified analyzing power and volume data during cycling grand tours.
- Performance reductions during cycling grant tours are preceded by a decrease in time spent in moderate to high intensity zones.
- The second rest day during cycling grand tours has the best impact on performance increase for subsequent stages.
- Cyclists develop two different intensity zones distribution (clusters) in the time-volume to complete the grand tour without differences in average power output.

2.3 Introduction

For professional men cycling athletes, there are three main grand tours with similar characteristics of consecutive days of racing and extreme exigence in terms of performance. The grand tours have a mileage of 3,300 to 3,500 km divided into 21 stages, with single days of rest distributed along the stages. In these races, athletes achieve an average power output of around 260 W (1). However, little knowledge about stage profiles has been considered (2).

Consecutive days of racing induce cumulative fatigue (1). Muscle fatigue reduces the ability to produce force over time (3) and causes muscle damage that triggers physiological events i.e. oxidative stress and inflammation (4). The inflammatory reaction (a cycle lasting up to 120 h) starts restoring the muscle integrity process (muscle homeostasis and regeneration) (5). Unfortunately, consecutive days of exercise interrupt the recovery cycle and reinforce the production of muscle damage, oxidative stress, and inflammation resulting in the cumulative fatigue condition (6). Previous studies have explored the effects of cumulative fatigue on isolated muscle conditions (7), in incremental exercise protocols (8), in diverse populations (9), as well as its interactions with other aspects of exercise like psychological and cognitive conditions (10). However, the description of cumulative fatigue over multistage professional races is difficult to obtain and analyze. Hence the evidence is limited.

In this regard, the current tools of performance monitoring and data sharing can allow the in-field monitoring of athletes' performance. This is the case of power output reported during the races, which allows a reliable description of the race demands (11). Therefore, a common way to describe the exercise characteristics during a race is to quantify the volume (time) in different intensity

zones according to the power output. These intensity zones can be defined as a percentage of the individual functional power threshold (12,13).

Because the performance in multistage races, like a professional cycling grand tour composed of 21 stages with at least two rest days, generates cumulative fatigue, the distribution of volume between the intensity zones could be altered, denoting a performance change. Finally, these races also include rest days. The rest days can benefit an athlete's recovery after strong efforts in consecutive days, in which the race is completed spending around 5,000 Kcal/day with high demands for hydration (around 6.7 L/day) (14). Currently, it is not clear how the variables volume and power output vary in response to rest days or during the race. Therefore, we conducted an exploratory analysis of the time course of cumulative fatigue effects on the volume and power output of professional male cyclists racing during two editions of a grand tour. In addition, we analyzed how the rest days impact cumulative fatigue indicators.

2.4 Material and methods

2.4.1 Participants and experimental design

Twelve professional cyclists from the same UCI World-Tour professional cycling team and racing two editions of the Giro d'Italia participated in this study. The participants had 26.9 (3.6) years, 178.5 (6.6) cm of height, 69.0 (7.8) kg of body mass, and 21.8 (1.6) kg/m^2 of body mass index. All signed an informed consent form. This study was approved by the local institution's ethics committee, and procedures followed the Declaration of Helsinki.

Data collection during the Giro d'Italia 2015 and 2016 included the individual recording of power output and volume distribution for each stage of the

race while the athletes followed the planning and protocols defined by the team management. We chose to analyze two editions of the grand tour to make the data generalization more robust. Regarding the characteristics of the race, we considered the number of stages, distance of each stage, and description of each stage considering the information from the official competition website.

2.4.2 Data collection

Data were recorded using the same device model and configuration for all cyclists (Garmin 510, Garmin Inc., Kansas, United States). The instrument was a power meter, a portable crank-based device (Power2Max type S, Zossen, Germany) that measures the mechanical power considering torque data obtained from an instrumented crankset with strain gages. All power meters were factory calibrated at least once per season, and a zero-offset was performed before each session attending to manufacturers' instructions. Potential spikes were checked and removed using specific software (Data Spike ID and FIX chart, WKO5 Build 576; TrainingPeaks LLC, Boulder, CO). Hence, volume and power output data were available to be obtained from cyclists' bicycles. The device measured power output every 1 s with an accuracy of 2% (15). Finally, when each stage ended, the volume and power output data were uploaded to a cloud service (TrainingPeaks, Boulder, United States) and subsequently, analyses were performed using specific software (WKO5 Build 576; TrainingPeaks LLC, Boulder, CO).

2.4.3 Intensity zones

Seven exercise intensity zones were determined based on the individual functional threshold power (FTP) (12): zone 1 (Z1; ≤ 55% of FTP), zone 2 (Z2; between 56 and 75% of FTP), zone 3 (Z3; between 76 and 90% of FTP), zone 4 (Z4; between 91 and 105% of FTP), zone 5 (Z5; between 106 and 120% of FTP), zone 6 (Z6; between 121 and 150% of FTP) and zone 7 (Z7; ≥151% of FTP). Z0 corresponds to the time without pedalling. We determined seven intensity zones representing a wide range of intensities, including aerobic and anaerobic efforts. These intensities distribution is commonly used by these cyclists during training and racing. Zones were determined based on the individualized FTP estimated by the best 20-min power output record (16) obtained during the month before the start of the competition in each of the years. In addition, whether cyclists recorded higher 20-min power during the competition, the intensity zones were updated to accurately quantify the intensities distribution.

2.4.4 Data analysis

We described the time-normalized stages' duration, which made all stage times equal to 100% in the time domain. Data (time volume normalized by stages duration and power output) were described for each intensity zone as mean and standard deviation considering the normal data distribution verified with Shapiro-Wilk and Levene's tests with error type 1 equal to 5%. The associations between the time spent in the different intensity zones and the stage duration were described using a non-linear fitting with an exponential series [$f_{(x)} = a*e^{(bx)} + c*e^{(dx)}$ + error]. The coefficients, 95%CI (confident interval), and the determination coefficient (R^2) were described. The association between total time volume and

each stage duration was described using a linear model [$f_{(x)} = mx + f + error$] to identify whether higher or lower slopes of intensity zones are dependent on the period stages (positive slopes >0.1 vs constants <0.1). The slope (m), inclination angle (θ), correlation and determination coefficient (R^2) were described. The peak of higher declines in the normalized volume was measured as the negative slopes across stages before the next normalized volume showed an increment (positive slopes). The slope changes in normalized time were tracked in the zone intensity with the highest dispersion that could show the compromise of the time-volume output. Additionally, the intensity increases and decreases strategies along a stage were explored by the slope changes normalized by their magnitudes (absolute values), resulting in -1 (negative slope) or +1 (positive slope) indicators. Finally, the principal component analysis (PCA) was used to understand how the intensity zones (Z1, Z2, Z3, Z4, Z5, Z6, and Z7) explained the total variance of normalized time volume for each stage. A threshold of 80% of the total variance was used to choose the principal component and understand the structure of the data. In addition, a mixed Gaussian fitting was used to define data clusters in the principal component space. The Akaike information criterion was used to determine the number of components [$AIC = 2k - 2\ln(L)$], with k equal to the number of clusters and L equal to the maximum value of the likelihood function for the Gaussian model. The posterior probability of pertinence of the main cluster fitted by mixed Gaussian distributions was described, and the normalized time volume and power output for each found cluster was also described. Finally, the clusters for normalized time and power output were described and compared using a two-way ANOVA and multiple comparisons with error type I of 5%.

2.5 Results

Table 1. Descriptive information from each Giro d'Italia edition analyzed

2015		**2016**	
Stage: location Date, distance Won how	Vertical meters Average speed winner Average power Average cadence	Stage: location Date, distance Won how	Vertical meters Average speed winner Average cadence Average power
1: San Lorenzo a Mare Saturday, May 9, 17.6 km Time trial	83 m 54.34 km/h 355.86 W 94.69 rpm	1: Apeldoorn ITT Friday, May 6, 9.8 km Time trial	37 m 53.21 km/h 378.62 W 93.24 rpm
2: Albenga → Genova Sunday, May 10, 177 km Sprint of large group	1868 m 41.93 km/h 190.21 W 73.08 rpm	2: Arnhem → Nijmegen Saturday, May 7, 190 km Sprint of a large group	732 m 40.93 km/h 153.94 W 62.67 rpm
3: Rapallo → Sestri Levante Monday, May 11, 136 km Sprint of large group	2797 m 38.15 km/h 222.70 W 74.42 rpm	3: Nijmegen → Arnhem Sunday, May 8, 190 km Sprint of a large group	691 m 43.22 km/h 184.23 W 70.46 rpm
4: Chiavari → La Spezia Tuesday, May 12, 150 km 14.1 km solo	3050 m 39.48 km/h 231.68 W 74.59 rpm	4: Catanzaro → Praia a Mare Tuesday, May 10, 200 km 9 km solo	2418 m 41.83 km/h 217.60 W 72.77 rpm
5: La Spezia → Abetone Wednesday, May 13, 152 km 10.7 km solo	3066 m 36.58 km/h 216.86 W 71.95 rpm	5: Praia a Mare → Benevento Wednesday, May 11, 233 km Sprint of a large group	3459 m 41.05 km/h 202.92 W 66.54 rpm

6: Montecatini Terme → Castiglione della Pescaia Thursday, May 14, 183 km Sprint of large group	1625 m 42.28 km/h 205.16 W 72.51 rpm	6: Ponte → Roccaraso Thursday, May 12,157 km 15 km solo	3749 m 33.63 km/h 226.29 W 70.97 rpm
7: Grosseto → Fiuggi Friday, May 15, 264 km Sprint of a large group	2873 m 35.81** km/h 193.73 W 68.79 rpm	7: Sulmona → Foligno Friday, May 13, 211 km Sprint of a large group	2301 m 42.04 km/h 223.20 W 69.85 rpm
8: Fiuggi → Campitello Matese Saturday, May 16, 186 km 3.4 km solo	3842 m 38.28* km/h 241.91 W 75.02 rpm	8: Foligno → Arezzo Saturday, May 14, 186 km 24.6 solo	1985 m 43.92 km/h 255.89 W 79.46 rpm
9: Benevento → San Giorgio del Sannio Sunday, May 17, 215 km 4 km solo	4264 m 38.34 km/h 259.87 W 74.34 rpm	9: Chianti ITT Sunday, May 15, 40.5 km Time trial	561 m 46.96 km/h 353.69 W 86.23 rpm
10: Civitanova Marche → Forlì Tuesday, May 19, 200 km Sprint of a small group	841 m 45.07 km/h 206.70 W 72.81 rpm	10: Campi Bisenzio → Sestola Tuesday, May 17, 219 km 14.5 km solo	4618 m 38.14 km/h 265.26 W 72.31 rpm

11: Forlì → Imola Wednesday, May 20, 153 km 25 km solo	2949 m 39.04 km/h 206.70 W 72.81 rpm	11: Modena → Asolo Wednesday, May 18, 229 km Sprint of a small group	777 m 45.93 km/h 215.85 W 72.12 rpm
12: Imola → Vicenza Thursday, May 21, 190 km Sprint of a large group	1288 m 43.37 km/h 212.21 W 74.98 rpm	12: Noale → Bibione Thursday, May 19, 182 km Sprint of a large group	122 m 42.66 km/h 196.20 W 71.82 rpm
13: Montecchio Maggiore → Jesolo Friday, May 22, 147 km Sprint of a large group	131 m 48.16 km/h 239.48 W 74.80 rpm	13: Palmanova → Cividale del Friuli Friday, May 20, 170 km 33.4 km solo	3669 m 37.53** km/h 272.35 W 71.89 rpm
14: Treviso → Valdobbiadene (ITT) Saturday, May 23, 59.2 km Time trial	593 m 45.77 km/h 295.88 W 82.78 rpm	14: Alpago → Corvara Saturday, May 21, 210 km Sprint of a small group	6001 m 34.4 km/h 253,49 W 70,54 rpm
15: Marostica → Madonna di Campiglio Sunday, May 24, 165 km Sprint of a small group	4634 m 37.70 km/h 325.41 W 81.13 rpm	15: Castelrotto → Alpe di Siusi ITT Sunday, May 22, 10.8 km Time trial	785 m 22.06*** km/h 389.37 W 81.23 rpm
16: Pinzolo → Aprica Tuesday, May 26, 174 km 4 km solo	4951 m 35.07 km/h 257.25 W 73.50 rpm	16: Bressanone → Andalo Tuesday, May 24, 132 km Sprint a deux	2737 m 44.27 km/h 289.97 W 75.64 rpm

17: Tirano → Lugano (CH) Wednesday, May 27, 134 km Sprint of a small group	1857 m 42.80 km/h 211.83 W 73.26 rpm	17: Molveno → Cassano d'Adda Wednesday, May 25, 196 km 0.4 km solo	1567 m 43.32 km/h 206.34 W 67.17 rpm
18: Melide (CH) → Verbania Thursday, May 28, 170 km 19.3 km solo	2195 m 41.76 km/h 212.96 W 74.82 rpm	18: Muggio → Pinerolo Thursday, May 26, 244 km Sprint of a small group	1637 m 44.97 km/h 211.56 W 71.84 rpm
19: Gravellona Toce → Cervinia Friday, May 29, 236 km 6 km solo	5113 m 36.85 km/h 252.22 W 74.32 rpm	19: Pinerolo → Risoul Friday, May 27, 162 km 5.1 km solo	3905 m 37.40 km/h 284.79 W 74.46 rpm
20: Saint Vincent → Sestriere Saturday, May 30, 196 km 1.6 km solo	3355 m 37.64 km/h 230.75 W 72.45 rpm	20: Guillestre → Sant'Anna di Vinadio Saturay, May 28, 134 km 14.1 km solo	4500 m 30.60 km/h 262.98 W 62.45 rpm
21: Torino → Milano Sunday, May 31, 185 km Sprint a deux	142 m 42.92 km/h 172.54 W 72.50 rpm	21: Cuneo → Torino Sunday, May 29, 163 km Sprint of a large group	879 m 42.84 km/h
Team athletes in the top 10 classification	1		2

* Winner was an athlete of the team. ** second place was an athlete of the team. *** third place was an athlete of the team. Source: PRO Cycling stats (https://www.procyclingstats.com/race/giro-d-italia/2015/stage-1/result/result; https://www.procyclingstats.com/race/giro-d-italia/2016/stage-1/result/result).

Cyclists spent more time (% stage time) in Z1, followed by Z2, Z3, Z0, Z4, Z5, Z6, and Z7. The average time spent (s), mean (standard deviation) in Z0, Z1, Z2, Z3, Z4, Z5, Z6, and Z7 were 14.6 (5.8), 26.3 (12.6), 17.3 (6.2), 14.7 (6.4), 13.0 (10.2), 7.3 (6.3), 4.8 (3.0), and 2.1 (1.6) % stage duration, respectively. The most variable zone was Z1, followed by Z4, Z3, Z5, Z2, Z0, Z6, and Z7. The mean (standard deviation) power output (expressed in Watts) in each of the intensity zones for Z0, Z1, Z2, Z3, Z4, Z5, Z6, and Z7 was 122.9 (13.9), 247.5 (17.2), 311.1(21.4), 366.0 (24.9), 421.1 (28.5), 496.5 (33.8), and 658.2 (47.6) Watts, respectively.

The association between mean power and stage time was non-linear modeled [$y = 334.8$ [95%CI 238.7- 430.9] $e^{(-0.0007997\ [95\%CI\ -0.001061 + 0.0005382]\ x)}$ + 306.8 [95%CI 204.2 - 409.5] $e^{(-0.0001052\ [95\%CI\ -0.000163 + 0.00004739]\ x)}$ $R^2 = 0.54$]. The highest intensity zones are related to longer time sustained at higher power output levels in shorter stages. In contrast, as Figure 1A depicts, the lower intensity zones were used to cover stages with longer durations, developing lower average power during the two analyzed editions of the Giro d' Italia.

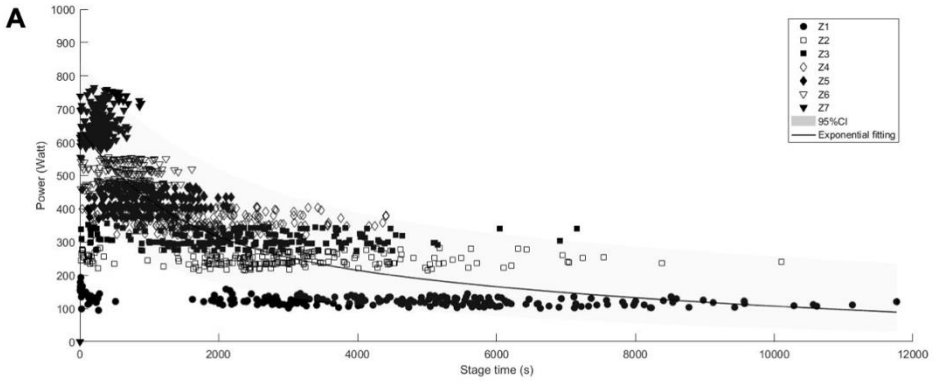
A
Power (Watt)
Stage time (s)
Z1
Z2
Z3
Z4
Z5
Z6
Z7
95%CI
Exponential fitting

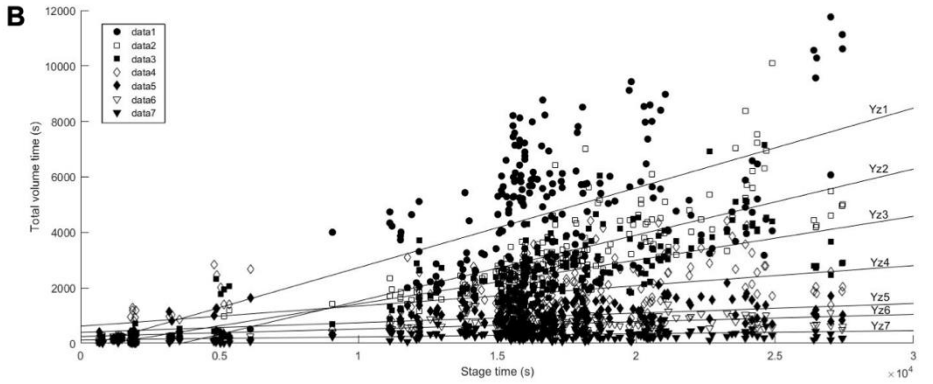
B
Total volume time (s)
Stage time (s)
data1
data2
data3
data4
data5
data6
data7
Yz1
Yz2
Yz3
Yz4
Yz5
Yz6
Yz7

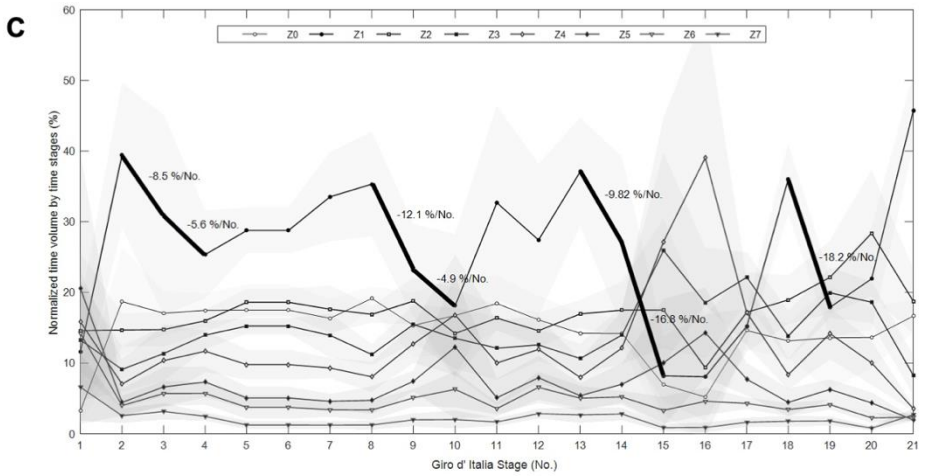
C
Normalized time volume by time stages (%)
Giro d' Italia Stage (No.)
Z0
Z1
Z2
Z3
Z4
Z5
Z6
Z7
-8.5 %/No.
-5.6 %/No.
-12.1 %/No.
-4.9 %/No.
-9.82 %/No.
-16.8 %/No.
-18.2 %/No.

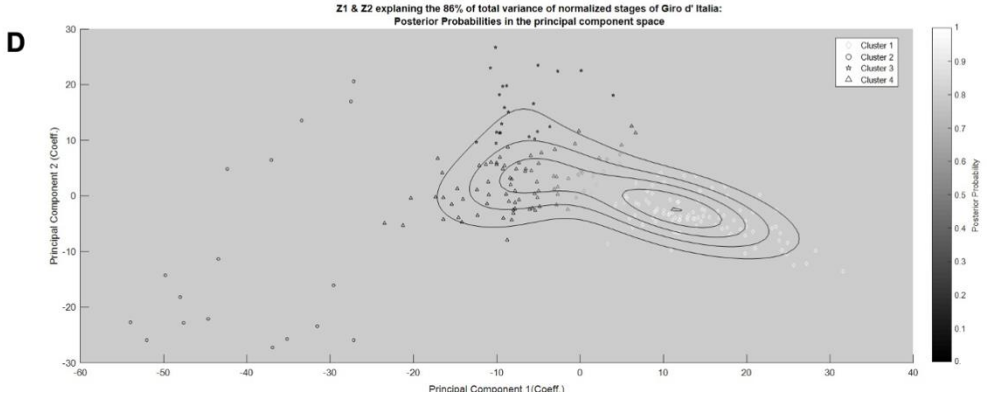
D
Z1 & Z2 explaning the 86% of total variance of normalized stages of Giro d' Italia:
Posterior Probabilities in the principal component space
Principal Component 2 (Coeff.)
Principal Component 1(Coeff.)
Cluster 1
Cluster 2
Cluster 3
Cluster 4
Posterior Probability

Figure 1. A: Power vs stage time for intensity zones entitled Z1 to Z7 during two editions of the Giro d' Italia. The power was measured in Watts and the stage time was measured in seconds. The figure shows the non-linear association between power and time during two editions of the Giro d' Italia. The highest intensity zones were predominant in stages of shorter duration requesting athletes to develop higher average power, while the lower intensity zones were predominant in longer stages requiring lower average power. Note the double distribution of Z1 and Z2 that suggest the lowest race period predominantly involve time in Z1 and Z2 intensity zones. **B:** Total volume time vs stage time for intensity zone Z1 to Z7 during two editions of the Giro d' Italia. The intensity zones are entitled Z1, Z2, Z3, Z4, Z5, Z6, and Z7, and each slope is entitled Yz1, Yz2, Yz3, Yz4, Yz5, Yz6, and Yz7, respectively. The total volume time was measured in seconds, and each stage duration was measured in seconds. **C:** Normalized time volume by time stage during the Giro d' Italia. The intensity zones are entitled Z0, Z1, Z2, Z3, Z4, Z5, Z6, and Z7. The mean and standard deviation are shown with black lines and gray shadows, respectively. The thick lines show the higher decrease of time volume tracked in Z1, the intensity zone with the most dispersion. The rest days occurred between stages 9 and 10, and stages 14 and 15. The first rest day of 2016 edition was not considered. **D:** The posterior probability of cluster pertinence of the main Gaussian cluster (cluster 1) in the principal component space explained 86% of the total data variance. Four clusters were identified in the principal component space from the Akaike information criterion [AIC = $2k - 2\ln(L)$ with k equal to the number of clusters and L equal to the maximum value of the likelihood function for the Gaussian model].

The association between total time volume (time to finish the grand tour) and the time volume for each stage (Figure 1B) showed higher slopes and inclination angles for Z1 [m = 0.29, θ = 16.2º, R^2 = 0.45], followed by Z2 [m = 0.24, θ =13.5º, R^2 = 0.71], Z3 [m = 0.16, θ =9.1º, R^2 = 0.53], Z4 [m = 0.08, θ = 4.6º, R^2 = 0.23], Z5 [m = 0.04, θ =2.3º, R^2 = 0.20], Z6 [m = 0.03, θ =1.7º, R^2 = 0.26], and Z7 [m = 0.01, θ = 0.6º, R^2 = 0.15].

The analysis of mean normalized time spent in the different intensity zones across each of the 21 stages from each year edition (Figure 1C) showed that higher peak declines of normalized volume, measured as the negative slopes,

across stages before the next increment that occurred between stages 2 and 4 [Δ= -8.5 % No.$^{-1}$], 8 and 10 [Δ= -12.2 % No.$^{-1}$], 13 and 15 [Δ= -19.0 % No.$^{-1}$], and 18 and 19 [Δ= -18.2 % No.$^{-1}$] tracked in the zone intensity with the highest dispersion (Z1).

Higher peak slope increment of normalized volume by stage until the next slope decrease after stage 4 [Δ= 4.8 % No.$^{-1}$, between 4 and 8], after stage 10 [Δ= -4.6 % No.$^{-1}$, between 10 and 13], after stage 15 [Δ= 20.8 % No.$^{-1}$, between 15 and 18], and after stage 19 [Δ= 23.8 % No.$^{-1}$, between 19 and 21] tracked in the zone intensity with the highest dispersion (Z1), see Figure 1C.

Negative slopes of Z3, Z4, Z5, and Z6 occurred four times and three times in Z7 before one or two stages before Z1 presented negative slopes (Table 2). In contrast, positive slopes of higher intensity zones (Z3 three times, Z4 four times, Z5 four times, Z6 three times, and Z7 twice during the competition) were observed, accompanied by a negative slope of Z1 (Table 2).

Table 2. Slope changes of normalized mean volume patterns across the *Giro d' Italia.*

	Giro d' Italia Stages																			
	1	2	3	4	5	6	7	8	9	10	11	12	13	14	15	16	17	18	19	20
Z0	1	-1	1	1	0	-1	1	-1	1	1	-1	-1	-1	-1	-1	1	-1	1	1	1
Z1	1	-1	-1^{R}	1	0	1	1	-1	-1^{R}	1	-1	1	-1	-1	-1^{R}	1	1	-1	1	1
Z2	1	1	1	1	0	-1	-1	1	-1	1	-1	1	1	1	-1	1	1	1	1	-1
Z3	-1	1	1	1	0	-1	-1	1	-1	-1	1	-1	1	1	-1	1	-1	1	-1	-1
Z4	-1	1	1	-1	0	-1	-1	1	1	-1	1	-1	1	1	1	-1	-1	1	-1	-1
Z5	-1	1	1	-1	0	-1	1	1	1	-1	1	-1	1	1	1	-1	-1	1	-1	-1
Z6	-1	1	1	-1	0	-1	-1	1	1	-1	1	-1	1	-1	1	-1	-1	1	-1	1
Z7	-1	1	-1	-1	0	-1	1	1	1	-1	1	-1	1	-1	1	1	1	1	-1	1

R = rest stage
-1 = negative slope (volume increase)
1 = positive slope (volume decrease)
Z0 = intensity zone zero
Z1 = intensity zone one
Z2 = intensity zone two
Z3 = intensity zone three
Z4 = intensity zone four
Z5 = intensity zone five

Z6 = intensity zone six
Z7 = intensity zone seven
In black is shown the slope decrease (-1) follow by a slope increase (+1) in Z1.
In light gray is shown the increase slope (+1) pattern of higher Z.
In dark gray is shown the decrease slope (-1) pattern of higher Z before the decrease of Z1 in the next one or two stages.

The principal component analysis showed that time spent in intensity zones Z1, Z2, Z3, Z4, Z5, Z6, and Z7 explained 63.62%, 18.20%, 8.12%, 5.84%, 2.98%, 1.20%, and 0.02% of the total variance in the normalized time by each time stage, respectively. The best number of mixed Gaussian components was four from the Akaike information criterion. The posterior probability of pertinence of the main cluster fitted by mixed Gaussian distributions in the principal component space that explained 86% of the total variance is summarized in Figure 1D.

There was a main effect for clusters and intensity zones in normalized time-volume ($p<0.001$), and there was interaction ($p<0.001$). Clusters one and two differed ($p<0.001$), as well as clusters one and four differed ($p<0.001$). There were differences between all intensities ($p<0.001$, Table 3). There was a main effect for intensity zones in power ($p<0.001$) without interaction ($p>0.05$) or effect for clusters ($p>0.05$). All intensity zones differed ($p<0.001$, Table 3).

Table 3. Volume and power cluster differences.

Normalized volume										
Cluster	Size	Stage	Z0	Z1	Z2	Z3	Z4	Z5	Z6	Z7
	n	mode	Mean (sd)	Mean (sd)	Mean (sd)	Mean (sd)	Mean (sd)	Mean (sd)	Mean (sd)	Mean (sd)
One	17	14	2.8 (3.4)*,ɣ	3.0 (2.6)*,ɣ	5.7 (6.0)*,ɣ	18.1 (15.2)*,ɣ	41.5 (16.8)*,ɣ	22.0 (14.9)*,ɣ	5.8 (4.4)*,ɣ	1.23 (1.4)*,ɣ
Two	122	12	16.6 (4.1)*	35.9 (7.5)*	17.1 (2.7)*	11.6 (3.1)*	8.1 (2.5)*	4.7 (1.7)*	4.0 (1.4)*	2.0(0.9)*
Three	20	16	12.8 (3.8)*	15.2 (3.2)*	28.2 (6.5)*	23.4 (4.8)*	11.6 (2.1)*	4.7 (1.2)*	3.0 (1.1)*	1.4 (0.8)*
Four	69	19	10.8 (6.0)*	14.4 (5.7)*	17.9 (4.0)*	16.6 (4.9)*	17.1 (3.2)*	3.8 (8.9)*	8.9 (2.6)*	6.5 (3.9)*

Power										
Cluster	Size	Stage	Total	Z1	Z2	Z3	Z4	Z5	Z6	Z7
	n	mode		Mean (sd)	Mean (sd)	Mean (sd)	Mean (sd)	Mean (sd)	Mean (sd)	Mean (sd)
One	17	14	2626.3	125.5 (13.5)*	247.5 (19.3)*	310.4 (22.7)*	365.3 (26.1)*	422.2 (30.7)*	499.3 (36.4)*	656.5 (44.1)*
Two	122	12	2628.9	121.8 (11.8)*	247.8 (17.0)*	311.6 (21.2)*	366.9 (24.8)*	422.4 (28.2)*	498.0 (33.9)*	660.0 (48.1)*
Three	20	16	2644.1	129.8 (14.4)*	251.2 (19.5)*	312.6 (23.1)*	366.4 (27.8)*	421.8 (33.0)*	497.1 (40.5)*	665.2 (61.7)*
Four	69	19	2602.3	122.1 (16.7)*	245.5 (16.1)*	309.6 (21.1)*	364.0 (24.4)*	417.8 (27.0)*	492.3 (31.2)*	651.0 (42.0)*

Z0 = intensity zone zero
Z1 = intensity zone one
Z2 = intensity zone two
Z3 = intensity zone three
Z4 = intensity zone four
Z5 = intensity zone five
Z6 = intensity zone six
Z7 = intensity zone seven
** = $p < 0.001$ between all intensity zones*
ɣ = $p < 0.001$ between cluster one and two, and between cluster one and four.

2.6 Discussion

A strong novelty of our study is that the analysis of two grand tour editions allowed the verification of cumulative fatigue during consecutive days of racing at a high level of competition. Importantly, cumulative fatigue has negative effects on performance and can cause overuse muscle injuries (26), the third largest cause of professional athlete absence in Grand Tours (17). Our main findings here were that cyclists i) develop higher mean power during shorter time stages using higher intensity zones and develop lower mean power during longer time stages using lower intensity zones, ii) use lower intensity zones to cover long-time stages while higher intensity zones are used to cover lower-time stages, iii) experienced cumulated fatigue during the competition (there was four recognizable performance decreases indicating fatigue effects) and the second rest day had the best impact on performance increase for subsequent stages, iv) decrease the time-volume of Z3, Z4, Z5, Z6 and Z7 in two or three stages before the performance decrease, which suggests those intensities being predictors, while higher zone intensities suggest compensating the performance decrease, and v) develop almost two different intensity zones distribution (clusters) in the time-volume to complete the competition without power generation differences.

Our findings have applicability in sports because high mileage cycling events such as Giro d'Italia, Vuelta a España, and Tour de France have similar energy expenditure and intensity development (18). We consider our findings can help both specific race strategies during the Giro d'Italia and planning training. The grand tours involve several consecutive days of high-level physical effort (19). Thus, adequate training planning should consider not only experimental laboratory knowledge but also in-field race characteristics and performance

analysis because not always the in-field conditions are possible to reproduce fully in laboratory testing (20).

Along the two editions of the Giro, we found how the stage distances determine the distribution of effort zones. Accordingly, longer stages use mainly lower intensities that represent low-intensity exercise below the first lactate or ventilatory threshold (21). Lower intensity zones showed how relevant they were to be completing the stages. Even shorter stages have shown activity in lower zone intensities (double distribution for Z1 to Z3) in coherence with the maximum efforts cannot be sustained for the entire stage because fatigue will limit performance (high-intensity exercise over the lactate or ventilatory threshold (22)), either by peripheral or central pathways (23,24). Thus, higher intensities are chosen for shorter time stages during the Giro d' Italia in accordance that each stage's intensity is modulated by total race duration in elite cycling (25).

Therefore, it is crucial to make an appropriate choice of the mechanical power provided by cyclists (mechanical power being defined by: the aerodynamic friction, the ascending term, and the accelerating term) in each stage of the competition to increase the cyclist's performance (26). Hence, the adequate use of intensity zones during the competition directly impacts the cycling dynamics. This choice suggests helping prevent fatigue episodes and increased fatigue intensity (lower cumulated fatigue) when the mechanical power is opportunely delivered. Likely, intensified training strategies may favor power production that will improve critical moments of the tour (27) complemented with aerobic exercise intensity (28), and might explain why shorter stages seem to be decisive for cyclist performance in the race (1).

Regarding cumulative fatigue, there were four recognizable performance decreases (negative slopes during the time-volume across the stages). The negative slopes tracked in the most variable intensity zone, which explained the main variance of the total data studied by principal component analysis (29), could be interpreted as the incapacity to sustain a stable peripheral effort in low-intensity zones. The main cause of performance losses in repetitive tasks is caused by cumulative fatigue (6). The high correlation between blood lactate transition thresholds and endurance performance, and the aerobic and anaerobic indices of cycling performance (30) support our effort to track the decrease in cycling performance in the time course of the competition. However, It is also possible that performance decreases allow athletes to save energy, especially for the final moments of a race, when habitually the classification tends to be decided (31).

In our exploration, three of four slope decreases fitted with the given rest stages (stage 3 in 2016, stage 9 in 2015 and 2016, and stage 15 in 2015 and 2016), showing an immediate reversion after the rest day. This influence of the rest day suggests the ability to choose to stay longer at higher intensity zones (except for the opening stage). Therefore, we argue that the variation in the distribution of intensities over time can describe the process of accumulated fatigue installation and the effect of rest days on time at different intensity zones. In addition, we also observed a decrease in time-volume in Z3, Z4, Z5, Z6, and Z7 in two or three stages before the drop in performance. These factors need to be further studied to be discussed as possible performance predictors. In the same way, time-volume at higher zone intensities increased when the

performance drops, which seems to be a compensation strategy during the competition.

Finally, there were almost two intensity zone pattern distributions in the time volume to complete the competition without differences in the power delivery. The main percentual differences were in Z1, Z4, and Z5, where one cluster completed the competition with a lower time in Z1 but stayed more time in Z4 and Z5. Zone intensities 4 and 5 permitted production of more than 320 W and lower than 450 W. It suggests a strategy that favors the use of intensity zones that can deliver satisfactory values of power. This kind of pattern may risk more cumulative fatigue if the athletes do not have enough preparation or induce more muscle damage, oxidative stress, and inflammation events during the competition. Therefore, the surveillance of how the time-volume in different intensity zones is used, the athlete's characteristics, the race conditions, and the athlete's interaction with these conditions are crucial to define adequate planning training and evaluate if the athletes are under risk cumulative fatigue conditions during the race, decreasing the athlete’s and team performance.

Our study has limitations. The first one is the fact that our participants are all men, and we know that the behavior of women for these same tests is different (32). Therefore, the extrapolation of these results to female athletes is not possible. In addition, we know that different athletes perform specific tasks within the strategy of a team in the competition and that this specialization generates differences in performance in the tests for each athlete (33). Finally, we also recognize that a real-world condition for data collection is subject to confounding factors that rely on the variables mentioned, but also the motivation of the athletes, soreness, effort perception, and individual goals. Despite these

limitations, we consider that the uniqueness of our exploratory analysis ensures sufficient novelty and relevance to our study.

2.7 References

1. Muriel X, Valenzuela PL, Mateo-March M, Pallarés JG, Lucia A, Barranco-Gil D. Physical Demands and Performance Indicators in Male Professional Cyclists During a Grand Tour: WorldTour Versus ProTeam Category. Int J Sports Physiol Perform. 2022 Jan 1;17(1):22–30.
2. Padilla S, Mujika I, Orbañanos J, Santisteban J, Angulo F, José Goiriena J. Exercise intensity and load during mass-start stage races in professional road cycling. Med Sci Sports Exerc. 2001 May;33(5):796–802.
3. Enoka RM, Duchateau J. Muscle fatigue: what, why and how it influences muscle function. J Physiol. 2007/08/19 ed. 2008 Jan 1;586(1):11–23.
4. Proske U, Morgan DL. Muscle damage from eccentric exercise: mechanism, mechanical signs, adaptation and clinical applications. J Physiol. 2001 Dec 1;537(Pt 2):333–45.
5. Owens DJ, Twist C, Cobley JN, Howatson G, Close GL. Exercise-induced muscle damage: What is it, what causes it and what are the nutritional solutions? Eur J Sport Sci. 2019 Jan 2;19(1):71–85.
6. Machado AS, da Silva W, Souza MA, Carpes FP. Green Tea Extract Preserves Neuromuscular Activation and Muscle Damage Markers in Athletes Under Cumulative Fatigue. Front Physiol. 2018/09/04 ed. 2018;9(1):9.
7. Marshall PW, Melville GW, Cross R, Marquez J, Harrison I, Enoka RM. Fatigue, pain, and the recovery of neuromuscular function after

consecutive days of full-body resistance exercise in trained men. Eur J Appl Physiol. 2021 Nov;121(11):3103–16.

8. Rodríguez-Marroyo JA, Villa JG, Pernía R, Foster C. Decrement in Professional Cyclists' Performance After a Grand Tour. Int J Sports Physiol Perform. 2017 Nov 1;12(10):1348–55.

9. Stewart RD, Duhamel TA, Rich S, Tupling AR, Green HJ. Effects of Consecutive Days of Exercise and Recovery on Muscle Mechanical Function. Med Sci Sports Exerc. 2008 Feb;40(2):316–25.

10. Lastella M, Roach GD, Halson SL, Martin DT, West NP, Sargent C. The impact of a simulated grand tour on sleep, mood, and well-being of competitive cyclists. J Sports Med Phys Fitness. 2015 Dec;55(12):1555–64.

11. Vogt S, Heinrich L, Schumacher YO, Blum A, Roecker K, Dickhuth HH, et al. Power output during stage racing in professional road cycling. Med Sci Sports Exerc. 2006 Jan;38(1):147–51.

12. Allen H, Coggan AR, McGregor S. Training and racing with a power meter. VeloPress; 2019.

13. Javaloyes A, Mateo-March M, Carpes FP, Moya-Ramon M, Lopez-Grueso R, Zabala M. Bilateral asymmetries in professional cyclists during a Grand Tour. Isokinet Exerc Sci. 2021;29(4):455–61.

14. Saris WHM, van Erp-Baart MA, Brouns F, Westerterp KR, Hoor F ten. Study on Food Intake and Energy Expenditure During Extreme Sustained Exercise: The Tour de France. Int J Sports Med. 2008 Mar 14;10(S 1):S26–31.

15. Maier T, Schmid L, Müller B, Steiner T, Wehrlin J. Accuracy of Cycling Power Meters against a Mathematical Model of Treadmill Cycling. Int J Sports Med. 2017 Jun;38(06):456–61.

16. Borszcz FK, Tramontin AF, Bossi AH, Carminatti LJ, Costa VP. Functional Threshold Power in Cyclists: Validity of the Concept and Physiological Responses. Int J Sports Med. 2018 Oct;39(10):737–42.

17. Haeberle HS, Navarro SM, Power EJ, Schickendantz MS, Farrow LD, Ramkumar PN. Prevalence and Epidemiology of Injuries Among Elite Cyclists in the Tour de France. Orthop J Sports Med. 2018 Sep;6(9):232596711879339.

18. Van Erp T, Hoozemans M, Foster C, De Koning JJ. Case Report: Load, Intensity, and Performance Characteristics in Multiple Grand Tours. Med Sci Sports Exerc. 2020 Apr;52(4):868–75.

19. El Helou N, Berthelot G, Thibault V, Tafflet M, Nassif H, Campion F, et al. Tour de France, Giro, Vuelta, and classic European races show a unique progression of road cycling speed in the last 20 years. J Sports Sci. 2010 May;28(7):789–96.

20. Abbiss CR, Menaspà P, Villerius V, Martin DT. Distribution of Power Output When Establishing a Breakaway in Cycling. Int J Sports Physiol Perform. 2013 Jul;8(4):452–5.

21. Cerezuela-Espejo V, Courel-Ibáñez J, Morán-Navarro R, Martínez-Cava A, Pallarés JG. The Relationship Between Lactate and Ventilatory Thresholds in Runners: Validity and Reliability of Exercise Test Performance Parameters. Front Physiol. 2018 Sep 25;9:1320.

22. Farrell PA, Wilmore JH, Coyle EF, Billing JE, Costill DL. Plasma lactate accumulation and distance running performance. Med Sci Sports. 1979;11(4):338–44.

23. Marcora SM, Staiano W. The limit to exercise tolerance in humans: mind over muscle? Eur J Appl Physiol. 2010 Jul;109(4):763–70.

24. Secher NH, Seifert T, Van Lieshout JJ. Cerebral blood flow and metabolism during exercise: implications for fatigue. J Appl Physiol. 2008 Jan;104(1):306–14.

25. Rodriguez-Marroyo JA, Garcia-Lopez J, Juneau CE, Villa JG. Workload demands in professional multi-stage cycling races of varying duration. Br J Sports Med. 2009 Mar 1;43(3):180–5.

26. Cohen C, Brunet E, Roy J, Clanet C. Physics of road cycling and the three jerseys problem. J Fluid Mech. 2021 May 10;914:A38.

27. Valenzuela PL, Gil-Cabrera J, Talavera E, Alejo LB, Montalvo-Pérez A, Rincón-Castanedo C, et al. On- Versus Off-Bike Power Training in Professional Cyclists: A Randomized Controlled Trial. Int J Sports Physiol Perform. 2021 May 1;16(5):674–81.

28. Jones TW, Eddens L, Kupusarevic J, Simoes DCM, Furber MJW, van Someren KA, et al. Aerobic exercise intensity does not affect the anabolic signaling following resistance exercise in endurance athletes. Sci Rep. 2021 Dec;11(1):10785.

29. Jolliffe IT, Cadima J. Principal component analysis: a review and recent developments. Philos Transact A Math Phys Eng Sci. 2016 Apr 13;374(2065):20150202.

30. Craig NP, Norton KI, Bourdon PC, Woolford SM, Stanef T, Squires B, et al. Aerobic and anaerobic indices contributing to track endurance cycling performance. Eur J Appl Physiol. 1993;67(2):150–8.

31. Swart J, Lamberts RP, Lambert MI, Lambert EV, Woolrich RW, Johnston S, et al. Exercising with reserve: exercise regulation by perceived exertion in relation to duration of exercise and knowledge of endpoint. Br J Sports Med. 2009 Sep 15;43(10):775–81.

32. Sanders D, van Erp T, de Koning JJ. Intensity and Load Characteristics of Professional Road Cycling: Differences Between Men's and Women's Races. Int J Sports Physiol Perform. 2019 Mar 1;14(3):296–302.

33. Gandia Soriano A, Carpes FP, Rodríguez Fernández A, Priego-Quesada JI. Effect of cycling specialization on effort and physiological responses to uphill and flat cycling at similar intensity. Eur J Sport Sci. 2021 Jun;21(6):854–60.

CAPITULO III

ARTIGO ORIGINAL

Distance and camera feature measurements affect the detection of temperature asymmetries using infrared thermography

Álvaro S. Machado[1]; Mar Cañada-Soriano[2], Irene Jimenez-Perez[3,4]; Marina Gil-Calvo[3,5]; Felipe Pivetta Carpes[1]; Pedro Perez-Soriano[3]; Jose Ignacio Priego-Quesada[3,4*]

[1] Applied Neuromechanics Group, Laboratory of Neuromechanics, Federal University of Pampa, Uruguaiana, Brazil.

[2] Applied Thermodynamics Department (DTRA), Universitat Politècnica de València, Valencia, Spain

[3] Research Group in Sports Biomechanics (GIBD), Department of Physical Education and Sports, University of Valencia, Valencia, Spain.

[4] Research Group in Medical Physics (GIFIME), Department of Physiology, University of Valencia, Valencia, Spain.

[5] Faculty of health and sport sciences, Department of physiatry and nursing, University of Zaragoza, Huesca, Spain.

3.1 Abstract

Small skin temperature asymmetries are claimed to indicate injuries, but the influence of measurement conditions and technical aspects of image acquisition are concerns for determining temperature asymmetries. This research determines whether distance and camera specifications affect thermal asymmetries detection. We simulated thermal asymmetries filling two glasses with water at different temperatures measured at two distances (0.7 and 1.5 m) using four different infrared cameras (T1020, E60BX, C2 and FLIR ONE). Linear regression verified the similarity between each camera and the T1020 camera (gold standard). The intraclass correlation coefficient assessed inter-camera reproducibility. Linear regression reported increasing adjustment using mean temperature, with lower values at 1.5 m between the T1020 and FLIR ONE (0.7 m, r= 0.58; 1.5 m, r= 0.34), C2 (0.7 m, r= 0.90; 1.5 m, r= 0.62) and E60BX (0.7 m, r= 0.96; 1.5 m, r= 0.68). Higher inter-camera reproducibility was observed at 0.7 m than 1.5 m. It is preferable to take thermal images with shorter distances and to prioritise cameras with superior hardware characteristics. The portability of FLIR ONE and C2 may be an advantage in studies investigating expected differences greater than 0.05 ºC and larger regions of interest.

Keywords: diagnostic imaging; injury; medicine; thermal asymmetries; thermal imaging; thermal sensitivity.

3.2 Introduction

Skin temperature symmetry is usually defined as the degree of similarity between the mean skin temperature of two Regions of Interest (ROIs) mirrored across the human body's longitudinal axis (1). Symmetrical skin temperature between human body sides is considered when absolute differences are lower than 0.5-0.7°C (1,2). Previous studies argued that asymmetries higher than 0.5-0.7°C could indicate physiological dysfunction related to pathologies and injuries. (3–5). When asymmetries are detected, a higher skin temperature of one body side would relate to inflammation or higher vascularity, and a lower skin temperature is associated with nerve dysfunction or lower vascularity (3,6). For this reason, and because the analysis of asymmetries has good reliability and reproducibility (7), some studies suggest screening skin temperature symmetries as a strategy for the diagnosis and prevention of injuries (8,9).

Skin temperature can be determined using infrared thermography (IRT), a technique used in medical sciences since the 1960s (10). IRT has the advantage of being contactless and non-invasive (6), which made the tool of special interest in medicine, being a safe and easy to conduct measure for when carrying out follow-ups or screenings since it does not have any perjury on patients. The growing interest in applying IRT in the medical areas is benefited by the availability of reasonably affordable cameras, but with recognized low resolution (11). It results that the camera focal plane array size (FPA) can influence the detection of temperature asymmetries, since low FPA and/or high instantaneous field of view (IFOV) might not identify the small magnitudes of change in skin temperature associated with an skin temperature asymmetry (12). On the other hand, the concerns about camera quality and its impact on the field

measurements is growing, motivating development of methods to improve camera resolution (13).

Another aspect of using IRT to determine thermal asymmetries is that camera FPA can affect the definition of the size of the regions of interest (ROI) from where temperature data are extracted, and therefore influence the detection of skin temperature asymmetries. ROI dimensions are limited by the distance between the measuring site and the camera (14). Although 25 pixels is recommended as the minimum size for properly defining a ROI (15), a larger ROI is always preferable (14,16). Furthermore, when analyzing asymmetries, the ROI from both body sides needs to be recorded within the same image, highlighting the role of camera FPA. However, when it comes to use in the clinical field, it is frequently important to measure the highest number of participants as fast as possible and therefore, higher distances between the camera and participants are performed (4) resulting in smaller ROIs, with few pixels than the recommended. From this point of view, the relationship between camera's hardware characteristics, ROI dimensions, and distance for image capture could influence estimation of skin temperature asymmetries.

The objective of this study was to determine whether distance and camera specifications affect the detection of thermal asymmetries. It has been hypothesized that at a larger distance, cameras with a lower FPA and a high IFOV could present a lower capacity to detect thermal asymmetries.

3.3 Methods

In this study, we compared four different IRT camera models from FLIR (FLIR, Wilsonville, Oregon, USA): T1020, E60BX, C2, and One Pro LT (FLIR

ONE). All cameras work in the long-wave wavelength range (7-14μm) and their hardware characteristics are described in table 1. The correct calibration of the cameras was verified before the experiment started using a black body (BX-500 IR Infrared Calibrator, CEM, Shenzhen, China) (17).

Table 1. Hardware characteristics from the four thermographic cameras used in this study.

	T1020	E60BX	C2	FLIR ONE
Spectral range	7.5 – 14.0 μm	7.5 – 13 μm	7.5 – 14 μm	8 – 14 μm
FPA (Focal plane array)	1024 x 768	320 x 240	80 x 60	80 x 60
FOV (Field of view)	28° x 21°	25° × 19°	41° × 31°	50° x 38°
IFOV (Instantaneous field of view)	0.47 mrad	1.36 mrad	11 mrad	12 mrad
NETD*	< 20 mK	45 mK	100 mK	150 mK
Temperature range	-40°C to 150°C	–20°C to 120°C	–10°C to 150°C	-20°C to 120°C
Measurement uncertainty	± 2°C	± 2°C	± 2°C	± 5°C

*At 30°C. NETD: Noise Equivalent Temperature Difference.

Measurements were performed in a specialized laboratory for IRT measurements, in a space where environmental conditions were controlled (e.g. without light and airflow, with the room temperature controlled, and no person apart from the investigator in the measurement environment) (18). IRT measurements were obtained from water samples placed in two 115 x 65 mm glass crystallizers (Kavalierglass, Prague, Czech Republic) positioned at 0.7 m

and 1.5 m far from the cameras. To produce temperature asymmetries, one of the glasses (G1) was filled with water (350 ml) and then heated to 40°C using a heater (Agimatic-E, JP Selecta, Barcelona, Spain). Immediately after reaching the target temperature, half of the water was poured into a second empty glass (G2), and both were placed on the ground, with 5 cm of distance in between, and in front of a black cloth to avoid the radiation reflection (3). Moreover, reflected temperature was measured according to the standard method ISO 18434-1:2008 and recorded in the camera settings. Because of the different transient temperature response from each glass, temperature asymmetries between them would be obtained as a result. Figure 1 illustrates the water temperature manipulation. To determine the temperature asymmetries, infrared images from all cameras were taken simultaneously obtaining the upper view of the glasses. For each of the cameras, images were recorded every 30 s during 15 minutes. There were 5 sets of images obtained, with a 30-minute waiting period in between. For each set of photos, the process of heating the water and preparing the glasses was repeated. At first, the entire water heating and image-taking protocol was performed for the lowest height. Subsequently, the protocol was repeated for all data from the highest height. Regions of interest contained the water, in a upper view, and not included the glass region.

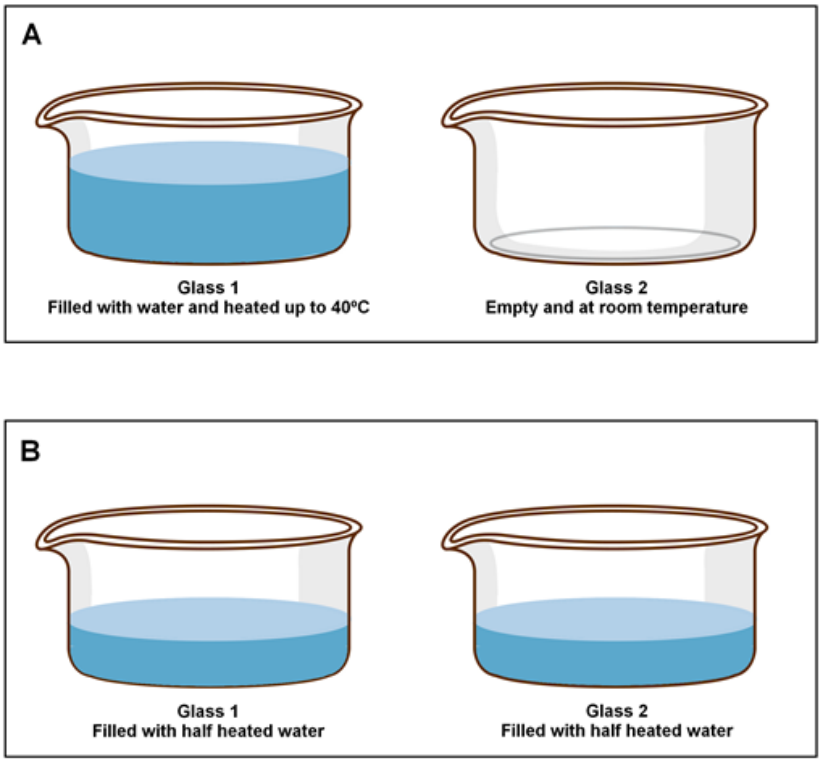

Figure 1. Firstly (A), the glass 1 was filled with water to be heated to 40°C, while the glass 2 remained empty at room temperature. Secondly (B), glass 2 was half filled with heated water. Infrared thermography images were taken for situation B.

All cameras were switched on for at least 10 minutes before acquiring the infrared images for electronic stabilization (18). Cameras T1020 and E60BX were mounted on tripods and programmed to acquire automatically images every 30 seconds for 15 minutes. On the other hand, cameras C2 and FLIR ONE were positioned and triggered manually, at the same distance from the glasses and following both the same time span between images and the 15 minutes recording period. Additionally, when C2 and FLIR ONE cameras were used, the image acquisition order was randomized for each trial.

The threshold defined to indicate temperature asymmetry was set at 0.5 °C, in agreement with previous studies addressing as this topic in medical studies

threshold is usually considered in medicine for skin temperature (1,2). The values obtained by each T1020 camera's thermogram were used as a reference to define the existence of asymmetries for each time point (since the asymmetry would have a variable behavior over time) by simple subtraction of temperature between both glasses of water. The presence of false positives and/or negatives were verified, which means T1020 showing values lower than 0.5 °C, whereas values greater than 0.5 °C were obtained from any of the remaining cameras, and/or T1020 showing values greater than 0.5 °C, whereas lower values were obtained from any of the remaining cameras, respectively.

Infrared images were analyzed using a commercial thermography software (Thermacam Researcher Pro 2.10 software, FLIR, Wilsonville, USA). ROIs were defined as the total visible area of the water for each sample, excluding the glass itself, and mean and maximum temperature data were extracted. ROIs size of each camera at the distance of 0.7 m was: 88516 ± 1184 pixels for T1020, 8130 ± 171 for E60BX, 212 ± 20 for C2, and 8012 ± 798 for FLIR ONE. ROIs size at the distance of 1.5 m was: 16215 ± 254 pixels for T1020, 1976 ± 85 for E60BX, 37 ± 0 for C2, and 1511 ± 81 for FLIR ONE. On all cameras, emissivity was fixed at 0.97 for water surface temperatures (19,20). Figure 2 shows the arrangement of the data collection setup and the determination of ROI in the thermogram processing.

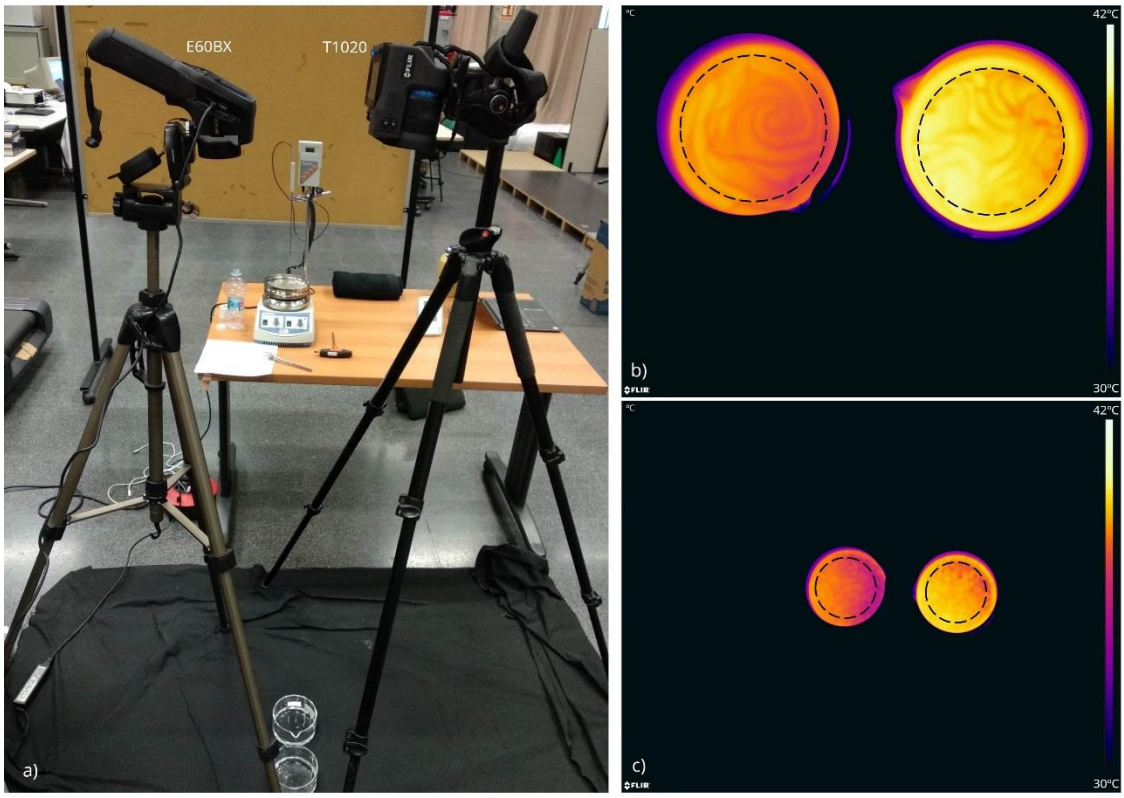

Figure 2. a) Experimental setup and thermal images performed with T1020 showing the ROIs (dashed lines) within the water in both glasses at b) 0.7 m and c) 1.5m.

Statistical analysis was performed using the software RStudio (version 1.2.5033). Linear regression analysis was performed to analyze the adjustment between T1020 and each camera for asymmetry calculation using mean and maximum temperature at the two distances. r-values, adjusted R^2, p-values, and equations of the adjustment were provided. Normal distribution of the residuals of the regressions models was verified ($p>0.05$) using the Kolmogorov-Smirnov test with Lilliefors correction. Bland-Altman plots were created to assess the agreement between T1020 and each of the other cameras, and to obtain the bias with 95% limits of agreement. Finally, the intraclass correlation coefficient was obtained to assess inter-camera reproducibility, based on a single rater-measurement, absolute-agreement, and 2-way random-effects model, between

the T1020 and each of the other cameras for asymmetry calculation using mean and maximum temperature at the two distances. Intraclass correlation coefficients were classified from 1.00 to 0.81 as excellent reproducibility, 0.80 to 0.61 as very good reproducibility, 0.60 to 0.41 as good reproducibility, 0.40 to 0.21 as reasonable reproducibility, and 0.20 to 0.00 as poor reproducibility (21).

3.4 Results

Table 2 shows the percentage of false positives and negatives obtained for each camera. Percentages were higher for 1.5 m distances than for 0.7 m for all cameras. FLIR ONE presented the highest percentages of false negative using mean and maximum water temperature, and for both distances (>20%). At 1.5 m, C2 presented the highest percentages of false positives for mean and maximum water temperature (>15%).

Linear regression analysis (Figure 3) reported increasing adjustment using mean temperature, with lower values at the 1.5 m, between the T1020 and FLIR ONE (distance 0.7 m, r= 0.58; distance 1.5 m r= 0.34), C2 (distance 0.7 m, r= 0.90; distance 1.5 m, r= 0.62), and E60BX (distance 0.7 m, r= 0.96; distance 1.5 m, r= 0.68). Similar results were observed using maximum temperature

Table 2. Percentage of false positives and negatives observed for mean and maximum temperatures for each camera and distance in comparison to the T1020 camera.

	Distance = 0.7 m			**Distance = 1.5 m**		
	E60BX	C2	FLIR ONE	E60BX	C2	FLIR ONE
			Mean temperature			
False Positive	0	4.4	0	14.7	21.6	7.8
False Negative	8.2	3.4	23.2	11.9	7.9	20.0
			Maximum temperature			
False Positive	0	0.6	1.7	12.6	15.8	4.3
False Negative	9.8	2.8	26.0	9.8	9.4	26.2

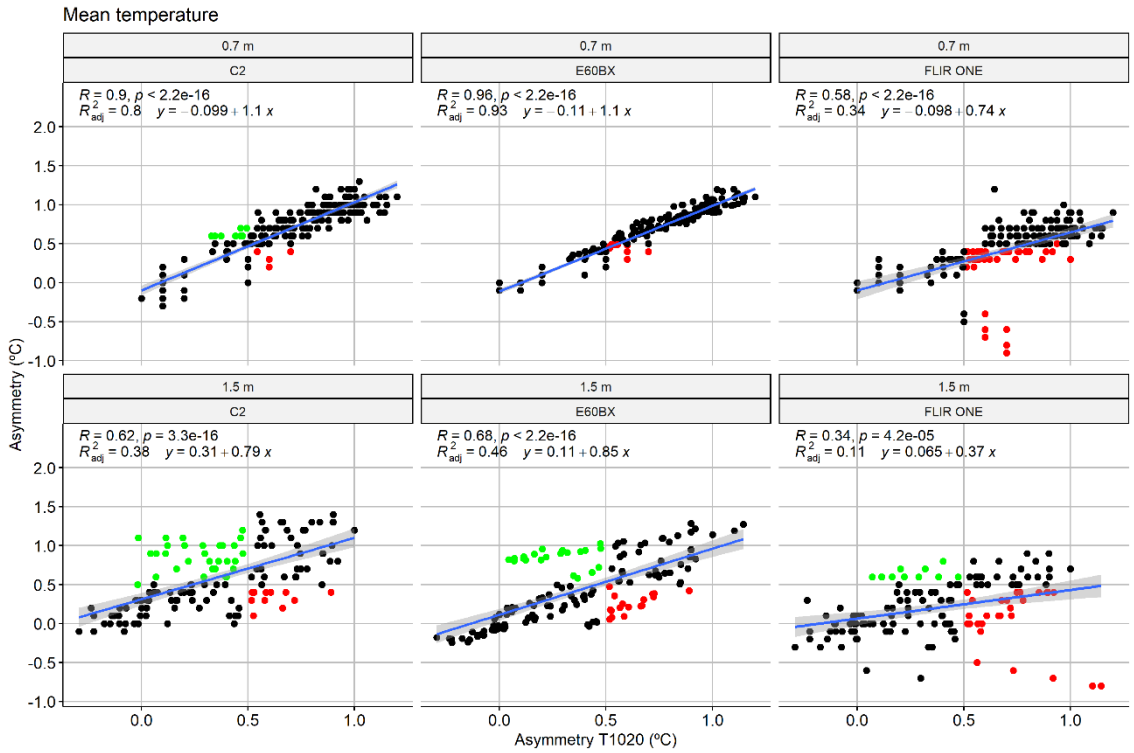

Figure 3. Linear regression analyses for the temperature asymmetry obtained at two camera distances (0.7 m and 1.5 m). False positives (green points) and negatives (red points).

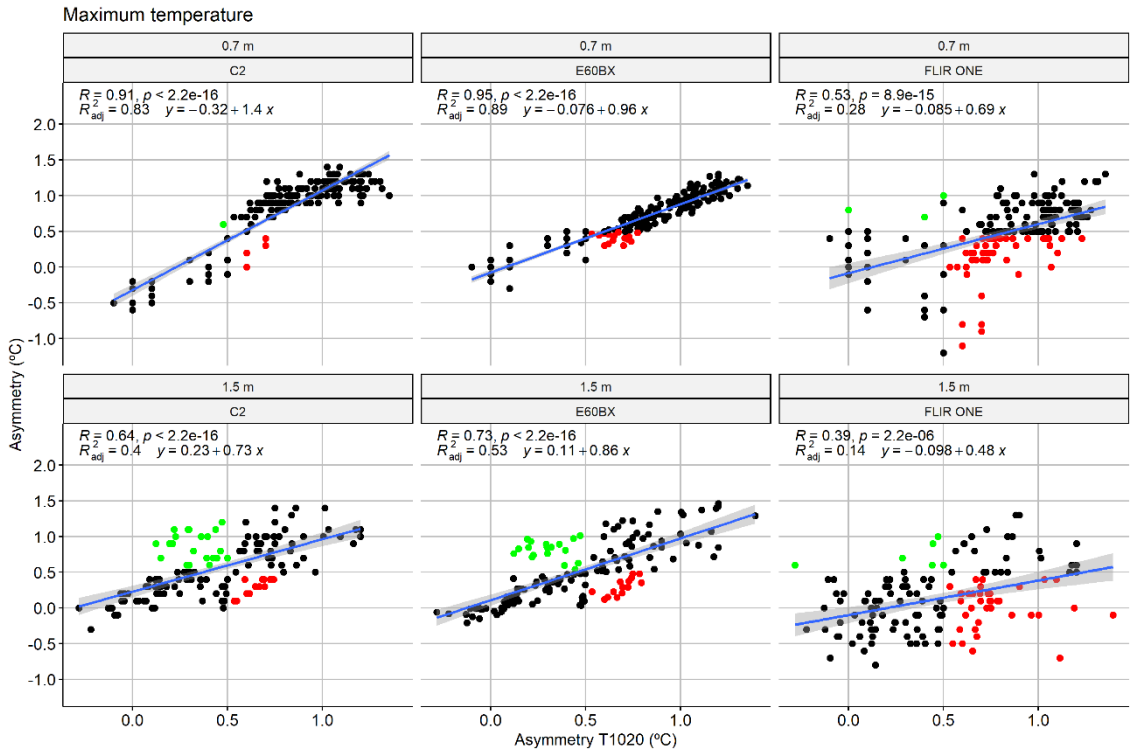

Figure 4. Linear regression analyses for the maximum temperature asymmetry obtained at two camera distances (0.7 m and 1.5 m). False positives (green points) and negatives (red points).

Bland Altman plots revealed increasing bias using mean temperature between the T1020 and E60BX, C2, and FLIR ONE at a distance of 0.7 m (Figure 5; bias: E60BX: 0.0 ±0.1 vs. C2: 0.0 ± 0.2 vs. FLIR ONE: 0.3 ± 0.3 °C). Higher biases were observed in distance of 1.5 m (bias: E60BX: -0.1 ± 0.3 vs. C2: -0.2 ± 0.3 vs. FLIR ONE: 0.2 ± 0.4 °C). Similar results were observed for maximum temperature (Figure 6; distance 0.7 m bias: E60BX: 0.1 ± 0.1 vs. C2: 0.0 ± 0.3 vs. FLIR ONE: 0.3 ± 0.4 °C; distance 1.5 m bias: E60BX: 0.0 ± 0.3 vs. C2: -0.1 ± 0.3 vs. FLIR ONE: 0.3 ± 0.4 °C).

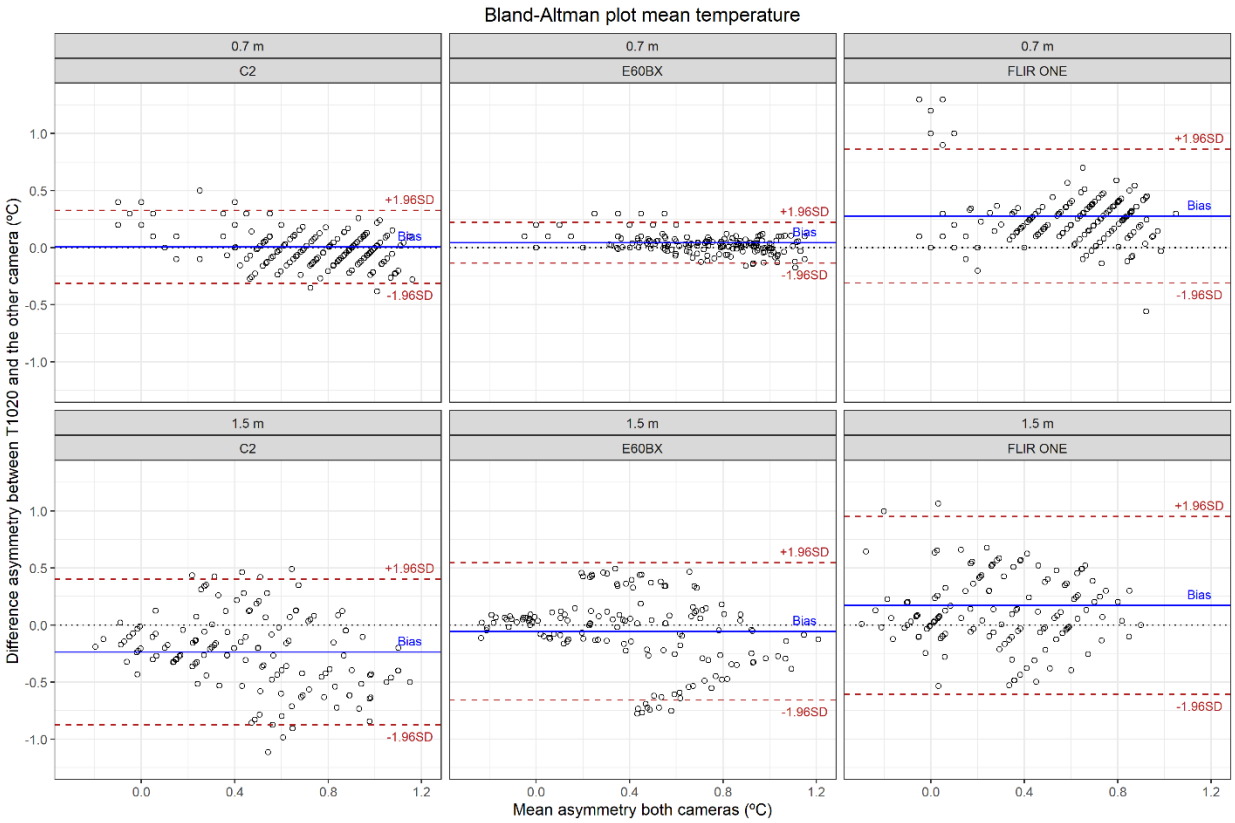

Figure 5. Difference of temperature asymmetry for the two distances (0.7 m and 1.5 m). Bland–Altman plots with 95% limits.

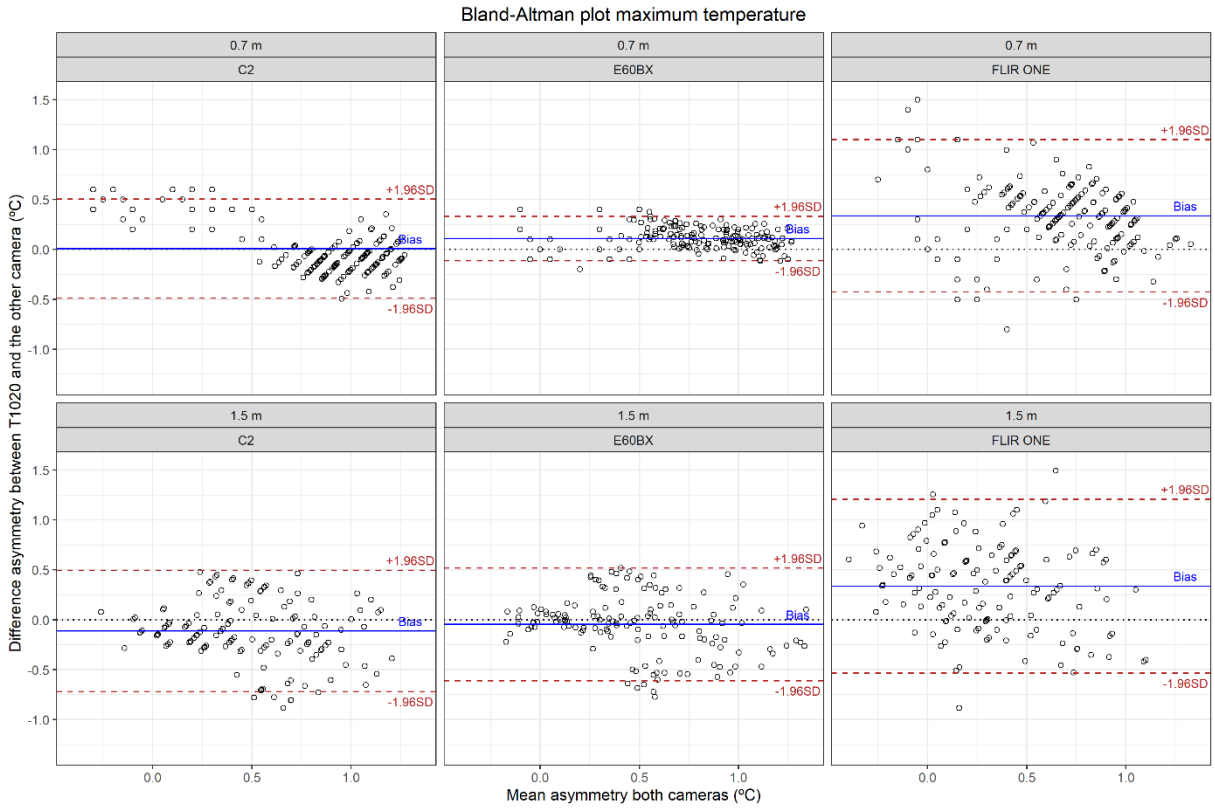

Figure 6. Difference of maximum temperature asymmetry for the two distances (0.7 m and 1.5 m). Bland–Altman plots with 95% limits.

Inter-camera reproducibility (Table 3) at a distance of 0.7 m was excellent for E60BX and C2 cameras, and moderately reasonable and good for FLIR ONE. At 1.5 m, the inter-camera reproducibility was very good for E60BX, moderately good and very good for C2, and reasonable for FLIR ONE.

Table 3. Intraclass correlation coefficients of inter-camera reproducibility between T1020 and the other three cameras for asymmetry calculation at two distances (0.7 m and 1.5 m).

	Distance = 0.7 m			**Distance = 1.5 m**		
	E60BX	C2	FLIR ONE	E60BX	C2	FLIR ONE
Mean	0.95 [0.90, 0.97]	0.87 [0.83, 0.90]	0.42 [0.01, 0.65]	0.66 [0.56, 0.74]	0.50 [0.16, 0.70]	0.30 [0.13, 0.45]
Maximum	0.90 [0.52, 0.96]	0.84 [0.79, 0.88]	0.38 [0.03, 0.61]	0.72 [0.63, 0.79]	0.60 [0.46, 0.71]	0.28 [0.02, 0.48]

3.5 Discussion

This study aimed to determine whether temperature asymmetry determination is affected by characteristics of four different thermographic cameras recording IRT images at two different distances from the region of interest. We set up an experiment considering measurements of water samples with temperature being manipulated to induce asymmetries of 0.5°C or higher, a reference often assumed as the cut-off point to discuss the relevance of temperature asymmetries (1,2,22). It was found that cameras of lower hardware characteristics (C2 and FLIR ONE) are more likely to present higher error rates. In addition, the closer distance between the camera and the region of interest was a determining factor for the results' accuracy.

FPA influences the infrared camera performance (23). Considering T1020 as the reference camera, due to its FPA of 1020 x 768 pixels, E60BX camera (320 x 240 pixels) provided results, with a higher level of correlation with the reference camera (T1020). In the opposite direction, the other cameras (C2 and FLIR ONE), both with FPA of 80 x 60 pixels, showed higher false positives and negatives, a lower correlation index, and a greater bias for both maximum and mean temperatures, especially for the 1.5 m distance. FPA influences the ability to detail an image, especially at larger distances, and the FPA difference between cameras can determine a difference in temperature outcomes (11,12). It also affects the ROI delimitation. In our study, even though the images were circles with a relatively low level of demand to subjectively define de ROIs edges by the evaluator, images taken at 1.5 m still generated highly discrepant results in lower FPA cameras, which is in agreement with a previous study (18).

The distance between the camera and the region of interest may affect the accuracy of thermographic measurements. The measurements performed at 1.5 m generated higher levels of both false positives and negatives, including E60BX camera, which has better performance parameters. In a previous study, differences of up to 0.2 °C were found when thermographic measurements were conduct at 0.2 m and 2.5 m far from region of interest (25). In this study, where we used artificial samples and, therefore, free of intervening factors typical of experiments with humans (such as thermoregulation, sex, menstrual period, food, smoking, etc.), we further advance on the concept that even small variations in distance measurement can have an impact on the temperature outcomes, and invalidate discussions about asymmetries that show small magnitudes. Lower FPA cameras register images with less precision. It is important to be sure about

the minimum region of interest dimension, which can be obtained by multiplying the camera’s IFOV by the distance.

Bland Altman's graphics visually present that it is preferable to take pictures from shorter distances, and that the bias and scattering of results is overstated for the FLIR ONE camera, suggesting the possibility that data from this camera may result in misleading information. It is important to emphasize the effect of the distance between the camera and the region of interest on the results of IRT images, since there is a need to cover both legs within the image in some experiments, which end up leading to measurements at distances larger than 1.5 m between the camera and the region of interest (26,27).

FPA influences asymmetry determination, but it is important to note that even cameras with similar FPA may provide different results. The Noise Equivalent Temperature Difference (NETD), which quantifies the thermal sensitivity of the camera and also refers to the ability of the system to detect small temperature differences within the image, can be a source of differences between cameras with similar FPA. As lower is the NETD value, lower is the noise, and the smaller is the temperature differences that can be detected by the camera in an image (28).

Cameras with worse thermal sensitivity (higher NETD values at the same defined temperature) are less capable of avoiding false data homogeneity (29). It could impair the detection of relatively high temperature differences within the same thermogram, and therefore misleading injury diagnosis. The higher false negative rates found with cameras with worse thermal sensitivity, mainly the FLIR ONE, could explain this limitation. The large amount of false positives in FLIR ONE results may also result of its overestimation of temperature (12), possibly

producing images with false zones with heat peaks. Given that camera temperature ranges are related to NETD (30), when a certain temperature can be measured using two different temperature ranges, it would be advisable to select the narrowest one, since it would exhibit the lowest noise.

Although they are advantageous in terms of portability and low cost, the lack of adjustable focus in both the FLIR ONE and C2 cameras could be a disadvantage compared to the other cameras used in this research. Fixed focus prevents sharper thermograms and ROIs from being delineated, resulting in limitations for the distance between the camera and the region of interest (31). Although results with closer images indicate a low impact of the focal adjustment (32), we observed that the low sharpness of images taken at 1.5 m distance was determinant for inaccurate results.

In conclusion, cameras with better hardware characteristics produce accurate and consistent results in a wide range of practical situations. In these cases, both at maximum and mean temperature the results were solid, and the level of error as a function of distance was low. The C2 and FLIR ONE cameras have advantages such as portability, which can facilitate use in several situations including external environment and clinical setting. Their lower hardware characteristics may compromise the determination of temperature asymmetry results depending on the distance of image recording. These cameras may not be recommended for measures far than 0.7 m and for small ROIs (less than 25 pixels (15) or 3-4 times the IFOV (30)), for example in the analysis of diabetic foot (33).

The distance between the infrared camera and the sample also affects the results, and it is preferable to take a closer shot. Furthermore, cameras with

superior hardware characteristics (e.g., ≥ 320 x 240 pixels, ≤ 1.3 mrad of IFOV or ≤ 45 mK of NETD) ensure greater data reliability when investigating thermal asymmetries of at least 0.5°C. For application fields with less need for precision (high size of ROIs and high asymmetries to detect), C2, which has the advantage of portability, seems to be sufficient.

A limitation of this study could be that the equations obtained have not been validated, for example employing a ROC curve (receiver operating characteristic curve) analysis with other data. However, our objective was not to use the equations, it was an approximation to know the degree of relationship between each camera and the T1020, as well as to evaluate the effect of distance on the detection of thermal asymmetries.

From an applied point of view, through the findings of this study we consider that researchers interested in evaluating thermal asymmetries may have better parameters to choose the most suitable thermographic cameras and will be able to observe that images taken closer present more consistent results. Altogether, this results also indicate that the standardization of the measurement protocols is a determining factor for the validity of analysis of temperature asymmetries.

3.6 References

1. Vardasca R, Ring EFJ, Plassmann P, Jones C. Termal symmetry of the upper and lower extremities in healthy subjects. Thermol Int. 2012 Apr 15;22:53–60.
2. Niu HH, Lui PW, Hu JS, Ting CK, Yin YC, Lo YL, et al. Thermal symmetry of skin temperature: normative data of normal subjects in Taiwan.

120 Zhonghua Yi Xue Za Zhi Chin Med J Free China Ed. 2001 Aug;64(8):459–
121 68.
122 3. Hildebrandt C, Raschner C, Ammer K. An Overview of Recent Application
123 of Medical Infrared Thermography in Sports Medicine in Austria. Sensors.
124 2010 May 7;10(5):4700–15.
125 4. Fernández-Cuevas I, Arnáiz Lastras J, Escamilla Galindo V, Gómez
126 Carmona P. Infrared Thermography for the Detection of Injury in Sports
127 Medicine. In: Priego Quesada JI, editor. Application of Infrared
128 Thermography in Sports Science [Internet]. Cham: Springer International
129 Publishing; 2017 [cited 2021 Jun 2]. p. 81–109. (Biological and Medical
130 Physics, Biomedical Engineering). Available from:
131 http://link.springer.com/10.1007/978-3-319-47410-6_4
132 5. Sanchis-Sánchez E, Vergara-Hernández C, Cibrián RM, Salvador R,
133 Sanchis E, Codoñer-Franch P. Infrared thermal imaging in the diagnosis
134 of musculoskeletal injuries: a systematic review and meta-analysis. AJR
135 Am J Roentgenol. 2014 Oct;203(4):875–82.
136 6. Priego Quesada JI, editor. Application of Infrared Thermography in Sports
137 Science. 1st ed. 2017. Cham: Springer International Publishing : Imprint:
138 Springer; 2017. 1 p. (Biological and Medical Physics, Biomedical
139 Engineering).
140 7. Molina-Payá J, Ríos-Díaz J, Martínez-Payá J. Inter and intraexaminer
141 reliability of a new method of infrared thermography analysis of patellar
142 tendon. Quant InfraRed Thermogr J. 2021 Mar 15;18(2):127–39.
143 8. Côrte AC, Pedrinelli A, Marttos A, Souza IFG, Grava J, José Hernandez
144 A. Infrared thermography study as a complementary method of screening

and prevention of muscle injuries: pilot study. BMJ Open Sport Amp Exerc Med. 2019 Jan 1;5(1):e000431.

9. Gómez-Carmona P, Fernández-Cuevas I, Sillero-Quintana M, Arnaiz-Lastras J, Navandar A. Infrared Thermography Protocol on Reducing the Incidence of Soccer Injuries. J Sport Rehabil. 2020 Nov 1;29(8):1222–7.

10. Jones BF. A reappraisal of the use of infrared thermal image analysis in medicine. IEEE Trans Med Imaging. 1998 Dec;17(6):1019–27.

11. Machado ÁS, Priego-Quesada JI, Jimenez-Perez I, Gil-Calvo M, Carpes FP, Perez-Soriano P. Influence of infrared camera model and evaluator reproducibility in the assessment of skin temperature responses to physical exercise. J Therm Biol. 2021 May;98:102913.

12. Kirimtat A, Krejcar O, Selamat A, Herrera-Viedma E. FLIR vs SEEK thermal cameras in biomedicine: comparative diagnosis through infrared thermography. BMC Bioinformatics. 2020 Mar 11;21(Suppl 2):88.

13. Lai F, Kandukuri J, Yuan B, Zhang Z, Jin M. Thermal Image Enhancement through the Deconvolution Methods for Low-Cost Infrared Cameras. Quant Infrared Thermogr J. 2018;15(2):223–39.

14. Priego Quesada JI, Kunzler MR, Carpes FP. Methodological Aspects of Infrared Thermography in Human Assessment. In: Priego Quesada JI, editor. Application of Infrared Thermography in Sports Science [Internet]. Cham: Springer International Publishing; 2017 [cited 2021 Jun 2]. p. 49–79. (Biological and Medical Physics, Biomedical Engineering). Available from: http://link.springer.com/10.1007/978-3-319-47410-6_3

15. ISO (2009). Medical electrical equipment-deployment, implementation and operational guidelines for identifying febrile humans using a screening thermograph. TR 13154:2009 ISO/TR 8-600.
16. Bach AJ, Stewart IB, Minett GM, Costello JT. Does the technique employed for skin temperature assessment alter outcomes? A systematic review. Physiol Meas. 2015;36(9):R27.
17. Machin G, Simpson R, Broussely M. Calibration and validation of thermal imagers. Quant InfraRed Thermogr J. 2009 Dec;6(2):133–47.
18. Moreira DG, Costello JT, Brito CJ, Adamczyk JG, Ammer K, Bach AJE, et al. Thermographic imaging in sports and exercise medicine: A Delphi study and consensus statement on the measurement of human skin temperature. J Therm Biol. 2017 Oct;69:155–62.
19. Robinson PJ, Davies JA. Laboratory Determinations of Water Surface Emissivity. J Appl Meteorol Climatol. 1972 Dec 1;11(8):1391–3.
20. Rees WG, James SP. Angular variation of the infrared emissivity of ice and water surfaces. Int J Remote Sens. 1992 Oct;13(15):2873–86.
21. Weir JP. Quantifying Test-Retest Reliability Using the Intraclass Correlation Coefficient and the SEM. J Strength Cond Res. 2005;19(1):231.
22. Vainionpää M, Tienhaara EP, Raekallio M, Junnila J, Snellman M, Vainio O. Thermographic Imaging of the Superficial Temperature in Racing Greyhounds before and after the Race. Sci World J. 2012;2012:1–6.
23. Steketee J. Spatial resolution of thermographic cameras. Bibl Radiol. 1975;(6):25–32.

24. Liu G, Xia Y, Yang C, Zhang L. The Review of the Major Entropy Methods and Applications in Biomedical Signal Research. In: Zhang F, Cai Z, Skums P, Zhang S, editors. Hong Kong, City University of Hong Kong: Springer International Publishing; 2018. p. 87–100.

25. Danko M, Hudak R, Foffová P, Zivcak J. An importance of camera - subject distance and angle in musculoskeletal application of medical thermography. Acta Electrotech Inf. 2010 Jan 1;10.

26. Menezes P, Rhea MR, Herdy C, Simão R. Effects of Strength Training Program and Infrared Thermography in Soccer Athletes Injuries. Sports Basel Switz. 2018 Nov 19;6(4).

27. Adamczyk JG, Krasowska I, Boguszewski D, Reaburn P. The use of thermal imaging to assess the effectiveness of ice massage and cold-water immersion as methods for supporting post-exercise recovery. J Therm Biol. 2016 Aug;60:20–5.

28. Chrzanowski K, Bielecki Z, Szulim M. Comparison of temperature resolution of single-band, dual-band, and multiband infrared systems. Appl Opt. 1999 May 1;38(13):2820.

29. Obinah MPB, Nielsen M, Hölmich LR. High-end versus Low-end Thermal Imaging for Detection of Arterial Perforators. Plast Reconstr Surg Glob Open. 2020 Oct;8(10):e3175.

30. Vollmer M, Möllmann KP. Infrared Thermal Imaging: Fundamentals, Research and Applications [Internet]. Weinheim, Germany: Wiley-VCH Verlag GmbH & Co. KGaA; 2017 [cited 2021 Jun 8]. Available from: http://doi.wiley.com/10.1002/9783527693306

31. Okada K, Takemura K, Sato S. Investigation of Various Essential Factors for Optimum Infrared Thermography. J Vet Med Sci. 2013;75(10):1349–53.

32. Vogel B, Wagner H, Gmoser J, Wörner A, Löschberger A, Peters L, et al. Touch-free measurement of body temperature using close-up thermography of the ocular surface. MethodsX. 2016;3:407–16.

33. van Doremalen RFM, van Netten JJ, van Baal JG, Vollenbroek-Hutten MMR, van der Heijden F. Validation of low-cost smartphone-based thermal camera for diabetic foot assessment. Diabetes Res Clin Pract. 2019 Mar;149:132–9.

CAPÍTULO IV

ARTIGO ORIGINAL

Influence of infrared camera model and evaluator reliability in the assessment of skin temperature responses to physical exercise

Álvaro S. Machado[1]; Jose Ignacio Priego-Quesada[2,3*]; Irene Jimenez-Perez[2,3]; Marina Gil-Calvo[2]; Felipe Pivetta Carpes[1]; Pedro Perez-Soriano[2]

[1] Applied Neuromechanics Group, Laboratory of Neuromechanics, Federal University of Pampa, Uruguaiana, Brazil.

[2] Research Group in Sports Biomechanics (GIBD), Department of Physical Education and Sports, University of Valencia, Valencia, Spain.

[3] Research Group in Medical Physics (GIFIME), Department of Physiology, University of Valencia, Valencia, Spain.

4.1 Abstract

As infrared thermography (IRT) has gain popularity in clinical and scientific research, different infrared cameras are available in the market. The aim of this study is to verify the similarity between three IRT models for assessment of skin temperature pre and post physical exercise. Three models of Flir thermographic cameras (E60bx, Flir-One Pro LT, and C2) were tested. Thermographies were taken of the foot sole, anterior leg and anterior thigh from 12 well-trained men, before and after a 30-min run on a treadmill. The images files were blinded and processed by 3 evaluators extracting the mean, maximum, and standard deviation temperature of the region of interest. Time for processing data and rate of perceived effort were also recorded. E60bx takes longer time for data processing (CI95% E60 vs C2 [0.2, 2.6 min], p=0.02 and ES=0.6); vs. Flir-One [0.0, 3.4 min], p=0.03 and ES=0.6) and elicits lower effort perception (E60 3.0 ± 0.1 vs. Flir-One 5.6 ± 0.2 vs C2 7.0 ± 0.2 points; p<0.001 and ES>0.8). The C2 camera overestimates the temperature, while the One underestimated the values. In general, there was a higher intra-class correlation between cameras and inter-examiners in the mean temperature variable, especially in the pre-exercise situation. However, when measures are performed after exercise, mean temperature seems to provide more consistent values across cameras and examiners. We recommend caution when using more than one camera model in a study. In the need to do so, we recommend the use of mean temperature.

Keywords: thermal imaging; physical exercise, running, thermoregulation

4.2 Introduction

Infrared thermography (IRT) is a non-contact method to measure superficial skin temperature (de Andrade Fernandes et al., 2014; Priego Quesada

et al., 2017). The broad interest in IRT relies on the fact that variation in skin temperature can be related to different medical conditions, from acute to chronic, from local to systemic issues (Jones, 1998; Lahiri et al., 2012). In sports, IRT is investigated concerning its possibilities to detect and monitor acute adaptations for different types of exercise (Hillen et al., 2020). It includes associations between skin temperature and injury risk (dos Santos Bunn et al., 2020; Gómez-Carmona et al., 2020; Menezes et al., 2018). The relative low cost and non-invasive use of IRT seduce sports medicine professionals to implement IRT as a tool for injury prevention or exercise physiology measurement (dos Santos Bunn et al., 2020; Hillen et al., 2020; Menezes et al., 2018).

Data acquisition is a matter of concern when employing IRT. Cameras or mobile gadgets detect electromagnetic radiation over the infrared spectrum at wavelengths of around 0.75–1000 μm, and record them in images that are further analyzed considering regions of interest (ROI) (Costello et al., 2012; Lahiri et al., 2012). Despite the effort to promote standardization of the IRT methods, which include the participant preparation for data collection (Moreira et al., 2017), technical aspects of data collection and analysis still have relevant impact on IRT research outcomes. A main limitation is the reliability considering the different technical characteristics of IRT devices (Rossignoli et al., 2016) and tools for data analysis (de Jesus Guirro et al., 2017; Silva et al., 2018). Furthermore, reliability is important when aiming to develop tools that should work with data input from different devices recording the thermal images (Bauer et al., 2020).

The reliability of the IRT affects the image resolution. High-resolution cameras tend to be more expensive, so the industry has made efforts to provide more affordable versions (Vardasca, 2019; Villa et al., 2020). The variability in

reliability and resolution of the cameras affect the results from studies by over or underestimation of the temperature. These imprecise measures are due to equipment error, as well the comparison of data from different cameras, even with similar spatial resolution (Kirimtat et al., 2020; Nguyen et al., 2010). For example, a minimum of 25 pixels is recommended for determination of a ROI (ISO, 2008b, 2009). It is recommended to minimize the difficulties in data analysis due to low resolution, and to permit automation in the data processing (Gauci et al., 2018). All these factors of influence suffer effects of the different devices and characteristics for image acquisition.

The availability of affordable infrared cameras has contributed to the popularization of IRT. However, studies aiming to provide technical guidance to data analysis and interpretation did not follow this growth, and questions still remain about the reliability of data from different cameras, especially in the context of sports, a field where IRT is widely applied (Gómez-Carmona et al., 2020; Hildebrandt et al., 2010; Menezes et al., 2018). The impact of image resolution and the overall quality of IRT equipment on data reliability can be estimated by the quantification of inter-examiner repeatability while using the same camera (Tan et al., 2016). Furthermore, cameras accuracy can be influenced by manufacturer calibration, and therefore the reliability of different cameras (of different costs, for example) is important to ensure proper comparison of results from different studies. A good example is the assessment of IRT responses to physical exercise, when skin temperature change due to thermo physiological mechanisms including peripheral vasodilation/vasoconstriction and sweat activity (Cramer & Jay, 2016).

Taken together, these questions indicate the gaps claiming for attention when implementing routines of IRT acquisition and analysis, in order to provide proper recommendation for its application in different contexts, for example, hospitals, clinics and sports clubs. Therefore, the aim of the study was to evaluate the inter-camera and inter-examiner reliability between three commercial thermographic cameras with different spatial resolution considering measures performed before and after physical exercise.

4.3 Materials and methods

4.3.1 Participants and experimental design

Twelve male recreational runners with mean ± standard deviation age 25 ± 8 years, body mass 71.3 ± 11.6 kg, height 1.79 ± 0.08 m, body mass index 22.1 ±2.1 kg/m^2, and running training volume 43.4 ± 44.2 km/week, signed an informed consent before start participation in the study. All procedures complied with the Declaration of Helsinki and were approved by the local university ethics committee (record number 1252705).

After signing the informed consent form, participants were placed, one at a time, in a temperature-controlled room where they remained seated for 10 min with thighs, legs and feet un-covered for thermal adaptation to the room temperature. After these 10 min, thermographic measurements of the soles of the feet (in seated position), anterior thighs and anterior legs (both in standing position) were taken. Then, the participants were instructed to run on a treadmill for 30 min. At the end of the race, a new period of 5 min, in the same rest posture, for thermal adaptation to the room temperature was carried out and the same

342 thermographic measurements were taken. Participants were evaluated after
343 exercise as a form to induce thermal stress that is useful to assess the
344 performance of cameras in different situations (de Andrade Fernandes et al.,
345 2014). Laboratory environmental conditions were: air temperature 23.1 ± 0.9ºC
346 and relative humidity 28.1 ± 5.1%.

347

348 **4.3.2 Running exercise**

349 Participants ran continuously for 30 min on a treadmill (Excite Run 900,
350 TechnoGymSpA, Gambettola, Italy) with a 1% of slope at a self-selected speed.
351 Exercise intensity was controlled by the treadmill speed to elicit report of 12 points
352 (between light intensity and somewhat hard) in the 6-20 points Borg scale (Borg,
353 1982). Exercise started with a 5-min warm-up where speed was set at 8 km/h for
354 the first 2 min and then increased by 1 km/h every 30 s until participants reported
355 12 points in the Borg scale. If the rate of perceived effort increased, small adjusts
356 in the speed were conducted. Once the speed was set, it was kept unchanged
357 for the 30 minutes of running. The average self-selected speed of the participants
358 was 10.2 ± 0.6 km/h.

359

360 **4.3.3 Infrared thermography measurements**

361 Skin temperature was measured using three different infrared
362 thermography cameras from Flir Systems Inc. (Wilsonville, USA): E60bx
363 (resolution of 320x240 pixels, noise equivalent temperature difference (NETD) <
364 0.05°C, and measurement uncertainty of ± 2ºC); C2 (resolution of 80×60 pixels,
365 NETD < 0.1°C and measurement uncertainty of ± 2 ºC for temperatures >25ºC);

366 and Flir-One Pro LT (resolution of 80×60 pixels, NETD of 0.1°C, and
367 measurement uncertainty of ± 5 ºC).

368 Measurements were taken in an area absent of sunlight 5 m far from any
369 electronic equipment, and other people (except for the thermographer and the
370 evaluator). An antireflective panel was placed behind the participant to minimize
371 the influence of the radiation reflected by the wall (Hildebrandt et al., 2010).
372 Reflected temperature was measured according to the standard method ISO
373 18434-1:2008 (ISO, 2008a). Moreover, the Thermographic Imagining in Sport
374 and Exercise Medicine checklist was used to corroborate that all factors that
375 could affect thermographic measurements were taken into account (Moreira et
376 al., 2017).

377 For image analysis, ROIs were defined for the feet (according to the
378 regions of rearfoot, midfoot, forefoot, toes, and hallux), anterior leg and anterior
379 thigh. Hallux and the toes were delimited, and from this delimitation, the rest of
380 the sole was divided into three equal longitudinal areas: rearfoot, midfoot and
381 forefoot. The leg was delimited at the top by the center of the muscular belly of
382 the calf and at the bottom by the narrowness of the ankle. The thigh was limited
383 at the top by the groin line and at the bottom by a tape placed as a mark above
384 the knee (Figure 1).

385 All the ROIs were analyzed bilaterally for each participant. The absolute
386 mean, the maximal and standard deviation of each ROI were computed using a
387 commercial software (Thermacam Researcher Pro 2.10 software, FLIR,
388 Wilsonville, USA). All images were processed using an emissivity factor of 0.98
389 to obtain skin surface temperatures (Steketee, 1973).

The images were coded with the participant's number, the time of measurement and a number associated with the camera. Three evaluators (3 ± 2 years of experience in thermographic evaluations) analysed the images in a blinded way: they did not know the association between the codification of the camera in the file with the camera model. At the end of the analysis of the images of each participant (6 in total: three pre and three post exercise) for each of the cameras, the time to conclude and the rate of perceived exertion (RPE, in a 0 to 10 Borg scale) were recorded for each evaluator. Order of the cameras in each participant was randomized in the three evaluators.

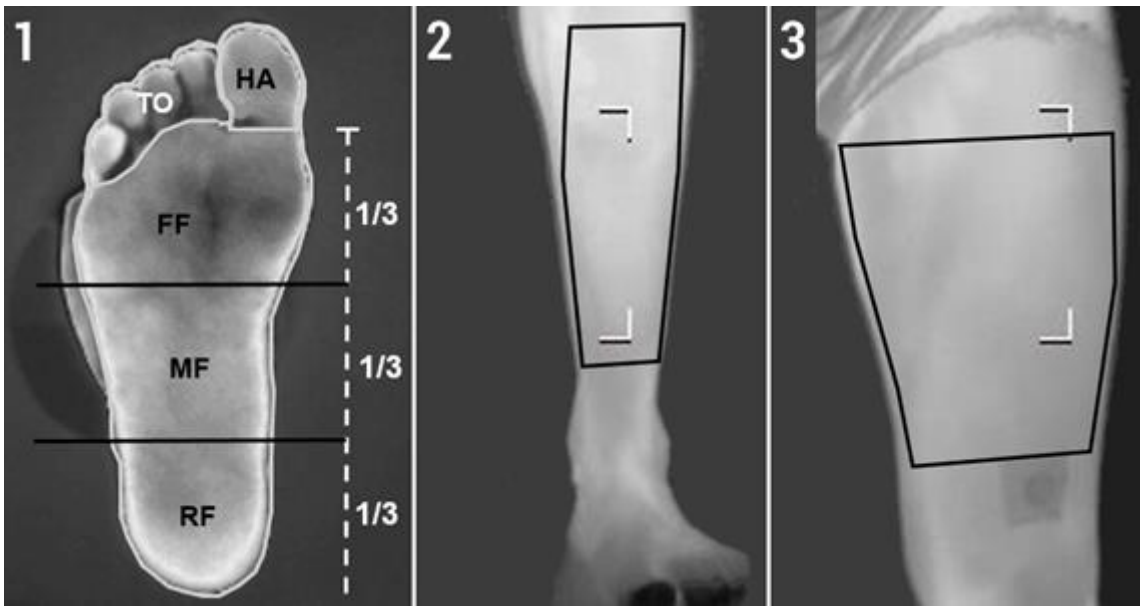

Figure 1. Regions of interest (ROIs) defined: (1) foot (RF: rearfoot, MF: midfoot, FF: forefoot, TO: toes, HA: hallux; (2) anterior leg; and (3) anterior thigh.

4.3.4 Statistical analysis

Statistical analyses were performed using SPSS 26 (SPSS Inc., Chicago, USA). Normality of data distribution was confirmed using the Shapiro-Wilk test

(p>0.05), except for the RPE data (p<0.05). Data with normal distribution are reported as mean ± standard deviation with 95% confidence intervals of the differences between comparisons (CI95%), and data without normal distribution are reported as median ± standard error. Time analysis was analyzed using a repeated measures ANOVA with Bonferroni post-hoc. Evaluators RPE was assessed using the Friedman test with Wilcoxon post-hoc. Except for inter-evaluator reliability, rest of analysis were performed with the data obtained by the most experienced evaluator. Repeated measures ANOVA with Bonferroni post-hoc were applied to compare the mean, maximum and standard deviation temperatures from each ROI considering three factors: measurement points in time (before and after exercise), side (right and left) and camera (E60bx, C2 and Flir-One Pro LT). The significance level was set at p<0.05. For significant pair differences, Cohen's effect sizes (ES) were computed and classified as small (ES 0.2–0.5), moderate (ES 0.5–0.8), or large (ES>0.8) (Cohen, 1988). The agreement between the three cameras was analyzed using Bland–Altman plots. The intraclass correlation coefficient (ICC) from model "2,1" (Shrout & Fleiss, 1979) was calculated between the three cameras at each of the measurement points in time and each ROI (inter-camera reliability), and between the three evaluators for each camera (inter-evaluator reliability). The following ICC considered indexes from 1.00 to 0.81 as excellent reliability, 0.80 to 0.61 as very good reliability, 0.60 to 0.41 as good reliability, 0.40 to 0.21 as reasonable reliability, and 0.20 to 0.00 as poor reliability (Weir, 2005). Differences in ICC values between measurement points in time and cameras were assessed using repeated measures ANOVA with Bonferroni post-hoc.

4.4 Results

4.4.1. Effect of camera type on time analysis and evaluator effort perception

The E60bx camera required longer time for images analysis (13 ± 3 min) than the other models (C2: 11 ± 3 min, CI95% of the difference [0.2, 2.6 min], p=0.02 and ES=0.6); Flir-One Pro LT: 11 ± 3 min, CI95% of the difference [0.0, 3.4 min], p=0.03 and ES=0.6). Time for images analysis did not differ between C2 and Flir-One Pro LT (p>0.05).

Evaluators reported crescent RPE for the use of E60bx, Flir-One Pro LT, and C2 (3.0 ± 0.1 vs. 5.6 ± 0.2 vs 7.0 ± 0.2 points, respectively; all comparisons presented a p<0.001 and ES>0.8).

4.4.2. Effect of camera type on thermographic results

Seven images recorded with Flir-One Pro LT had files corrupted and could not be used (2 of the feet, 2 of the anterior thigh and 3 of the anterior leg) presenting invalid results (temperatures lower than -40ºC). Therefore, the repeated measures ANOVAs were performed with the data from 10 participants for most of the ROIs, except for the anterior leg, which was performed with data from 9 participants.

Images from left and right were merged due to the absent of asymmetries for images from the different cameras (p>0.05). In general, C2 camera presented lower mean and maximum skin temperature, and higher standard deviation than the other cameras (Figure 2). Flir-One Pro LT showed higher mean and maximum skin temperature than the other cameras in the ROIs from the lower limbs

456 (anterior leg and anterior thigh). Most of the observed differences had a large
457 effect size (ES>0.8)

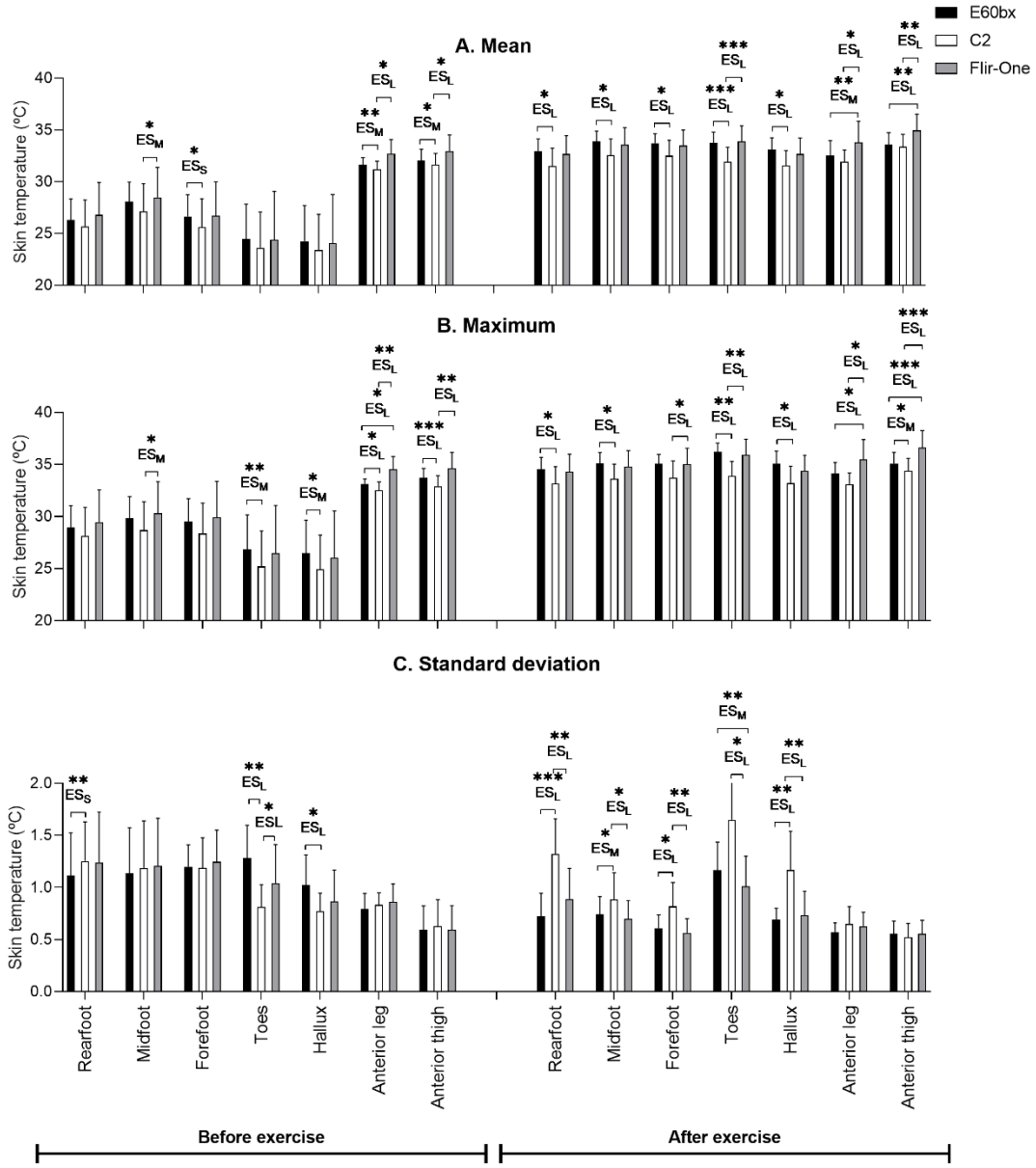

458

459 **Figure 2.** Mean ± standard deviation of the mean (A), maximum (B) and standard
460 deviation temperature (C) of each thermographic camera before and after
461 exercise. Differences are identified by symbols (*p < 0.05; **p < 0.01; ***p <
462 0.001) and the effect size with letters (small effect size ES_S; moderate effect size
463 ES_M; large effect size ES_L).

Bland–Altman plots (Figure 3) showed lower 95% limits of agreement between E60bx and Flir-One Pro LT than between C2 and the other cameras before exercise (Bias E60bx vs C2 0.8 ± 1.0ºC; E60bx vs. Flir-One Pro LT -0.2 ± 1.6ºC; C2 vs. Flir-One Pro LT -1.1 ± 1.8ºC) and after exercise (Bias E60bx vs C2 1.2 ± 1.2ºC; E60bx vs. Flir-One Pro LT -0.4 ± 1.2ºC; C2 vs. Flir-One Pro LT -1.6 ± 1.4ºC) on mean skin temperature (Figure 3) and maximum skin temperature (Figure 4): before exercise (Bias E60bx vs C2 1.1 ± 1.1ºC; E60bx vs. Flir-One Pro LT -0.2 ± 1.8ºC; C2 vs. Flir-One Pro LT -1.5 ± 1.8ºC) and after exercise (Bias E60bx vs C2 1.5 ± 1.4ºC; E60bx vs. Flir-One Pro LT -0.3 ± 1.4ºC; C2 vs. Flir-One Pro LT -1.9 ± 1.6ºC).

Similar results were found between cameras and measurement points for standard deviation skin temperature (Figure 5): before exercise (Bias E60bx vs C2 0.1 ± 0.3ºC; E60bx vs. Flir-One Pro LT 0.0 ± 0.2ºC; C2 vs. Flir-One Pro LT -0.1 ± 0.2ºC) and after exercise (Bias E60bx vs C2 -0.2 ± 0.4ºC; E60bx vs. Flir-One Pro LT 0.0 ± 0.2ºC; C2 vs. Flir-One Pro LT 0.3 ± 0.4ºC).

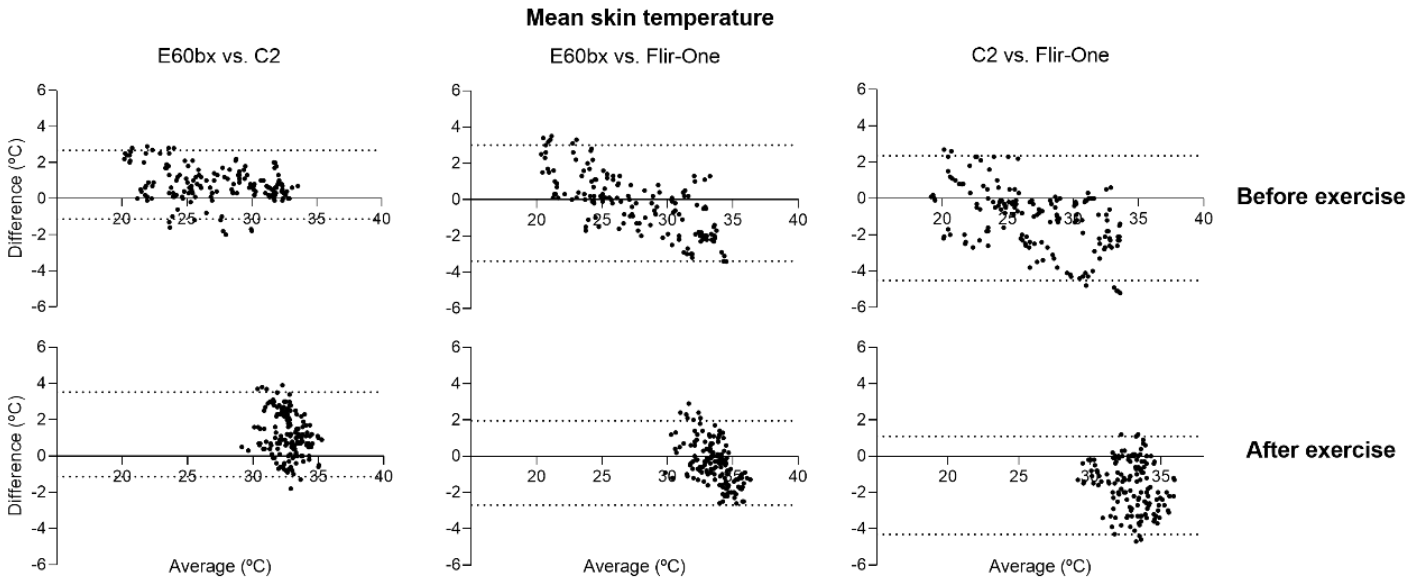

481

482 **Figure 3.** Bland–Altman plot with 95% limits of agreement illustrates the
483 difference in mean skin temperature measurements between values obtained in
484 all the ROIs by the three cameras assessed.

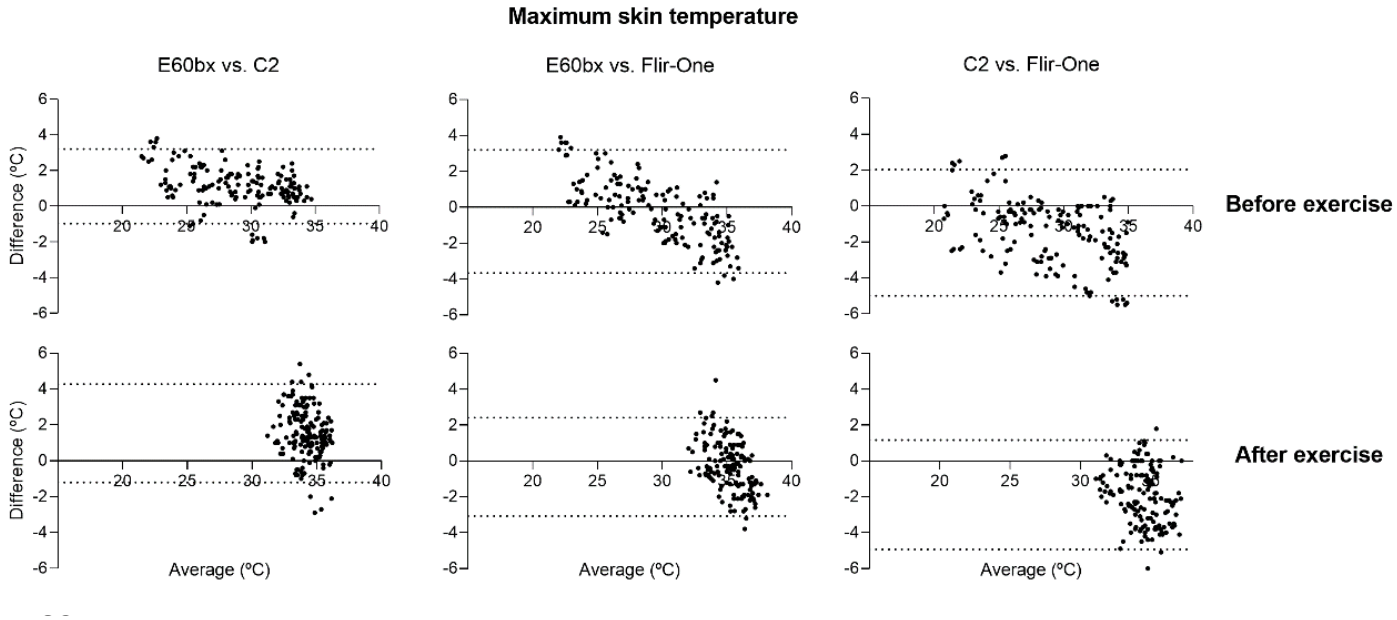

486 **Figure 4.** Bland–Altman plot with 95% limits of agreement illustrates the
487 difference in maximum skin temperature measurements between values
488 obtained in all the ROIs by the three cameras assessed.

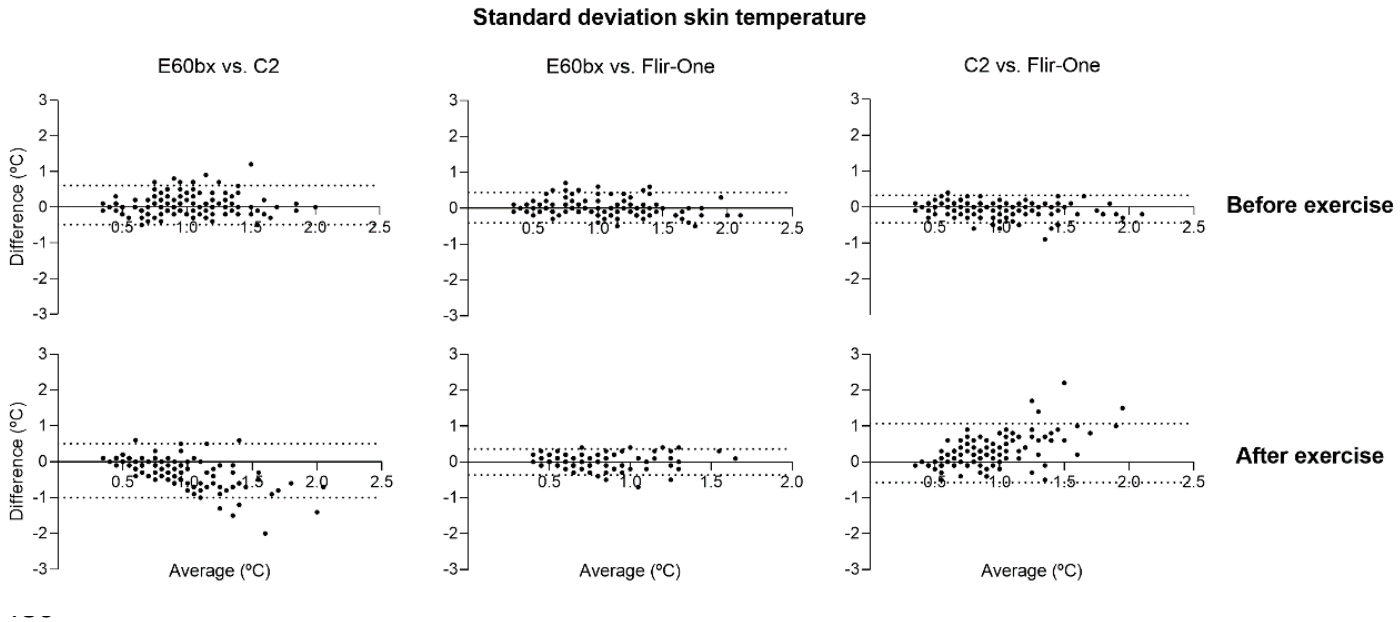

490 **Figure 5.** Bland–Altman plot with 95% limits of agreement illustrates the
491 difference in standard deviation skin temperature measurements between values
492 obtained in all the ROIs by the three cameras assessed.

493

494 **4.4.3. Effect of camera type on reliability**

495 Table 1 shows the inter-camera reliability. ICC values were lower after
496 exercise than before for the mean (0.76 ± 0.17 vs. 0.48 ± 0.13, CI95% of the
497 difference [0.09, 0.46], p=0.01 and ES=1.8), maximum (0.71 ± 0.20 vs. 0.35 ±
498 0.15, CI95% of the difference [0.16, 0.55], p<0.01 and ES=2.0), and standard
499 deviation skin temperature (0.71 ± 0.23 vs. 0.37 ± 0.22, CI95% of the difference
500 [0.10, 0.58], p=0.01 and ES=1.5). C2-Flir-One Pro LT comparison presented
501 lower ICC values than E60bx-Flir-One Pro LT comparison for mean [0.54 ± 0.18
502 vs. 0.69 ± 0.14, CI95% of the difference (0.07, 0.25), p<0.01 and ES=1.0] and
503 maximum skin temperature (0.46 ± 0.21 vs. 0.61 ± 0.19, CI95% of the difference
504 [0.06, 0.24], p<0.01 and ES=0.8). E60bx-Flir-One Pro LT comparison presented

higher ICC values of standard deviation skin temperature than E60bx-C2 comparison (0.68 ± 0.13 vs. 0.42 ± 0.29, CI95% of the difference [0.04, 0.47], p=0.02 and ES=1.2) and C2-Flir-One Pro LT comparison (0.68 ± 0.13 vs. 0.51 ± 0.24, CI95% of the difference [0.03, 0.32], p=0.03 and ES=0.9).

Table 1. Intraclass correlation coefficients (ICC) of inter-camera reliability from the three infrared cameras considering the mean, maximum, and standard deviation skin temperature.

	Mean skin temperature					
	Before exercise			After exercise		
	E60bx-C2	E60bx-Flir-One Pro LT	C2-Flir-One Pro LT	E60bx-C2	E60bx-Flir-One Pro LT	C2-Flir-One Pro LT
Rearfoot	.84	.85	.77	.37	.70	.55
Midfoot	.82	.83	.77	.29	.63	.50
Forefoot	.83	.83	.80	.33	.62	.48
Toes	.92	.90	.86	.23	.73	.27
Hallux	.90	.90	.85	.21	.67	.38
Anterior leg	.78	.35	.23	.61	.67	.28
Anterior thigh	.89	.50	.47	.80	.53	.31
	Maximum skin temperature					
Rearfoot	.84	.86	.74	.36	.69	.49
Midfoot	.78	.83	.70	.15	.62	.37
Forefoot	.82	.83	.76	.10	.45	.42
Toes	.84	.89	.84	.04	.56	.25
Hallux	.82	.85	.83	.01	.40	.34
Anterior leg	.65	.14	.10	.27	.46	.09
Anterior thigh	.78	.56	.40	.62	.46	.19
	Standard deviation skin temperature					
Rearfoot	.86	.86	.93	.13	.46	.23
Midfoot	.90	.95	.89	.22	.58	.13
Forefoot	.71	.75	.85	.14	.45	.13
Toes	.14	.58	.49	.01	.69	.02
Hallux	.25	.63	.64	.06	.45	.06
Anterior leg	.35	.76	.49	.55	.68	.66
Anterior thigh	.93	.94	.94	.67	.73	.66

Table 2 shows inter-evaluator reliability. No differences were observed between measurement points on ICC of the mean skin temperature (p=0.21),

516 maximum skin temperature (p=0.29), and standard deviation skin temperature
517 (p=0.31). C2 camera presented lower ICC values for mean skin temperature than
518 E60bx (0.80 ± 0.18 vs. 0.96 ± 0.07, CI95% of the difference [0.03, 0.28], p=0.02
519 and ES=1.3) and Flir-One Pro LT (0.80 ± 0.18 vs. 0.96 ± 0.06, CI95% of the
520 difference [0.04, 0.28], p=0.02 and ES=1.3). Maximum skin temperature (p=0.08)
521 and standard deviation (p=0.40) did not differ between the cameras.

522

523 **Table 2.** Intraclass correlation coefficients (ICC) of inter-evaluator
524 reliability of the three infrared cameras for mean, maximum and standard
525 deviation skin temperature.

	Mean skin temperature					
	Before exercise			After exercise		
	E60bx	C2	Flir-One Pro LT	E60bx	C2	Flir-One Pro LT
Rearfoot	.99	.93	.99	.96	.77	.96
Midfoot	.99	.92	.99	.98	.89	.99
Forefoot	.99	.93	.99	.99	.88	.99
Toes	.99	.94	.99	.83	.27	.80
Hallux	.99	.96	.99	.90	.39	.90
Anterior leg	.80	.70	.88	.98	.75	.99
Anterior thigh	.99	.96	.99	.99	.94	.99
	Maximum skin temperature					
Rearfoot	.87	.96	.97	.97	.96	.99
Midfoot	.99	.94	.98	.99	.95	.99
Forefoot	.98	.92	.98	.73	.79	.84
Toes	.99	.92	.97	.99	.84	.96
Hallux	.98	.93	.98	.97	.77	.83
Anterior leg	.93	.93	.98	.94	.84	.98
Anterior thigh	.89	.98	.92	.99	.96	.97
	Standard deviation skin temperature					
Rearfoot	.91	.82	.89	.20	.20	.17
Midfoot	.90	.84	.78	.41	.26	.36
Forefoot	.84	.80	.71	.31	.27	.05
Toes	.75	.34	.48	.14	.27	.09
Hallux	.59	.19	.50	.15	.46	.24
Anterior leg	.33	.61	.25	.09	.04	.46
Anterior thigh	.93	.01	,81	.71	.18	.31

526

4.5 Discussion

Here we investigate the reliability of IRT data obtained from three different thermographic cameras before and after exercise, and the inter-examiner repeatability of the results. Considering the E60bx camera as a reference due to its higher resolution, we found that the C2 model underestimates skin temperature, while the Flir-One Pro LT overestimates the results. Both the inter-examiner and inter-camera ICC remained higher when analyzing the mean temperature, especially in the pre-exercise condition. Finally, the higher resolution camera allows more detailed ROI, which takes more time to process the data, but generates less RPE for the evaluators.

The best overall results of thermal imaging data processing seems to depend on the combination of higher spatial resolution and better thermal sensitivity, or NETD (Usamentiaga et al., 2014). As we observed for the E60bx camera, this combination reduces variability, but also produces more detailed images, which resulted in longer time to finish processing. The longer time spent for image processing seems to result of a greater possibilities to detail the ROIs' contour, which also seems to have been more comfortable for the examiners. On the other hand, lower spatial resolution of cameras C2 and Flir-One Pro LT limits the ROI identification due to less detailed edges (Fernández-Cuevas et al., 2015).

The way ROIs are determined *a priori* enhances the possibility of errors in data processing (Nahm, 2013). Here we show that the smallest ROIs (toes and hallux), where detailing ROIs become more difficult, result in lower inter-examiner ICC. Small errors in the positioning of the ROIs generate higher variations in results when the image resolution is lower. Therefore, the error rate is attributed to the low accuracy in placing the ROI (Liu et al., 2020). Especially for the anterior

leg, the low inter-examiner ICC may result of difficulty in excluding the portion of the gastrocnemius that appears in the image recorded at the frontal plane. A possible solution is to delimit the ROI area with some reflective tape (Priego Quesada et al., 2017), which may also help to automatize the ROI determination (Gauci et al., 2018; Requena-Bueno et al., 2020).

Considering the E60bx as the reference camera, C2 model underestimates the temperature values, whereas Flir-One Pro LT overestimates. The overestimation of Flir-One camera is in agreement with previous studies (Curran et al., 2015; Vardasca, 2019), and difficult to correct even using a blackbody calibration (Curran et al., 2015). This limitation should be balanced with the lower cost of this camera model. The under and overestimation mentioned are supported by the Bland–Altman plots, especially for mean and maximum skin temperature above the measurement uncertainty. In this sense, we found inter-cameras ICC for maximum and average temperatures with large discrepancy. However, it is important to consider that we measured the temperature with specific cameras, and differences between cameras as expected also due to factory calibration parameters (Havenith & Lloyd, 2020). For now, we recommend caution in using more than one camera model when conducting scientific study.

The range of temperatures measured affects the accuracy of the infrared cameras. For example, manufacturer indicates higher measurement uncertainty to determine temperatures higher than 25ºC with the C2 camera. To test this hypothesis, we administrated the physical exercise to challenge body thermoregulation and induce changes in skin temperatures. Bland–Altman plots shows that Flir-One camera presented higher positive differences compared to

577 the other two models for measures of temperatures lower than ~22ºC, and higher
578 negative differences for measures of temperatures higher than ~33ºC. It may
579 result of factory calibration made to consider temperatures between 25 and 30ºC.
580 For measures from the C2 camera, the exercise produced higher variability,
581 which could explain the lower inter-camera ICC agreement. Such results indicate
582 that the cameras have a temperature range where they operate better, limiting
583 their reliability, and therefore the environment condition may play a fundamental
584 role due to variations in ambient temperature.

585 Ammer and Formenti (Ammer & Formenti, 2016) recommended to take
586 the standard deviation into account when planning a statistical analysis involving
587 a thermogram ROI. As it was observed, accuracy when drawing is crucial for the
588 inter-examiner and inter-camera similarity, especially for smaller ROIs. Variations
589 in the positioning of ROIs can generate different mean and maximum temperature
590 (Priego Quesada et al., 2015). As an illustrative example of an application of the
591 use of the standard deviation of the ROI, if an ROI is drawn by error covering an
592 small area outside the body, the mean and maximum temperature would be able
593 to dilute these outlier values, but these errors would be verifiable by observing
594 high standard deviations values of the ROI. In our study, although the Bland–
595 Altman plot showed great cameras agreement in standard deviation for both pre
596 and post exercise, standard deviation presented lower ICC inter-examiner
597 reliability than mean and maximum temperature. Firstly, the great camera
598 agreement in standard deviation could suggest that although mean or maximum
599 skin temperature could be different between cameras, the thermal distribution
600 within the ROI was similar. Secondly, the lower inter-examiner reliability is
601 understandable, since a difference of 0.1ºC between evaluators in a standard

deviation with a value of 1ºC represents 10%, while a difference of 0.1 or 1ºC for mean temperature of 30ºC represents a 0.3 and 3.3%, respectively. When evaluating the standard deviation in exercise investigation, it must be taken into account as significant differences between conditions above 0.3ºC, which is the maximum agreement limits observed by the Bland–Altman plot. The mean and maximum temperature suggested that the manual determination of the ROI impacted the results, and the standard deviation values indicated that this variation occurred in designs that covered only the skin, without adding part of the background of the thermograms.

The use of different cameras may be inevitable for large and multicenter studies, and in this case the main variables to be determined with different cameras deserves attention (Priego Quesada et al., 2017). In our study, mean temperature showed general better inter-camera ICC for foot and lower limbs, and Bland–Altman plots also showed a slightly better agreement between the cameras, mainly in the pre-exercise scenario. The predominantly high inter-examiner ICC and having the best agreement in the Bland-Altman plots places this variable as the most reliable to describe the real phenomenon. However, when it comes to the clinic or research practice, there is no consensus on the most recommendable IRT variable to use (Priego Quesada et al., 2017). It is important to emphasize that the advantage of mean temperature over the other variables in this study does not eliminate the need to assess the requirements of each experimental design. For studies within the same laboratory, if the laboratory has access to several cameras, it is recommended not to exchange different models, and within the same model, always use the same camera.

Future studies may extend the analysis to verify the effectiveness of the different cameras in diagnosing sports injuries or in respond to ice induced thermal stress. Finally, we highlight that testing one camera per model can be considered a limitation. Future studies may test the similarity between different cameras of the same model.

4.6. Conclusion

Cheaper cameras took less time for data analysis but increase the perception of effort in processing the data. We found higher intra-class correlation between cameras and inter-examiners in the mean temperature variable, but when effects of physical exercise are considered, data variability increases. We suggest to always use the same camera model for each project and when it is not possible, the mean temperature should be considered.

4.7 References

Ammer, K., & Formenti, D. (2016). Does the type of skin temperature distribution matter? *Themol. Int.*, *26*(2), 51–54.

Bauer, J., Hoq, M. N., Mulcahy, J., Tofail, S. A. M., Gulshan, F., Silien, C., Podbielska, H., & Akbar, Md. M. (2020). Implementation of artificial intelligence and non-contact infrared thermography for prediction and personalized automatic identification of different stages of cellulite. *EPMA Journal*, *11*(1), 17–29. https://doi.org/10.1007/s13167-020-00199-x

Borg, G. A. v. (1982). Psychophysical bases of perceived exertion. *Med Sci Sports Exerc*, *14*(5), 377–381.

Cohen, J. (1988). *Statistical Power Analysis for the Behavioral Sciences, Second Edition*. Routledge.

Costello, J. T., McInerney, C. D., Bleakley, C. M., Selfe, J., & Donnelly, A. E. (2012). The use of thermal imaging in assessing skin temperature following cryotherapy: A review. *Journal of Thermal Biology*, *37*(2), 103–110. https://doi.org/10.1016/j.jtherbio.2011.11.008

Cramer, M. N., & Jay, O. (2016). Biophysical aspects of human thermoregulation during heat stress. *Autonomic Neuroscience: Basic and Clinical*, *196*, 3–13. https://doi.org/10.1016/j.autneu.2016.03.001

Curran, A., Klein, M., Hepokoski, M., & Packard, C. (2015). Improving the accuracy of infrared measurements of skin temperature. *Extreme Physiology & Medicine*, *4*(Suppl 1), A140. https://doi.org/10.1186/2046-7648-4-S1-A140

de Andrade Fernandes, A., dos Santos Amorim, P. R., Brito, C. J., de Moura, A. G., Moreira, D. G., Costa, C. M. A., Sillero-Quintana, M., & Marins, J. C. B. (2014). Measuring skin temperature before, during and after exercise: A comparison of thermocouples and infrared thermography. *Physiological Measurement*, *35*(2), 189.

de Jesus Guirro, R. R., Oliveira Lima Leite Vaz, M. M., das Neves, L. M. S., Dibai-Filho, A. V., Carrara, H. H. A., & de Oliveira Guirro, E. C. (2017). Accuracy and Reliability of Infrared Thermography in Assessment of the Breasts of Women Affected by Cancer. *Journal of Medical Systems*, *41*(5), 87. https://doi.org/10.1007/s10916-017-0730-7

dos Santos Bunn, P., Elisa Koppke Miranda, M., Inoue Rodrigues, A., de Souza Sodré, R., Borba Neves, E., & Bezerra da Silva, E. (2020). Infrared

thermography and musculoskeletal injuries: A systematic review with meta-analysis. *Infrared Physics & Technology*, 103435. https://doi.org/10.1016/j.infrared.2020.103435

Fernández-Cuevas, I., Bouzas Marins, J. C., Arnáiz Lastras, J., Gómez Carmona, P. M., Piñonosa Cano, S., García-Concepción, M. Á., & Sillero-Quintana, M. (2015). Classification of factors influencing the use of infrared thermography in humans: A review. *Infrared Physics & Technology*, *71*, 28–55. https://doi.org/10.1016/j.infrared.2015.02.007

Gauci, J., Falzon, O., Formosa, C., Gatt, A., Ellul, C., Mizzi, S., Mizzi, A., Sturgeon Delia, C., Cassar, K., Chockalingam, N., & Camilleri, K. P. (2018). Automated Region Extraction from Thermal Images for Peripheral Vascular Disease Monitoring. *Journal of Healthcare Engineering*, *2018*. https://doi.org/10.1155/2018/5092064

Gómez-Carmona, P., Fernández-Cuevas, I., Sillero-Quintana, M., Arnaiz-Lastras, J., & Navandar, A. (2020). Infrared Thermography Protocol on Reducing the Incidence of Soccer Injuries. *Journal of Sport Rehabilitation*, 1–6. https://doi.org/10.1123/jsr.2019-0056

Havenith, G., & Lloyd, A. B. (2020). Counterpoint to “Infrared cameras overestimate skin temperature during rewarming from cold exposure.” *Journal of Thermal Biology*, *92*, 102663. https://doi.org/10.1016/j.jtherbio.2020.102663

Hildebrandt, C., Raschner, C., & Ammer, K. (2010). An overview of recent application of medical infrared thermography in sports medicine in Austria. *Sensors*, *10*(5), 4700–4715.

699 Hillen, B., Pfirrmann, D., Nägele, M., & Simon, P. (2020). Infrared Thermography
700 in Exercise Physiology: The Dawning of Exercise Radiomics. *Sports*
701 *Medicine (Auckland, N.Z.)*, *50*(2), 263–282.
702 https://doi.org/10.1007/s40279-019-01210-w
703 ISO. (2008a). *18434-1:2008: Condition monitoring and diagnostics of machines*
704 *– Thermography – Part 1: General procedures*.
705 ISO. (2008b). *Particular requirements for the basic safety and essential*
706 *performance of screening thermographs for human febrile temperature*
707 *screening*. *TC121/SC3-IEC SC62D*.
708 ISO. (2009). *Medical Electrical Equipment-Deployment, implementation and*
709 *operational guidelines for identifying febrile humans using a screening*
710 *thermograph*. *TR 13154:2009 ISO/TR 8-600*.
711 Jones, B. F. (1998). A reappraisal of the use of infrared thermal image analysis
712 in medicine. *IEEE Transactions on Medical Imaging*, *17*(6), 1019–1027.
713 https://doi.org/10.1109/42.746635
714 Kirimtat, A., Krejcar, O., Selamat, A., & Herrera-Viedma, E. (2020). FLIR vs SEEK
715 thermal cameras in biomedicine: Comparative diagnosis through infrared
716 thermography. *BMC Bioinformatics*, *21*(Suppl 2).
717 https://doi.org/10.1186/s12859-020-3355-7
718 Lahiri, B. B., Bagavathiappan, S., Jayakumar, T., & Philip, J. (2012). Medical
719 applications of infrared thermography: A review. *Infrared Physics &*
720 *Technology*, *55*(4), 221–235.
721 Liu, X., Feng, J., Luan, J., Dong, C., Fu, H., & Wu, Z. (2020). Intra- and Interrater
722 Reliability of Infrared Image Analysis of Facial Acupoints in Individuals with

Facial Paralysis. *Evidence-Based Complementary and Alternative Medicine : ECAM*, *2020*. https://doi.org/10.1155/2020/9079037

Menezes, P., Rhea, M. R., Herdy, C., & Simão, R. (2018). Effects of Strength Training Program and Infrared Thermography in Soccer Athletes Injuries. *Sports*, *6*(4). https://doi.org/10.3390/sports6040148

Moreira, D. G., Costello, J. T., Brito, C. J., Adamczyk, J. G., Ammer, K., Bach, A. J. E., Costa, C. M. A., Eglin, C., Fernandes, A. A., Fernández-Cuevas, I., Ferreira, J. J. A., Formenti, D., Fournet, D., Havenith, G., Howell, K., Jung, A., Kenny, G. P., Kolosovas-Machuca, E. S., Maley, M. J., … Sillero-Quintana, M. (2017). Thermographic imaging in sports and exercise medicine: A Delphi study and consensus statement on the measurement of human skin temperature. *Journal of Thermal Biology*, *69*, 155–162. https://doi.org/10.1016/j.jtherbio.2017.07.006

Nahm, F. S. (2013). Infrared Thermography in Pain Medicine. *The Korean Journal of Pain*, *26*(3), 219–222. https://doi.org/10.3344/kjp.2013.26.3.219

Nguyen, A. V., Cohen, N. J., Lipman, H., Brown, C. M., Molinari, N.-A., Jackson, W. L., Kirking, H., Szymanowski, P., Wilson, T. W., Salhi, B. A., Roberts, R. R., Stryker, D. W., & Fishbein, D. B. (2010). Comparison of 3 Infrared Thermal Detection Systems and Self-Report for Mass Fever Screening. *Emerging Infectious Diseases*, *16*(11), 1710–1717. https://doi.org/10.3201/eid1611.100703

Priego Quesada, J. I., Kunzler, M. R., & Carpes, F. P. (2017). Methodological Aspects of Infrared Thermography in Human Assessment. In *Application of Infrared Thermography in Sports Science* (pp. 49–79). Springer

International Publishing. http://link.springer.com/chapter/10.1007/978-3-319-47410-6_3

Priego Quesada, J. I., Martínez Guillamón, N., Cibrián Ortiz de Anda, R. M., Psikuta, A., Annaheim, S., Rossi, R. M., Corberán Salvador, J. M., Pérez-Soriano, P., & Salvador Palmer, R. (2015). Effect of perspiration on skin temperature measurements by infrared thermography and contact thermometry during aerobic cycling. *Infrared Physics & Technology*, *72*, 68–76. https://doi.org/10.1016/j.infrared.2015.07.008

Requena-Bueno, L., Priego-Quesada, J. I., Jimenez-Perez, I., Gil-Calvo, M., & Perez-Soriano, P. (2020). Validation of ThermoHuman automatic thermographic software for assessing foot temperature before and after running. *Journal of Thermal Biology*, 102639. https://doi.org/10.1016/j.jtherbio.2020.102639

Rossignoli, I., Fernández-Cuevas, I., Benito, P. J., & Herrero, A. J. (2016). Relationship between shoulder pain and skin temperature measured by infrared thermography in a wheelchair propulsion test. *Infrared Physics & Technology*, *76*, 251–258.

Shrout, P. E., & Fleiss, J. L. (1979). Intraclass correlations: Uses in assessing rater reliability. *Psychological Bulletin*, *86*(2), 420–428. https://doi.org/10.1037/0033-2909.86.2.420

Silva, N. C. M., Castro, H. A., Carvalho, L. C., Chaves, É. C. L., Ruela, L. O., & Iunes, D. H. (2018). Reliability of Infrared Thermography Images in the Analysis of the Plantar Surface Temperature in Diabetes Mellitus. *Journal of Chiropractic Medicine*, *17*(1), 30–35. https://doi.org/10.1016/j.jcm.2017.10.006

772 Steketee, J. (1973). Spectral emissivity of skin and pericardium. *Physics in*
773 *Medicine and Biology*, *18*(5), 686.
774 Tan, L. L., Sanjay, S., & Morgan, P. B. (2016). Repeatability of infrared ocular
775 thermography in assessing healthy and dry eyes. *Contact Lens and*
776 *Anterior Eye*, *39*(4), 284–292. https://doi.org/10.1016/j.clae.2016.01.010
777 Usamentiaga, R., Venegas, P., Guerediaga, J., Vega, L., Molleda, J., & Bulnes,
778 F. G. (2014). Infrared Thermography for Temperature Measurement and
779 Non-Destructive Testing. *Sensors (Basel, Switzerland)*, *14*(7), 12305–
780 12348. https://doi.org/10.3390/s140712305
781 Vardasca, R. (2019). Are the IR cameras FLIR ONE suitable for clinical
782 applications? *Thermology International*, *23*(3), 95–102.
783 Villa, E., Arteaga-Marrero, N., & Ruiz-Alzola, J. (2020). Performance Assessment
784 of Low-Cost Thermal Cameras for Medical Applications. *Sensors (Basel,*
785 *Switzerland)*, *20*(5). https://doi.org/10.3390/s20051321
786 Weir, J. P. (2005). Quantifying test-retest reliability using the intraclass correlation
787 coefficient and the SEM. *Journal of Strength and Conditioning Research /*
788 *National Strength & Conditioning Association*, *19*(1), 231–240.
789 https://doi.org/10.1519/15184.1

CAPÍTULO V

ARTIGO ORIGINAL

Can infrared thermography serve as an alternative to assess cumulative fatigue?

Álvaro Sosa Machado[1], Willian da Silva[1], Jose Ignacio Priego-Quesada[2], Felipe P Carpes[1]*

1 Applied Neuromechanics Group, Laboratory of Neuromechanics, Federal University of Pampa, Uruguaiana, Brazil.

2 Research Group in Sports Biomechanics (GIBD), Department of Physical Education and Sports, University of Valencia, Valencia, Spain.

5.1 Abstract

Fatigue muscle requires recovery time to return to normal performance. By not allowing that time and exercising again, we produce cumulative fatigue. Would infrared thermography (IRT) of the skin be able to indicate the effects of cumulative fatigue? In this article, we recruited 21 untrained women and induced cumulative fatigue in biceps brachii over two consecutive days of exercise. We measured delayed onset muscle soreness (DOMS), maximal strength, and IRT. On the day following cumulative fatigue induction, muscle strength remains reduced and DOMS remains elevated. The IRT indicated that the arm under cumulative fatigue has a higher temperature for minimum and mean temperature, being asymmetrical in relation to the control arm, mainly in the calculation of variation between the situation without and the situation with fatigue. The variation of the minimum and average temperatures correlated with the strength loss. In summary, IRT seems to be able to detect cumulative fatigue, being useful to explain strength losses and reduce injury risks.

Keywords: Exercise recovery, Muscle damage, Muscle fatigue, Skin temperature.

5.2 Introduction

Muscle fatigue is a physiological and transient phenomenon that reduces the ability of the skeletal muscle to produce and sustain strength production through voluntary contractions (Enoka and Duchateau, 2008). The process to recover from muscle damage resulting from fatigue takes place over time, requiring a period of rest to optimize muscle regeneration (Fredsted et al., 2008). When the muscle reaches the fatigue condition and the rest period is not allowed until a new exercise demand is imposed, a situation of cumulative fatigue is created (Rodríguez-Marroyo et al., 2017). We know that as a result of cumulative fatigue, there is a persistence of oxidative stress (Pizzino et al., 2017), intensification of muscle damage (Proske and Morgan, 2001), and an imbalance in muscle contractility parameters (Machado et al., 2018). All these consequences expose the musculature to an increased risk of injury and reduced ability to maintain performance (Proske and Morgan, 2001; Rodríguez-Marroyo et al., 2017).

Recently, this particularity of muscle physiology has been drawing attention due to the importance of knowing the conditions of possible muscle injuries and the need to plan a more efficient exercise period. Full body training on consecutive days is already known to be safe in terms of torque recovery and overall neuromuscular performance (Marshall et al., 2021). On the other hand, if muscle demand is imposed to exhaustion on consecutive days, the recovery pattern changes, and performance in terms of maximum strength can remain depressed for several days (Stewart et al., 2008). It becomes evident that monitoring exercise recovery is a useful approach to safely administrating exercise and training loads by both improving strategies for recovery and

anticipating the loss of performance (Mujika, 2017). However, it can be difficult to implement because requires several markers to be monitored. Muscle fatigue elicits high levels of oxidative stress, muscle damage, and inflammation (Accattato et al., 2017; MacIntyre et al., 1995; Proske and Morgan, 2001). In addition to the cost per sample and the need for high-precision readers, biochemical measurement has the disadvantage of requiring invasive procedures (Baird et al., 2012), while other techniques to monitor muscle activity like electromyography requires sophisticated data processing (Cifrek et al., 2009).

As the experimental muscle generates an inflammatory process it could increase the skin temperature (Cheung et al., 2003) which could be measured by infrared thermography (IRT), a non-invasive and affordable image technique for measuring skin temperature (Machado et al., 2021). This technique has been used in the context of sports medicine mainly to detect muscle injuries based on thermal asymmetry during baseline analysis (Fernández-Cuevas et al., 2017; Gómez-Carmona et al., 2020). However, although some studies have also tried to find a correlation between muscle damage and skin temperature in fatigue induction protocols, the no alteration of baseline skin temperature on the posterior days after muscle damage induction or its evolution during exercise not related to fatigue manifestation do not support IRT as a muscle damage or fatigue diagnostic method (Willian da Silva et al., 2018; Priego-Quesada et al., 2020). On the other hand, Korman et al (2021) found that exercises performed on consecutive days reduced baseline skin temperature. However, the exercise sequence interspersed power, resistance, and endurance exercises, which may have generated an alternation of focused muscles and therefore some periodic rest throughout the days (2021).

In this sense, we hypothesized that IRT would indicate the effects of cumulative fatigue on the muscle by changes in skin temperature. The objective of this study was to reproduce a situation of cumulative fatigue and to determine whether infrared thermography can assess its effects by serving as a monitoring tool.

5.3 Material and methods

We recruited 21 women from the local community (age of 23.6 ± 3 years old, body mass of 60.3 ± 9 kg, and height of 1.61 ± 0.4 m). A sample size of 21 untrained participants was estimated using the G * Power 3.1 software (University of Düsseldorf, Düsseldorf, Germany) and considering a repeated measures ANOVA design, with 90% power, α error of 0.05, and an effect size of 0.26 for data changes in skin temperature (Faul et al., 2007). To be included, they must have not performed any systematic physical exercise program for at least the previous three months and had not performed any exercise for at least three weeks before the measurements, and be free from severe injuries in the lower extremity in the last six months. In addition, they should not make use of any drug whose composition included anti-inflammatory, analgesic, or stimulant substances. Furthermore, the participants were instructed not to consume energy drinks, stimulants, food supplements, infusions, and fruits for one week before the end of the testing period (Priego Quesada, 2017). All participants signed a consent term following the Declaration of Helsinki and were approved by the local University Ethics Committee (registration number: IRB 60376216.4.0000.5323).

5.3.1. Protocol

The protocol consisted of 3 consecutive days of laboratory visits. On the first two days, exercises were performed to induce muscle fatigue in the non-dominant biceps brachii, thus generating the condition of cumulative fatigue on the third day. On day 1, baseline IRT measurements of the biceps brachii were performed bilaterally, in addition to the assessment of isometric maximal voluntary strength, and delayed onset muscle soreness (DOMS) was assessed at rest and under palpation. Isometric maximal voluntary strength was also performed after the fatigue induction on day 1. On day 2, no strength measurements were performed, but we evaluated IRT and DOMS. On day 3, we performed the IRT, DOMS, and strength measurement. Figure 1 shows the measurements performed for days 1, 2, and 3.

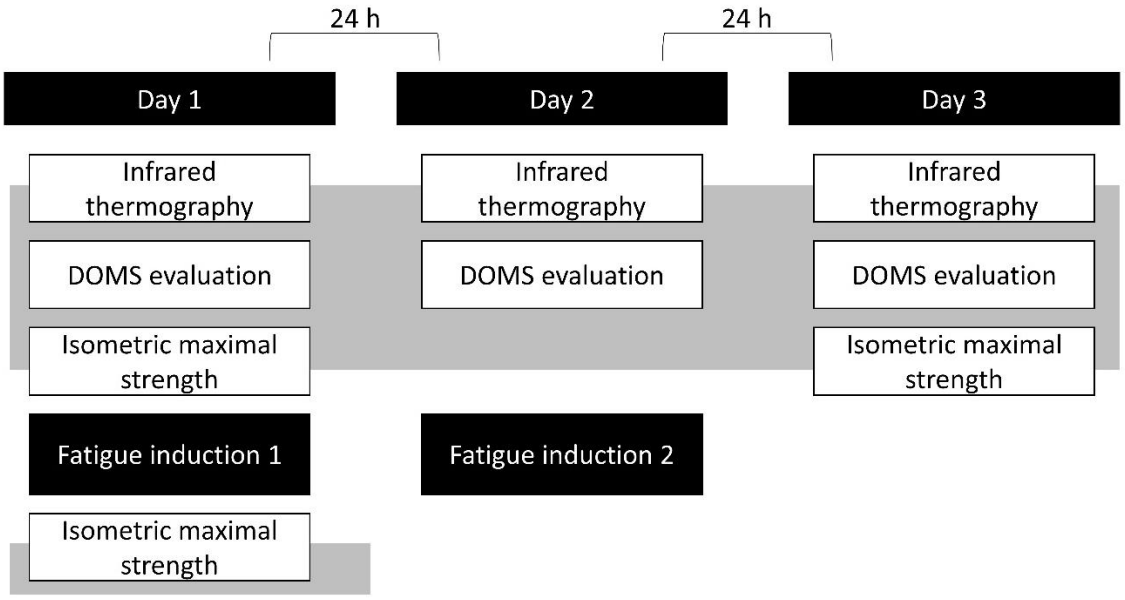

Figure 1. The illustration details the three days of evaluations performed. On the first two days, muscle fatigue was induced. On the third day, measurements were performed under the condition of cumulative fatigue. DOMS: delayed onset muscle soreness.

5.3.2 Exercise protocol

We induced cumulative muscle fatigue in the biceps brachii of the non-preferred arm of the participants. They were seated on a chair, with posture adjusted to keep the spine straight, arms along the body, hips, and knees flexed at 90º, and feet parallel aligned with the hips width (Oliveira et al., 2009). The task was to perform a bicep curl with a 2 kg dumbbell under a rhythm controlled by the beep of a metronome at 20 bpm, and the exercise range of motion was from the maximal elbow extension to the maximal elbow flexion, with 50% of the cycle involving an eccentric action (Marri and Swaminathan, 2016). The load was fixed and standardized and the target exercise volume was the maximum for each participant, guaranteeing the production of muscle damage and DOMS (Uchida, 2008).

They were instructed to perform as many repetitions as possible in an initial set. After 60 seconds of rest, they were instructed to perform successive secondary sets with 60 seconds of rest in between. Each secondary series should be performed to a achieve number of repetitions between 50% and 75% of the number of repetitions in the initial series. If the participant exceeded 75% of repetitions, the series was interrupted, and a new rest period was respected. If the participant did not reach 50% of the initial set, we considered that a fatigue condition was reached. The measurement was also terminated when the participant could not maintain the expected pattern for the movement (Priego-Quesada et al., 2020). Verbal encouragement was provided during the exercise. We multiplied the total number of protocol repetitions by the sets number and by

the load to determine the work volume performed on each fatigue-inducing day (Machado et al., 2022).

5.3.3 Infrared thermography

Skin temperature was quantified using an IRT camera (resolution of 320 x 240 pixels, NETD <0.05 °C, and measurement uncertainty of ± 2°C or 2%, E-60 model, Flir Systems Inc., Wilsonville, Oregon, USA). The camera was turned on at least 10 min before the evaluations. All images were captured at 1 m far from the participant and with the camera lens positioned perpendicular to the region of interest (ROI).

We defined the biceps brachii zones bilaterally as ROIs to analyze asymmetries. The demarcation of the ROIs had the axillary cleavage as a starting point, with a vertical line drawn up to the upper edge of the arm, which contoured the arm inferiorly until it found the upper line of the antecubital fossa of the elbow. Then, the line was conducted transversally to the arm up to the medial border, and, finally, it followed superiorly until finding the starting point (Figure 2). Since the position of the axillary cleavage can vary for each person according to their posture and body composition, we decided to superiorly contour the biceps and include the anterior deltoid in the ROI rather than risk losing some portion of the biceps brachii.

Participants were positioned at the evaluation site for at least 10 min before taking thermal images for acclimatization to the temperature and relative humidity conditions of the laboratory air (Priego Quesada, 2017). On the other hand, IRT post-measurement measurements were performed immediately after the completion of the protocol. All thermal images were collected in an air-conditioned

and controlled environment with room temperature 24.4 ± 1.6 ºC and air humidity 39.0 ± 8.4 %. All procedures followed the Thermographic Imaging in Sports and Exercise Medicine (TISEM) checklist (Moreira et al., 2017). The same researcher performed all image records. Infrared images were processed using commercial software (Thermacam Researcher Pro 2.10 software, FLIR, Wilsonville, Oregon, USA). From each ROI, we extract the values of the minimum, maximum, and mean temperature variables. Subsequently, we calculated skin temperature variation (ΔT) between day 3 and day 1 for each IRT variable.

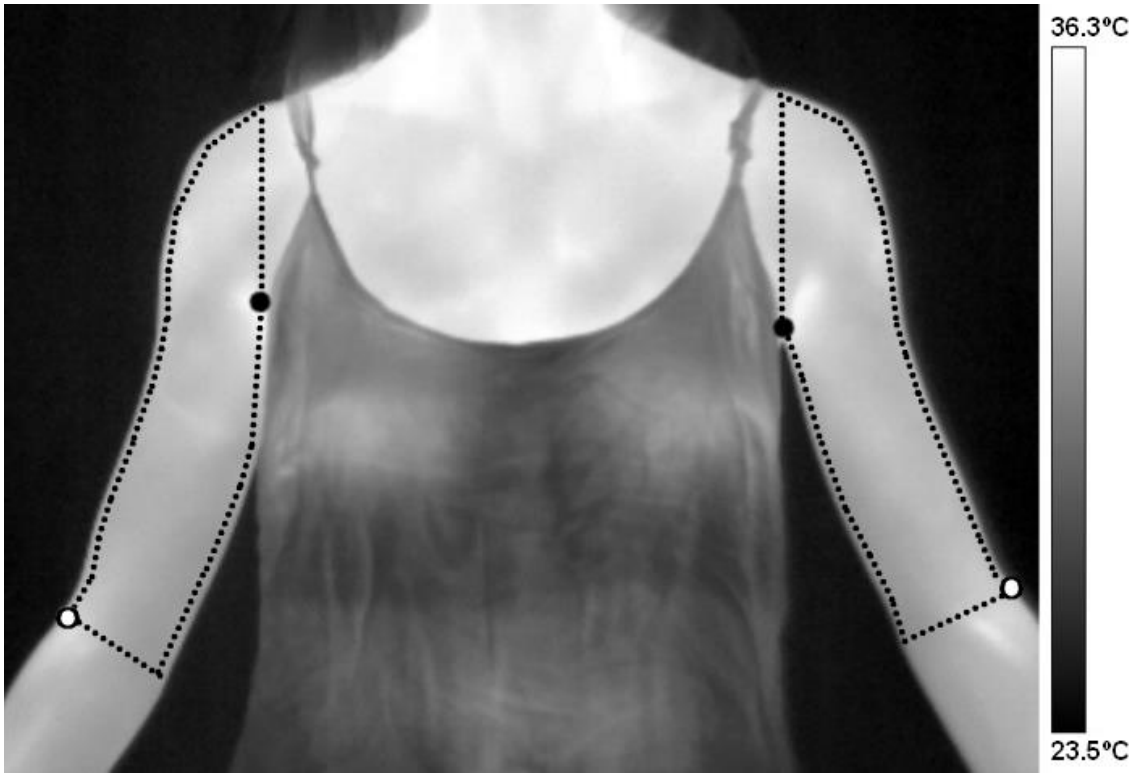

Figure 2. Regions of interest (ROIs) determined by the dotted lines for each arm. We considered the axillary cleavage as the initial reference (black circle) and the upper edge of the antecubital fossa as the lower limit reference (white circle).

5.3.4 Delayed onset muscle soreness

DOMS was assessed using a numeric pain rating scale (NPRS) based on a verbally reported soreness intensity score from 0 (minimum) to 10 (maximum) (Hawker et al., 2011). After familiarizing themselves with the scale, the participants were evaluated in two conditions: a) at rest, being asked about the intensity of soreness while the experimental arm was resting on the chair guard and without any movement or stimulus; and b) under palpation, in which soreness was rated after palpation of biceps brachii belly with similar intensity for all participants (W. da Silva et al., 2018). DOMS assessments were always performed by the same researcher.

5.3.5 Muscle strength assessment

We evaluated the maximal voluntary isometric strength during elbow flexion using load cell sampling force signals at 2000 Hz (Miotec Biomedical Inc., Porto Alegre, Brazil). The load cell was attached in the middle of a chain fixed to the ground and held by the hand of the participant at the other end with a handle. The strength assessment was performed with the same positioning and posture as for the fatigue induction exercise, except for the arm positioned at 90º of elbow flexion (Oliveira et al., 2009).

After familiarization with the setup by performing up to 3 repetitions and making themselves comfortable seated, the participant was instructed to produce the maximum strength by pulling the handle and sustaining the contraction for approximately 5 seconds. Verbal commands were used to start, stimulate the maximum, and end each attempt. A 60-seconds rest was allowed between attempts. Three attempts were performed if the last attempt did not have the

maximum strength value. In these cases, a new attempt was made, and the initial one was discarded.

We evaluated maximum strength in 3 moments: on day 1 pre-fatigue induction, on day 1 post-fatigue induction, and on day 3 (under the effect of cumulative fatigue from days 1 and 2). From each moment, we extracted the mean maximum strength of the three validated attempts registered. Strength was normalized by body mass (kg.f/kg).

5.3.6 Statistical analysis

Data are expressed as mean and standard deviation. The normality of the data distribution was verified with the Shapiro-Wilk test. The results of normalized strength and DOMS at palpation were compared between the different days with one-way ANOVA and post-hoc Bonferroni. DOMS at rest were compared with the Kruskal-Wallis test and Dunn's multiple comparisons. The work volume was compared between days 1 and 2 with a paired t-test. Minimum, mean, and maximum skin temperatures had main effects and interactions between days of the measurement (1 vs. 2 vs. 3) and arm (experimental vs. experimental) verified with two-way ANOVA and post-hoc Bonferroni. The effect size index f (ESf) was calculated for the main ANOVA results and determined as small (0.1-0.25), medium (0.25-0.4), and large (>0.4). The Cohen's *d* effect size (ES*d*) was determined for t-test and post-hoc and classified as small (0.01-0.059), medium (0.06-0.139), and large (≥ 0.14) (Cohen, 2013). We performed simple linear regression to verify the relationship between each IRT variable and strength loss. Finally, we analyzed the asymmetries between the experimental and control arms for the temperature variation data between day 1 and day 3 (Δ day 3 -day 1) with

paired t-test. The significance level was set at 0.05 for all analyses using the SPSS version 26 (SPSS Inc., Chicago, IL, US).

5.4 Results

5.4.1 Muscle strength, work volume, and doms

Maximal isometric strength was impaired by the fatigue induction with acute effects on day 1 post [$F_{(2,20)}$ = 55.980; $p < 0.001$; ESf = 0.78, Figure 3.a], persistent up to day 3 [$F_{(2,20)}$ = 55.980; $p < 0.001$; ESf = 0.34, Figure 3.a]. Although the acute effect of fatigue was recovered day 3 later with higher muscle strength values than day 2 [$F_{(2,20)}$ = 55.980; $p < 0.001$; ESf = 0.43, Figure 3.a], these values still was not recovered to the basal levels, supporting the persistent effect of cumulative fatigue. Work volume decreased on the second day of fatigue induction [$t_{(1,20)}$ = 4.191; $p < 0.001$; ES*d* = 0.03, Figure 3.b].

DOMS at rest increased from day 1 to day 3 [$H_{(5)}$ = 50.08; $p < 0.001$; ES*d* = 0.59, Figure 3.c]. Cumulative fatigue also resulted in higher DOMS at palpation from day 1 to day 2 [$F_{(5,20)}$ = 30.120; $p < 0.001$; ES*d* = 0.24, Figure 3.d] and day 3 [$F_{(5,20)}$ = 30.120; $p < 0.001$; ES*d* = 0.59, Figure 3.d].

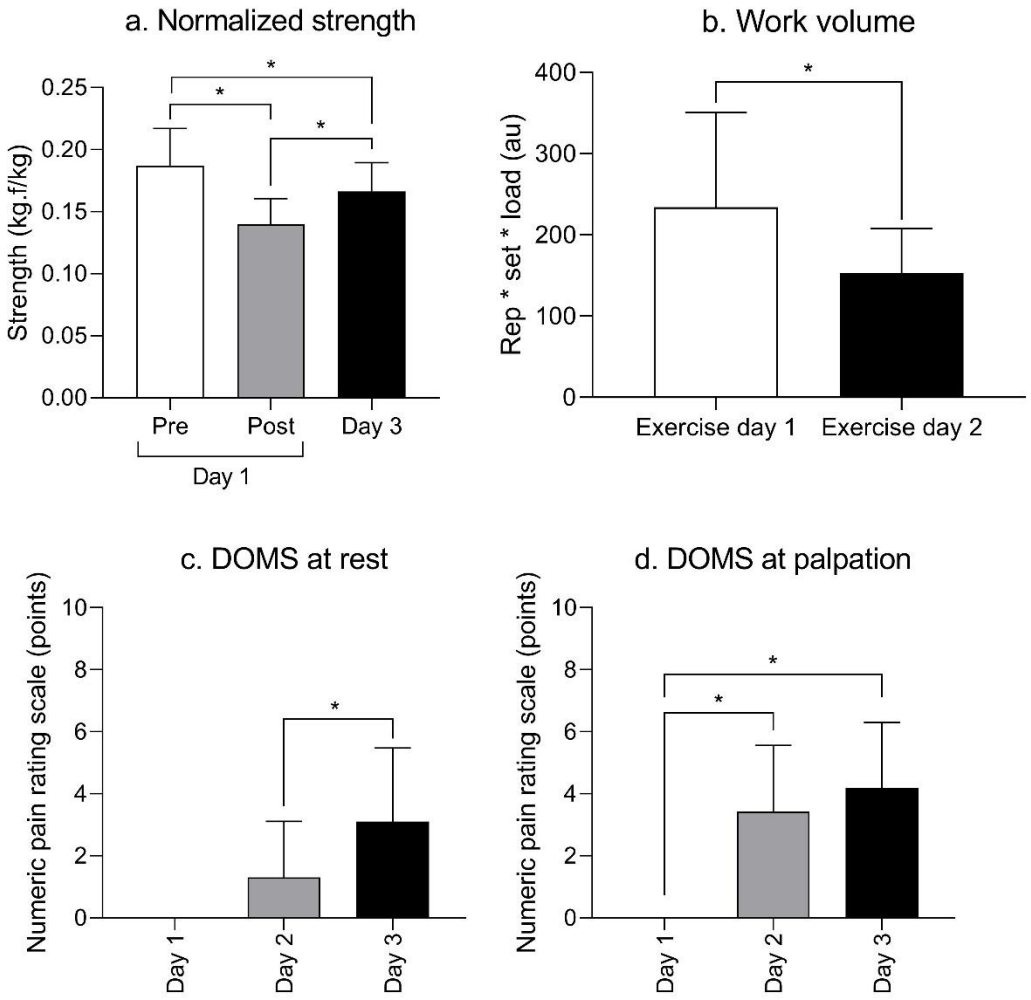

Figure 3. Mean (bars) and standard deviation (vertical lines) values for (a) maximal isometric strength normalized to the individual body mass, (b) work volume in arbitrary units (au), (c) delayed onset muscle soreness (DOMS) at rest and (d) DOMS at palpation. NRPS: numeric rate pain scale. For strength and DOMS results. * means $p < 0.05$.

5.4.2 Skin temperature

Minimum temperature showed main effects for day [$F = 4.992$; $p = 0.018$, $f = 0.72$]. We observed that the experimental arm showed an increase in the minimum temperature from day 1 to day 3 [$F_{(1,20)} = 6.931$; $p = 0.003$; ES*d* = 0.92, Figure 4.a]. Comparing arms for each day, we observed an asymmetry at day 1,

with lower values found for the experimental arm [$F_{(1,20)}$ = 12.397, p = 0.002; ES*d* = 0.59, Figure 4.a].

Mean temperature showed main effects for arm [F = 9.819; p = 0.005; ESf = 0.16] and day [F = 11.177; p = 0.001; ESf = 0.63]. Comparing temperature variation for each arm at each day, we observed that the experimental arm showed an increase in the mean temperature from day 1 to day 2 [$F_{(1,20)}$ = 7.578; p = 0.040; ES*d* = 0.47, Figure 4.b] and from day 1 to day 3 [$F_{(1,20)}$ = 7.578; p = 0.003; ES*d* = 0.76, Figure 4.b]. For control arm we observed increase in mean temperature from day 1 to day 2 [$F_{(1,20)}$ = 7.578; p = 0.028; ES*d* = 0.38, Figure 4.b], and from day 1 to day 3 [$F_{(1,20)}$ = 7.578; p = 0.004; ES*d* = 0.70, Figure 4.b].

In asymmetries analysis, we saw experimental arm with higher values at day 1 [$F_{(1,20)}$ = 7.517, p = 0.013; ES*d* = 0.18, Figure 4.b]. On day 2, experimental arm showed higher values [$F_{(1,20)}$ = 28.623, p < 0.001; ES*d* = 0.20, Figure 4.b]. Finally, at day 3, experimental arm had higher values at [$F_{(1,20)}$ = 10.535, p = 0.004; ES*d* = 0.25, Figure 4.b].

For maximal temperature, no effect for arm [$F_{(1,20)}$ = 2.284, p = 0.146, Figure 4.c] nor day [$F_{(1,20)}$ = 2.298, p = 0.128, Figure 4.c] were found.

The Δ day 3 - day 1 shows the temperature of experimental arm higher than control for minimum [$t_{(1,20)}$ = 3.030; p = 0.007; ES*d* = 0.58], maximum [$t_{(1,20)}$ = 10.965; p < 0.001; ES*d* = 0.90] and mean temperatures [$t_{(1,20)}$ = 4.834; p < 0.001; ES*d* = 0.98].

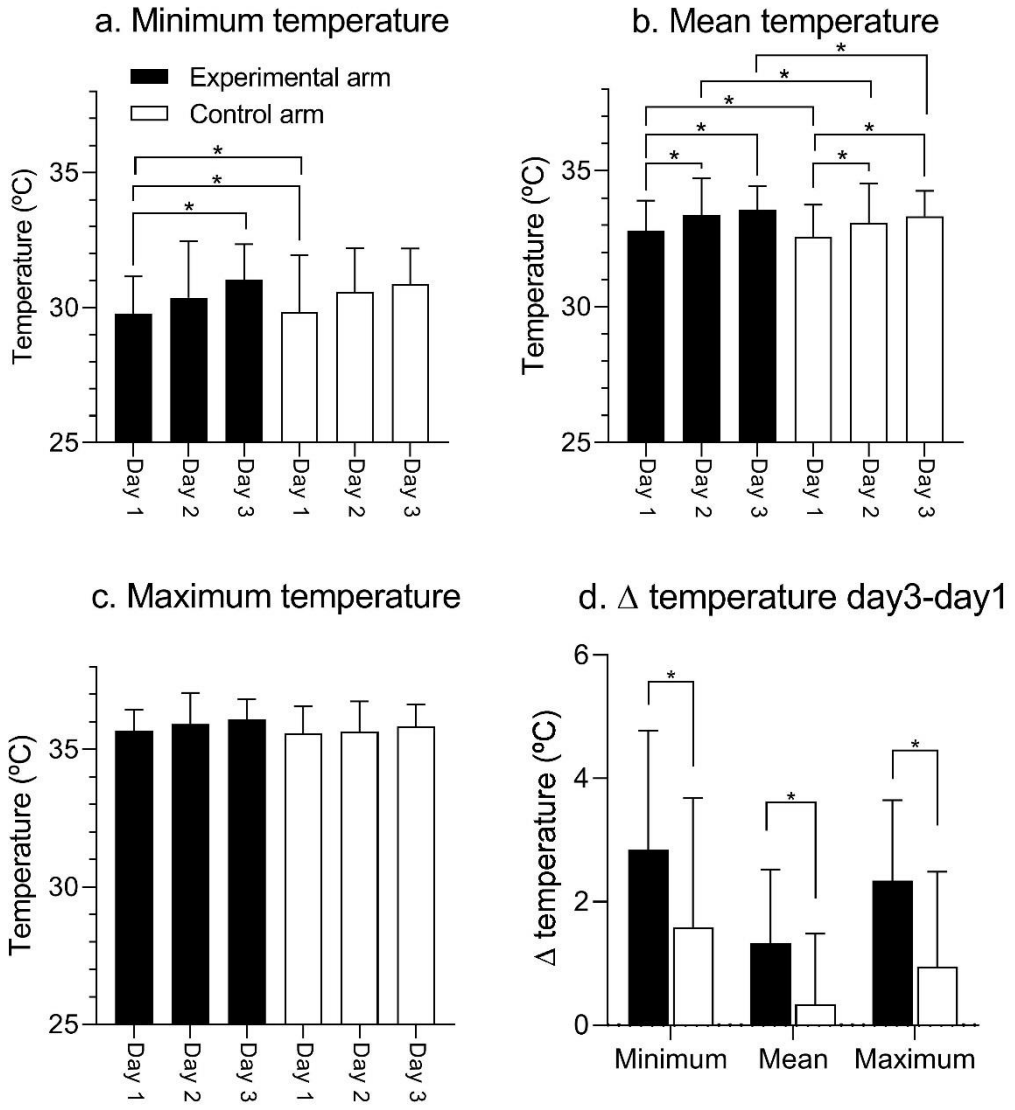

Figure 4. Mean (bars) and standard deviation (vertical lines) data of (a) minimum, (b) mean, and (c) maximum temperatures for days 1, 2, and 3 in the experimental and control arms. (c) Difference between the temperature on day 3 and day 1 (Δd3-d1) for each variable. * means $p < 0.05$.

5.4.3 Relationship between muscle strength and skin temperature

Simple linear regression was calculated to predict participant's strength loss based on their mean temperature variation. For minimum temperature a

significant regression equation was found [$F_{(1,19)}$= 6.591, p = 0.020], with an R^2 of 0.251. Participants' predicted strength loss (in %) is equal to 0.098 * (mean temperature variation in ºC) + 3.868. Also for mean temperature a significant regression equation was found [$F_{(1,20)}$= 6.531, p = 0.019], with an R^2 of 0.255. Participants' predicted strength loss (in %) is equal to 0. 067 * (mean temperature variation in ºC) + 3.043. Finally, for maximum temperature no significant regression was found [$F_{(1,20)}$= 0.468, p = 0.501].

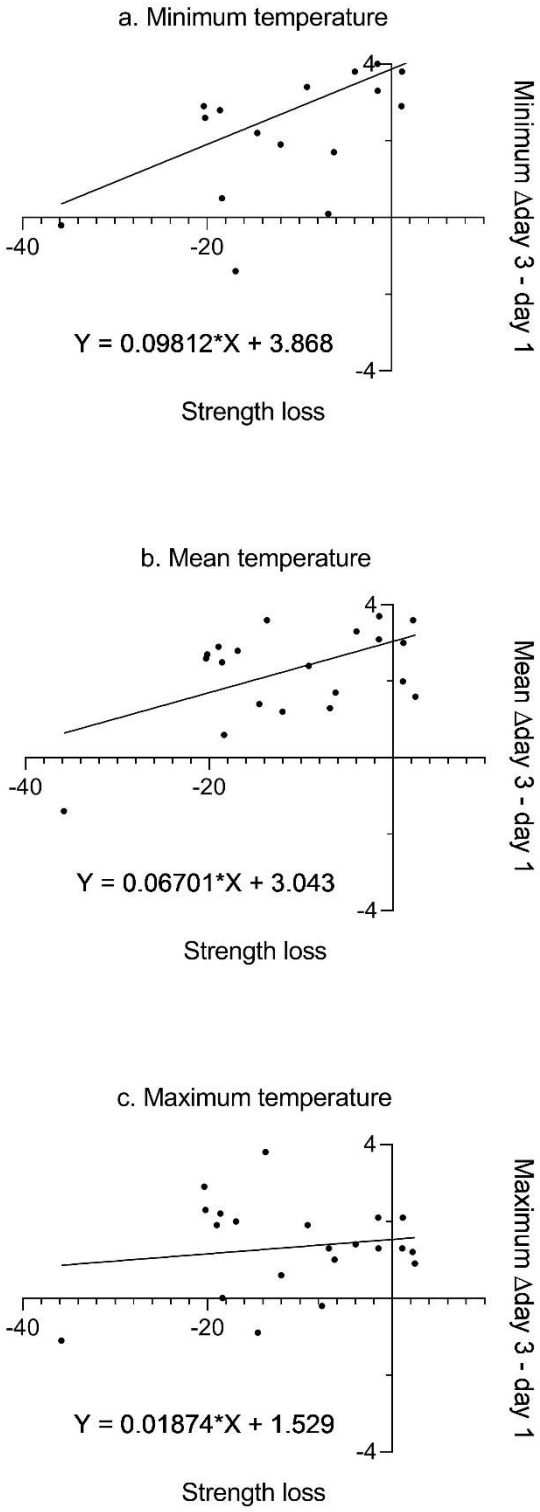

Figure 5. Simple linear regression plot for strength loss (%) and IRT ∆ day 3 - day 1 for minimum, mean and maximum temperature.

5.4 Discussion

In this study, we induced a condition of cumulative fatigue in the biceps brachii muscle and observed the feasibility of using IRT as a monitoring tool considering fatigue effects on muscle strength and DOMS. The cumulative fatigue resulted in delayed onset muscle soreness, a major marker of muscle damage, and significant muscle strength loss, a major marker for performance impairment. It was possible to relate the effects of cumulative fatigue with IRT outcomes, with higher temperatures observed in the experimental arm, and the correlation between the minimum and with the mean temperatures with muscle strength loss.

Cumulative fatigue reduced the maximal work volume performed. In the same sense, maximal isometric strength was also reduced by the fatigue induction protocol. During the three days of testing, strength capacity recovery is not able to achieve the basal performance, which we argue resultant of the magnitude of muscle damage and the fact that an adequate recovery time was not administrated (Fernandes et al., 2019). This disruption of the regeneration process potentiates inflammation and oxidative stress, factors that negatively affect muscle strength (MacIntyre et al., 1995; Prochniewicz et al., 2008).

In previous studies, a period of 48 h following strenuous exercise was associated with higher activity of both stress oxidative and damage markers for different muscles, including triceps sural (Willian da Silva et al., 2018) and quadriceps muscles (Machado et al., 2018). Our protocol also generated DOMS under spontaneous and under palpation conditions indicating that the protocol induced muscle damage. DOMS results from the sensitization of nociceptors as a result of the inflammatory process (Basbaum et al., 2009), which in turn

happens to regenerate muscle damage (Peake et al., 2017). Added together, the results of reduced workload, loss of maximal isometric strength, and development of DOMS confirm the cumulative fatigue situation of our protocol.

Observing the behavior of the IRT over the 3 days of measurements, we saw higher minimum and mean temperatures on day 3 compared to day 1 in the experimental but not in the control arm. This pattern is different from what occurred in protocols with a single day of exercise, in which the temperature 48 h after exercise did not differ from baseline values (DE Almeida Barros et al., 2020). Probably, exercises performed on consecutive days in our protocol prevented muscle recovery, and IRT seems to be able to detect the heat produced by the inflammatory process on the third day of measurements, a cumulative fatigue effect. Since muscle contraction during fatigue induction occurs over large areas of muscle (Marco et al., 2017), if the temperature rises because of inflammatory processes resulting from muscle damage, it is expected that the minimum temperature will be higher than without fatigue and that the mean temperature of the entire ROI is pulled up.

The control arm showed some variations in mean IRT over the days, with the temperature on the second and third day being higher than that of the first day. Although this limb did not perform any exercise, some temperature change is expected because thermoregulation has systemic effects. (Kenny, 2010). On the other hand, the changes differ from what occurred in the experimental arm, and this difference was confirmed by the asymmetry analysis mainly because the temperature of the experimental arm was higher than that of the control on the third day. Also, for this reason, we suggest that the conclusions of studies with IRT take into account the set of information provided by the different variables.

One way to verify the effects of exercise is the comparison between the experimental arm and the control arm. We found no differences between the experimental arm and the control arm when comparing the mean IRT raw data on day 3, where it would be possible to attest to the situation of accumulated fatigue. After that, we calculated the temperature variation between day 1 and day 3 both for the experimental and control arm, and saw asymmetries for all variables. It seems that the small margin of temperature variation in the post-exercise period prevents the verification of the difference between limbs (Formenti et al., 2016), but by calculating the variation between the days without and with accumulated fatigue, it is possible to affirm the asymmetries.

The identification of changes in skin temperature as related to or dependent on exercise characteristics is difficult due to individual factors that are difficult to control among participants. Previous studies performing cross-sectional measures of temperature in experimental and non-experimental conditions failed to show conclusive IRT outcomes (Côrte et al., 2019; de Carvalho et al., 2021; Menezes et al., 2018), but when the basal temperature measured is combined with a follow-up of measurements after exercise, some stronger conclusions can be drawn (Priego-Quesada et al., 2019). Therefore, the use of IRT to monitor exercise-induced fatigue effects might require repeated measures over different days.

Although the IRT does not seems to have the ability to monitor the development of fatigue in real-time (Bartuzi et al., 2012), and presents conflicting results regarding its ability to relate to DOMS after a proper recovery period (da Silva et al., 2021; W. da Silva et al., 2018; Priego-Quesada et al., 2020), we found that consecutive measurement of IRT can be related to DOMS magnitude. DOMS

is known to be related to loss of strength (Cleak and Eston, 1992), but its restrict to making inter-subject comparisons through subjective scales (Borg, 1982). Therefore, we investigated the direct relationship between IRT variables and strength values. Both minimum and mean but not maximum temperature were related to strength loss. This result is supported by evidence that when performing at a higher temperature, skeletal muscle reduces its ability to produce strength, in addition to being more vulnerable to injury risk (Castellani et al., 2016).

Our study has limitations. DOMS can occur in anyone, but is more likely to happen in sedentary people, which led us to not include physically active people in this study, limiting speculations about similar results in athletes. In addition, it was not possible to alternate the order of the measurements (transferring the situation without exercise to after the accumulated fatigue) since the protocol generated DOMS and waiting for recovery to be able to evaluate the muscle in the situation without fatigue again would take a long time for the participants to bond.

5.5 Conclusions

The Infrared thermography is capable of detecting skin heating due to cumulative fatigue. The minimum and mean skin temperature were related to muscle strength reductions when cumulative fatigue was induced by two consecutive days of exercise. The relationship between skin temperature and strength losses seems promising to help adjust exercise programs and minimize the risk of muscle injury.

5.6 References

Accattato, F., Greco, M., Pullano, S.A., Carè, I., Fiorillo, A.S., Pujia, A., Montalcini, T., Foti, D.P., Brunetti, A., Gulletta, E., 2017. Effects of acute physical exercise on oxidative stress and inflammatory status in young, sedentary obese subjects. PLoS ONE 12, e0178900. https://doi.org/10.1371/journal.pone.0178900

Baird, M.F., Graham, S.M., Baker, J.S., Bickerstaff, G.F., 2012. Creatine-kinase and exercise-related muscle damage implications for muscle performance and recovery. Journal of nutrition and metabolism 2012, 13. https://doi.org/10.1155/2012/960363

Bartuzi, P., Roman-Liu, D., Wiśniewski, T., 2012. The Influence of Fatigue on Muscle Temperature. International Journal of Occupational Safety and Ergonomics 18, 233–243. https://doi.org/10.1080/10803548.2012.11076931

Basbaum, A.I., Bautista, D.M., Scherrer, G., Julius, D., 2009. Cellular and Molecular Mechanisms of Pain. Cell 139, 267–284. https://doi.org/10.1016/j.cell.2009.09.028

Borg, G.A., 1982. Psychophysical bases of perceived exertion. Med Sci Sports Exerc 14, 377–381.

Castellani, J.W., Zambraski, E.J., Sawka, M.N., Urso, M.L., 2016. Does high muscle temperature accentuate skeletal muscle injury from eccentric exercise? Physiol Rep 4, e12777. https://doi.org/10.14814/phy2.12777

Cheung, K., Hume, P.A., Maxwell, L., 2003. Delayed Onset Muscle Soreness: Treatment Strategies and Performance Factors. Sports Medicine 33, 145–164. https://doi.org/10.2165/00007256-200333020-00005

Cifrek, M., Medved, V., Tonkovic, S., Ostojic, S., 2009. Surface EMG based muscle fatigue evaluation in biomechanics. Clin Biomech (Bristol, Avon) 24, 327–40. https://doi.org/10.1016/j.clinbiomech.2009.01.010

Cleak, M.J., Eston, R.G., 1992. Muscle soreness, swelling, stiffness and strength loss after intense eccentric exercise. Br J Sports Med 26, 267–272. https://doi.org/10.1136/bjsm.26.4.267

Cohen, J., 2013. Statistical Power Analysis for the Behavioral Sciences, 0 ed. Routledge. https://doi.org/10.4324/9780203771587

Côrte, A.C., Pedrinelli, A., Marttos, A., Souza, I.F.G., Grava, J., José Hernandez, A., 2019. Infrared thermography study as a complementary method of screening and prevention of muscle injuries: pilot study. BMJ OPEN SP EX MED 5, e000431. https://doi.org/10.1136/bmjsem-2018-000431

da Silva, W., Machado, Á.S., Lemos, A.L., de Andrade, C.F., Priego-Quesada, J.I., Carpes, F.P., 2021. Relationship between exercise-induced muscle soreness, pain thresholds, and skin temperature in men and women. Journal of Thermal Biology 100, 103051. https://doi.org/10.1016/j.jtherbio.2021.103051

da Silva, Willian, Machado, Á.S., Souza, M.A., Kunzler, M.R., Priego-Quesada, J.I., Carpes, F.P., 2018. Can exercise-induced muscle damage be related to changes in skin temperature? Physiol. Meas. 39, 104007. https://doi.org/10.1088/1361-6579/aae6df

da Silva, W., Machado, A.S., Souza, M.A., Mello-Carpes, P.B., Carpes, F.P., 2018. Effect of green tea extract supplementation on exercise-induced delayed onset muscle soreness and muscular damage. Physiology & behavior 194, 5. https://doi.org/10.1016/j.physbeh.2018.05.006

DE Almeida Barros, N., Aidar, F.J., DE Matos, D.G., DE Souza, R.F., Neves, E.B., DE Araujo Tinoco Cabral, B.G., Carmargo, E.A., Reis, V.M., 2020. Evaluation of Muscle Damage, Body Temperature, Peak Torque, and Fatigue Index in Three Different Methods of Strength Gain. Int J Exerc Sci 13, 1352–1365.

de Carvalho, G., Girasol, C.E., Gonçalves, L.G.C., Guirro, E.C.O., Guirro, R.R. de J., 2021. Correlation between skin temperature in the lower limbs and biochemical marker, performance data, and clinical recovery scales. PLoS One 16, e0248653. https://doi.org/10.1371/journal.pone.0248653

Enoka, R.M., Duchateau, J., 2008. Muscle fatigue: what, why and how it influences muscle function. The Journal of physiology 586, 11–23. https://doi.org/10.1113/jphysiol.2007.139477

Faul, F., Erdfelder, E., Lang, A.-G., Buchner, A., 2007. G*Power 3: A flexible statistical power analysis program for the social, behavioral, and biomedical sciences. Behavior Research Methods 39, 175–191. https://doi.org/10.3758/BF03193146

Fernandes, J., Lamb, K., Twist, C., 2019. Exercise-Induced Muscle Damage and Recovery in Young and Middle-Aged Males with Different Resistance Training Experience. Sports 7, 132. https://doi.org/10.3390/sports7060132

Fernández-Cuevas, I., Arnáiz Lastras, J., Escamilla Galindo, V., Gómez Carmona, P., 2017. Infrared Thermography for the Detection of Injury in Sports Medicine, in: Priego Quesada, J.I. (Ed.), Application of Infrared Thermography in Sports Science, Biological and Medical Physics, Biomedical Engineering. Springer International Publishing, Cham, pp. 81–109. https://doi.org/10.1007/978-3-319-47410-6_4

Formenti, D., Ludwig, N., Trecroci, A., Gargano, M., Michielon, G., Caumo, A., Alberti, G., 2016. Dynamics of thermographic skin temperature response during squat exercise at two different speeds. Journal of Thermal Biology 59, 58–63. https://doi.org/10.1016/j.jtherbio.2016.04.013

Fredsted, A., Clausen, T., Overgaard, K., 2008. Effects of Step Exercise on Muscle Damage and Muscle Ca2+ Content in Men and Women. Journal of Strength and Conditioning Research 22, 1136–1146. https://doi.org/10.1519/JSC.0b013e318173db9b

Gómez-Carmona, P., Fernández-Cuevas, I., Sillero-Quintana, M., Arnaiz-Lastras, J., Navandar, A., 2020. Infrared Thermography Protocol on Reducing the Incidence of Soccer Injuries. J Sport Rehabil 29, 1222–1227. https://doi.org/10.1123/jsr.2019-0056

Hawker, G.A., Mian, S., Kendzerska, T., French, M., 2011. Measures of adult pain: Visual Analog Scale for Pain (VAS Pain), Numeric Rating Scale for Pain (NRS Pain), McGill Pain Questionnaire (MPQ), Short-Form McGill Pain Questionnaire (SF-MPQ), Chronic Pain Grade Scale (CPGS), Short Form-36 Bodily Pain Scale (SF. Arthritis Care Res 63, S240–S252. https://doi.org/10.1002/acr.20543

Kenny, G., P., 2010. Human thermoregulation: separating thermal and nonthermal effects on heat loss. Front Biosci 15, 259. https://doi.org/10.2741/3620

Korman, P., Kusy, K., Kantanista, A., Straburzyńska-Lupa, A., Zieliński, J., 2021. Temperature and creatine kinase changes during a 10d taper period in sprinters. Physiol. Meas. 42, 124001. https://doi.org/10.1088/1361-6579/ac3d76

Machado, Á.S., da Silva, W., Andrade, C.F., De la Fuente, C., Souza, M.A., Carpes, F.P., 2022. Green tea supplementation favors exercise volume in untrained men under cumulative fatigue. Sci Sports.

Machado, A.S., da Silva, W., Souza, M.A., Carpes, F.P., 2018. Green Tea Extract Preserves Neuromuscular Activation and Muscle Damage Markers in Athletes Under Cumulative Fatigue. Frontiers in physiology 9, 9. https://doi.org/10.3389/fphys.2018.01137

Machado, Á.S., Priego-Quesada, J.I., Jimenez-Perez, I., Gil-Calvo, M., Carpes, F.P., Perez-Soriano, P., 2021. Influence of infrared camera model and evaluator reproducibility in the assessment of skin temperature responses to physical exercise. Journal of Thermal Biology 98, 102913. https://doi.org/10.1016/j.jtherbio.2021.102913

MacIntyre, D.L., Reid, W.D., McKenzie, D.C., 1995. Delayed Muscle Soreness: The Inflammatory Response to Muscle Injury and its Clinical Implications. Sports Medicine 20, 24–40. https://doi.org/10.2165/00007256-199520010-00003

Marco, G., Alberto, B., Taian, V., 2017. Surface EMG and muscle fatigue: multi-channel approaches to the study of myoelectric manifestations of muscle

fatigue. Physiol. Meas. 38, R27–R60. https://doi.org/10.1088/1361-6579/aa60b9

Marri, K., Swaminathan, R., 2016. Analyzing the influence of curl speed in fatiguing biceps brachii muscles using sEMG signals and multifractal detrended moving average algorithm. Presented at the Conf Proc IEEE Eng Med Biol Soc, pp. 3658–3661. https://doi.org/10.1109/EMBC.2016.7591521

Marshall, P.W., Melville, G.W., Cross, R., Marquez, J., Harrison, I., Enoka, R.M., 2021. Fatigue, pain, and the recovery of neuromuscular function after consecutive days of full-body resistance exercise in trained men. Eur J Appl Physiol 121, 3103–3116. https://doi.org/10.1007/s00421-021-04777-3

Menezes, P., Rhea, M.R., Herdy, C., Simão, R., 2018. Effects of Strength Training Program and Infrared Thermography in Soccer Athletes Injuries. Sports (Basel) 6. https://doi.org/10.3390/sports6040148

Moreira, D.G., Costello, J.T., Brito, C.J., Adamczyk, J.G., Ammer, K., Bach, A.J.E., Costa, C.M.A., Eglin, C., Fernandes, A.A., Fernández-Cuevas, I., Ferreira, J.J.A., Formenti, D., Fournet, D., Havenith, G., Howell, K., Jung, A., Kenny, G.P., Kolosovas-Machuca, E.S., Maley, M.J., Merla, A., Pascoe, D.D., Priego Quesada, J.I., Schwartz, R.G., Seixas, A.R.D., Selfe, J., Vainer, B.G., Sillero-Quintana, M., 2017. Thermographic imaging in sports and exercise medicine: A Delphi study and consensus statement on the measurement of human skin temperature. Journal of Thermal Biology 69, 155–162. https://doi.org/10.1016/j.jtherbio.2017.07.006

Mujika, I., 2017. Quantification of Training and Competition Loads in Endurance Sports: Methods and Applications. International Journal of Sports Physiology and Performance 12, S2-9-S2-17. https://doi.org/10.1123/ijspp.2016-0403

Oliveira, L.F., Matta, T.T., Alves, D.S., Garcia, M.A., Vieira, T.M., 2009. Effect of the shoulder position on the biceps brachii emg in different dumbbell curls. Journal of sports science & medicine 8, 24–9.

Peake, J.M., Neubauer, O., Della Gatta, P.A., Nosaka, K., 2017. Muscle damage and inflammation during recovery from exercise. Journal of Applied Physiology 122, 559–570. https://doi.org/10.1152/japplphysiol.00971.2016

Pizzino, G., Irrera, N., Cucinotta, M., Pallio, G., Mannino, F., Arcoraci, V., Squadrito, F., Altavilla, D., Bitto, A., 2017. Oxidative Stress: Harms and Benefits for Human Health. Oxid Med Cell Longev 2017, 8416763. https://doi.org/10.1155/2017/8416763

Priego Quesada, J.I. (Ed.), 2017. Application of Infrared Thermography in Sports Science, 1st ed. 2017. ed, Biological and Medical Physics, Biomedical Engineering. Springer International Publishing : Imprint: Springer, Cham. https://doi.org/10.1007/978-3-319-47410-6

Priego-Quesada, J.I., De la Fuente, C., Kunzler, M.R., Perez-Soriano, P., Hervás-Marín, D., Carpes, F.P., 2020. Relationship between Skin Temperature, Electrical Manifestations of Muscle Fatigue, and Exercise-Induced Delayed Onset Muscle Soreness for Dynamic Contractions: A Preliminary Study. Int J Environ Res Public Health 17, E6817. https://doi.org/10.3390/ijerph17186817

Priego-Quesada, J.I., Oficial-Casado, F., Gandia-Soriano, A., Carpes, F.P., 2019. A preliminary investigation about the observation of regional skin temperatures following cumulative training loads in triathletes during training camp. J Therm Biol 84, 431–438. https://doi.org/10.1016/j.jtherbio.2019.07.035

Prochniewicz, E., Spakowicz, D., Thomas, D.D., 2008. Changes in Actin Structural Transitions Associated with Oxidative Inhibition of Muscle Contraction. Biochemistry 47, 11811–11817. https://doi.org/10.1021/bi801080x

Proske, U., Morgan, D.L., 2001. Muscle damage from eccentric exercise: mechanism, mechanical signs, adaptation and clinical applications. J Physiol 537, 333–345. https://doi.org/10.1111/j.1469-7793.2001.00333.x

Rodríguez-Marroyo, J.A., Villa, J.G., Pernía, R., Foster, C., 2017. Decrement in Professional Cyclists' Performance After a Grand Tour. International Journal of Sports Physiology and Performance 12, 1348–1355. https://doi.org/10.1123/ijspp.2016-0294

Stewart, R.D., Duhamel, T.A., Rich, S., Tupling, A.R., Green, H.J., 2008. Effects of Consecutive Days of Exercise and Recovery on Muscle Mechanical Function. Medicine & Science in Sports & Exercise 40, 316–325. https://doi.org/10.1249/mss.0b013e31815adf02

Uchida, M.C., 2008. Efeito do exercício de força em diferentes intensidades com volume total similar sobre a dor muscular de início tardio, marcadores de lesão muscular e perfil endócrino. (Doutorado em Biologia Celular e Tecidual). Universidade de São Paulo, São Paulo. https://doi.org/10.11606/T.42.2008.tde-09092008-135446

CAPÍTULO VI

ARTIGO ORIGINAL

Green tea supplementation favors exercise volume in untrained men under cumulative fatigue

Machado, AS[1], da Silva, W[1], de Andrade, CF[1], De la Fuente, CI[1,2], de Souza, MA[3] and Carpes, FP[1*]

1 Applied Neuromechanics Research Group, Laboratory of Neuromechanics, Federal University of Pampa, Uruguaiana, RS, Brazil

2 LIBFE, Escuela de Kinesiologia, Universidad de los Andes, Santiago, Chile

3 Physiology Research Group, Laboratory of Neurochemistry, Federal University of Pampa, Uruguaiana, RS, Brazil

*** corresponding author**

Felipe P. Carpes, Ph.D.,

Associate professor at Federal University of Pampa

e-mail: carpes@unipampa.edu.br

Postal address: Federal University of Pampa - Laboratory of Neuromechanics

Po box 118 - ZIP 97500-970, Uruguaiana, RS, Brazil.

Phone office: +55 55 3911 0225

6.1 Abstract

Objectives: Cumulative fatigue is an unwanted result of consecutive days of exercise. We hypothesize that a natural antioxidant such as green tea extract from C*amellia sinensis* could reduce the effects of cumulative fatigue. Here we determine whether green tea extract could prevent muscle damage and preserve neuromuscular activity in a condition of cumulative fatigue. **Equipment and methods:** Sixteen untrained men were divided into intervention (500 g green tea extract) and placebo (500 g celulomax E) groups and tested for biceps brachii strength and neuromuscular electrical activity, muscle damage, and oxidative status before and after cumulative fatigue induced by two consecutive days of biceps curl exercise. In fatigue induction, work volume was assessed. The significance level adopted was 0.05. **Results:** Cumulative fatigue caused muscle damage in both groups ($P<0.01$) without affecting strength. The green tea extract group was able to sustain the exercise volume ($P=0.43$), while it was reduced for the placebo group ($P=0.04$). The green tea extract group showed preserved neuromuscular activity (entropy and frequency slope) compared to placebo. The green tea extract group showed stable oxidative status ($P=0.09$), which was increased in placebo ($P=0.03$). **Conclusion:** Green tea extract supplementation did not affect the magnitude of muscle damage after cumulative fatigue but helped preserve neuromuscular performance and maintain exercise volume by minimizing oxidative stress resulting from cumulative fatigue.

Keywords: Exercise recovery; exhaustion; muscle damage; oxidative status; electromyography.

6.2 Introduction

Muscle fatigue causes transient losses in producing and sustaining strength [1]. A standard paradigm to study muscle fatigue is having participants perform to exhaustion and then determining the short and long-term adaptations. Nevertheless, other conditions interest both scientists and exercise participants, which are the consequences of fatigue induced by exercise performed on consecutive days. In addition, late damage caused by muscle fatigue can facilitate the development of muscle injuries and affect neuromuscular performance. Therefore, prevention or muscle recovery strategies in this context are necessary.

Strenuous exercise evokes oxidative stress, characterized by an imbalance between reactive oxygen species (ROS) production, damaging membranes, proteins, DNA, and other essential structures [2]. Muscle damage is also an important event that may follow muscle fatigue. Muscle damage is characterized by the disruption of sarcomeres and myofibrils, usually due to eccentric exercise. The recovery may take 3 to 7 days, generally leading to muscle soreness and the rise of inflammatory markers. Together, these events reduce muscle performance and may increase the risk of a major injury [3].

Since both oxidative stress and muscle damage take a few days to end their cycles [4], recovery time may not be enough when consecutive bouts of exercise are imposed. However, with demands inducing fatigue on successive days, the muscles experience accumulation of metabolites, reinforcing ROS production and muscle damage, named here as cumulative fatigue. Such conditions result in a more extended period of impaired contractility and strength capacity [5].

Muscle damage requires tissue repair in the exercised muscles through the inflammatory cascade, but the inflammatory process itself produces high levels of ROS, which results in oxidative stress and muscle damage [6]. So far, the studies do not fully describe how the conflicting interdependence between ROS and inflammation affects the cycle of muscle damage. Therefore, could an antioxidant supplementation along with exercise-induced muscle damage be a strategy to balance the relationship between ROS and muscle damage?

Muscle damage was increased in cyclists performing six consecutive days of strenuous testing but attenuated by bromelain supplementation [5]. A previous study found that cumulative fatigue leads to muscle damage, increases oxidative stress, and reduces neuromuscular activation in master trained cyclists, but not for the group that received green tea extract (GTE) from *Camellia sinensis* [7]. Also, in exercises involving small muscle groups performing eccentric actions, GTE supplementation reduced blood markers of muscle damage [8].

Most of the studies on cumulative fatigue consider trained athletes. For example, untrained people, which do not have an endogenous antioxidant system so developed [9], may suffer differently from cumulative fatigue when starting participation in regular physical exercise. However, investigating this population may help highlight the effect of antioxidant supplementation. Benefits of GTE supplementation found for trained athletes may also depend on a predisposition to a faster recovery promoted by physical conditioning and fitness [10], limiting a broad inference of its effects in less or untrained people.

Until then, the antioxidant properties of GTE only generated benefits in physical exercise for an animal model, not being reproduced in humans [11]. Furthermore, establishing the GTE as a nutritional alternative for beginners in

physical exercise could be an advance in human nutrition due to its accessibility at low cost and the vast literature that attests to the safety of its use [12]. Therefore, the importance of this study relies on the need to explore the mechanisms of accumulated fatigue and assess the potential of GTE supplementation to minimize possible negative consequences of the accumulation of fatigue on muscle contraction.

Here we set out to determine whether GTE supplementation can minimize the effects of cumulative fatigue on biochemical markers and neuromechanical performance of untrained men under cumulative exercise. We hypothesize that GTE supplementation will prevent muscle damage and ensure adequate neuromuscular activity and, consequently, strength and exercise volume.

6.3 Materials and Methods

We conducted a triple-blinded placebo control study including untrained men, defined by a self-reported low history of adherence to regular physical exercise and no regular practice of physical exercise for at least two months. The protocol consisted of four visits to the laboratory to perform four tests: A) strength test without supplementation and fatigue; B) first exercise bout to induce fatigue; C) second exercise bout to induce fatigue; and D) strength test with supplementation and cumulative fatigue. To avoid task-learning effects, half of the participants from each group performed “A” one week after “D”. Before “A” and “D”, we collected blood samples to quantify biochemical markers. Figure 1 depicts the protocol.

We extract the workload information from the biceps curl exercise to measure isolated muscle endurance. From the isometric contraction, we

collected maximum strength and neuromuscular electrical activation parameters. To explore the discussion about the biochemical effects of green tea on fatigue, we selected a marker of muscle damage and indicators of oxidative status. We chose both fatigue induction with biceps curl exercise and the isometric strength test of biceps brachialis to isolate the target muscle of our intervention. Since our biochemical measurements are blood markers, a more global exercise would damage a larger muscle group and reduce CK specificity.

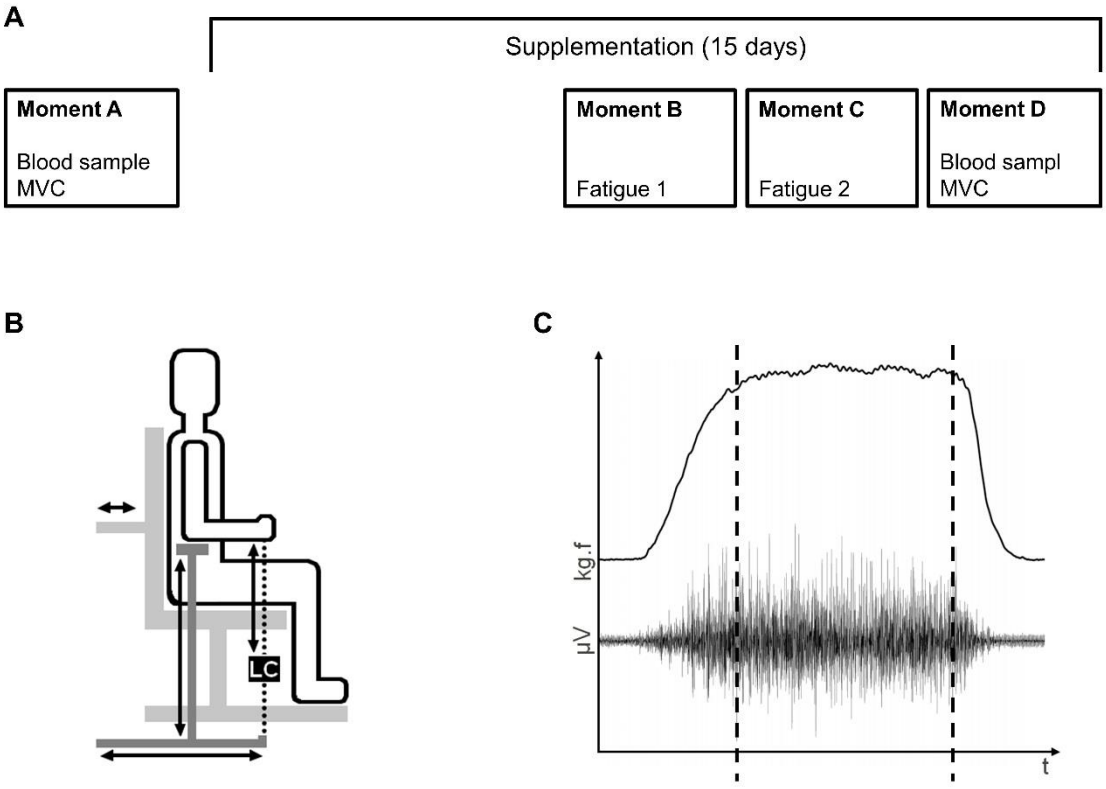

Figure 1. Protocol and experimental set-up. A) Temporal organization of the study. In half of the participants in each group, moment A was moved to at least one week after moment D. Moments B, C and D were arranged in consecutive days. B) Posture of the participant during the tests. Bilateral arrows indicate structures of adjustable length to maintain the desired alignment (neutral shoulder, elbow at 90°). The dotted line indicates the orientation of the chain where the load cell (LC) was attached. C) EMG burst and

strength signals representation during the isometric maximal voluntary contraction (MVC). Dotted lines indicate the cut off points that corresponds to the MVC hold time.

6.3.1 Subjects

Sample size calculation was performed using the PSS Health tool [13], estimating the difference between the CK means in the GTE and placebo groups, with a margin of error of 38 U/L, confidence level of 95%, and an expected standard deviation of 46 U/L [7]. A sample size of 26 subjects was determined (with 13 in each group). Thirty participants were contacted, 22 agreed to participate in the study, 8 did not complete all the tests, and their data were not added to the analyses. We were unable to replace the participants due to the restrictions to assess people in research during the coronavirus pandemic.

Participants were randomized to placebo group [n = 8, age 26 (4) years, body mass 79.3 (9) kg, 1.75 (0.06) m] or intervention (GTE) group [n = 8, age 27 (5) years, body mass 75.2 (7) kg, height 1.69 (0.12) m]. The participant should perform the proposed tasks and be free of musculoskeletal injuries to the upper limbs in the last six months. All of them received dietary advice to minimize the influence of diet on the measures. We also instructed them to avoid changes in sleep routine during the study period. All participants signed an informed consent form before starting participation. The ethics committee from the local institution approved this research (IRB 60376216.4.0000.5323). All procedures were performed following the Declaration of Helsinki.

6.3.2 Cumulative fatigue protocol

The fatigue protocol was induced during non-preferred biceps curl exercise with a 3 kg dumbbell, representing approximately 7% of individual body mass. This workload was defined based on a previous study that successfully induced muscle damage and soreness for the same exercise [14]. Participants were seated on a chair and instructed to perform the exercise under a metronome-controlled rhythm of 20 beats per minute (bpm).

The exercise range of motion was from the maximal elbow extension to the maximal elbow flexion, with 50% of the cycle involving an eccentric action. The first set was conducted to reach the maximum number of repetitions. The following sets (1 min for rest between sets) were maintained between 50% and 75% of the maximal number of repetitions. If the participant could not achieve 50% of the maximal number of repetitions, the fatigue condition was considered and the test concluded [15]. The exercise bouts were performed on two consecutive days, always at the same time of the day. The product between numbers of repetitions, numbers of series, and load determined the exercise volume for each day.

6.3.3 Green tea extract supplementation

Supplementation lasted 15 days and considered the daily oral ingestion of 500 mg of green tea extract (GTE) or placebo capsules (celulomax E), always before the first meal of the day. Chronic supplementation is required to achieve the antioxidant potential of GTE [7,8]. Therefore, we adopted 15 consecutive days of supplementation as our intervention. The dose of 500 mg per day is lower than the maximal dose that previous studies investigating the safety of this substance

ingestion and equal to the amount used in studies that showed the effectiveness of GTE to promote antioxidant defenses [16–18].

The capsules were identical in appearance and handled at a local pharmacy. A sample of the GTE was tested using high-performance liquid chromatography (HPLC), and we confirmed the presence of epigallocatechin gallate (1.60 mg/g), epicatechin (1.59 mg/g), epigallocatechin (16 mg/g), and epicatechin-gallate (17.80 mg/g). Furthermore, participants were requested to avoid consuming tobacco, medicines, supplements, green tea, energy drinks, fruits, milk, caffeine, and alcohol from two weeks before until the end of the tests [19–21].

6.3.4 Neuromechanical assessment

Neuromechanical assessments were performed at the beginning (“without fatigue”, basal measure) and the end of the protocol (“with fatigue” as an intervention measure) and included measurement of strength and electromyography (EMG) sampled at 2000 Hz through a 14-bit electronic device (Miotec Biomedical Inc., Porto Alegre, Brazil). The participants were seated on an adjustable chair in which they held a handle to tension a chain attached to a load cell (Miotec Biomedical Inc., Porto Alegre, Brazil). We aimed to maintain the participants seated with the hip and knee stable at 90°, shoulders at a neutral position, elbow at 90° and supine hand, with the load cell aligned perpendicularly to the ground (Fig. 1.B). The elbow of the tested arm was positioned on a padded cushion used as a position reference during the tests. After adjustments, three familiarization trials were performed.

We asked participants to perform three isometric maximal voluntary contractions (MVC) for elbow flexion to measure strength. The verbal command was given to gradually produce force until reach the maximum elbow flexion strength. Then, the participants sustain the maximal strength for 5 seconds until hearing the command to stop the contraction [22]. Between each MVC at least a 30-s rest time was given. EMG signals were recorded from the biceps brachii using a pair of Ag/AgCl electrodes (bipolar configuration; 22 mm in diameter; an inter-electrode distance of 20 mm, Kendall Meditrace Inc., Canada) placed on the skin following local hygiene. We also positioned a reference electrode at a bony protrusion, following the SENIAM standards [23].

The EMG and force signals were segmented at the 5-s plateau of the MVC (Fig 2.C) and normalized by body mass. The average of three MVC attempts was calculated. EMG signals were zero-mean centered and filtered using a band-pass digital Butterworth filter with a cut-off frequency of 20 – 400 [24]. The Shannon entropy was obtained from the root mean square (RMS) time-series of the EMG data resulting from a 50% overlapped rectangular window of 250 ms as an indicator of complexity and randomness of dynamic biological data [25]. The frequency spectrum was determined using the fast Fourier algorithm to extract the frequency peak using a 50% overlapped rectangular window of 500 [26]. The frequency slope of the linear regression applied for each frequency series was obtained and considered a myoelectric manifestation of muscle fatigue. We also determined the medium-to-low-frequency ratio (46-95/15-45 Hz; M/LBF ratio) to evaluate the shift of the spectrum [27]. All digital signals were offline analyzed using custom codes written in Matlab (2016a, Mathworks Inc., Massachusetts, USA).

6.3.5 Biochemical assays

Before moments A and D, a sample of 10 mL of blood was collected from the ulnar vein, being 5 mL stored in heparin tubes and 5 mL in EDTA tubes. All samples were centrifuged for 15 min at 2500 rpm, and plasma was separated and stored at -80°C. Heparinized samples were used for the determination of creatine kinase (CK) activity using commercial enzymatic kits (Labtest) to estimate muscle damage [28]. Other measures were conducted using EDTA samples.

The concentration of malondialdehyde (MDA) was measured using the thiobarbituric acid-reactive substances (TBARS) assay by a modification of the method of Ohkawa et al. [29]. Serum blood was mixed with SDS and thiobarbituric acid (TBA). Orthophosphoric acid, an antioxidant, was added to the mixture to avoid oxidation during subsequent heating. After incubation at 95°C for 60 min, the pink-red chromogen produced by the TBA-MDA adduct was used to quantify the level of TBARS by measuring its absorbance at 532 nm. The level of TBARS was calculated and expressed in nmol MDA/mL.

A fluorimetric assay determined the content of reduced glutathione (GSH). The sample was added in a medium with perchloric acid and potassium phosphate (TFK), and then ortho-phthalaldehyde (OPA) was added in the dark. The mixture was incubated for 15 min at room temperature, and the fluorimetric reading was performed with excitation at 350 nm and emission at 420 nm. The result is expressed under an average calibration factor [30].

The detection of intracellular reactive oxygen species (ROS) was performed using a liposoluble probe, 2,7 - dichlorodihydrofluorescein diacetate

(DCFH-DA), which diffuses into cells, and in the cytosol it is deacetylated by esterases, forming 2,7 - dichlorodihydrofluorescein (DCFH), which becomes available to act as a substrate for free radicals formed in the intracellular medium. After oxidation by free radicals, the probe emits fluorescence, which is measured in a fluorimeter. The technique has a high sensitivity for ROS detection and the probe used has increased specificity to H_2O_2. The samples were read at times 0, 15, 30, and 60 minutes with an emission rate of 520 and extinction 488, and the data were expressed as % of control [31].

6.3.6 Statistical analyses

The Shapiro-Wilk test identified data with parametric and non-parametric distributions. Parametric data are presented as mean and standard deviation. Nonparametric data are presented as median and interquartile ranges. Due to the final characteristic of the variables resulting from the final n, we decided to perform intragroup, intergroup, and delta pre x post comparisons separately. Strength and exercise volume showed a normal distribution and were compared between groups by independent t-tests. Changes due to fatigue were also expressed by the delta of change in relation to the basal measure and compared using the Mann-Whitney test. Except for the GSH activity (which were compared by t-test), biochemical results did not follow a normal distribution, and comparisons between groups were performed by Mann-Whitney test. For parametric data, the Cohen's effect size (*d*) was calculated to show the magnitude of the differences, considered: non effect <0.2, small 0.2 - 0.4, intermediate 0.5 – 0.7 and large > 0.8 [32]. The significance level adopted was 0.05.

6.4 Results

6.4.1 Neuromechanical assessment and exercise volume

The effect of cumulative fatigue on the strength [**Fig. 2A**, $t_{(1)}$ = 1.066; P =0.304] and median frequency of neuromuscular activation [P = 0291] did not differ between placebo and GTE groups. Exercise volume was not influenced by fatigue in GTE group [**Fig. 2B**, $t_{(1)}$ = 0.828; P = 0.434], but placebo group experienced a reduced exercise volume when fatigued [**Fig. 2B**, $t_{(1)}$ = 2.372; P =0.049; *d* = 0.41]. Deltas in RMS entropy [**Fig. 2C**, P = 0.002] and peak frequency of neuromuscular activation [**Fig. 2D**, P = 0.028] were larger in the GTE group than placebo. Fatigue increased the EMG M/LBF ratio in the placebo group, and reduced in the GTE group [**Fig. 2E**, $t_{(1)}$ = 2.594; P = 0.023; *d* = 1.35].

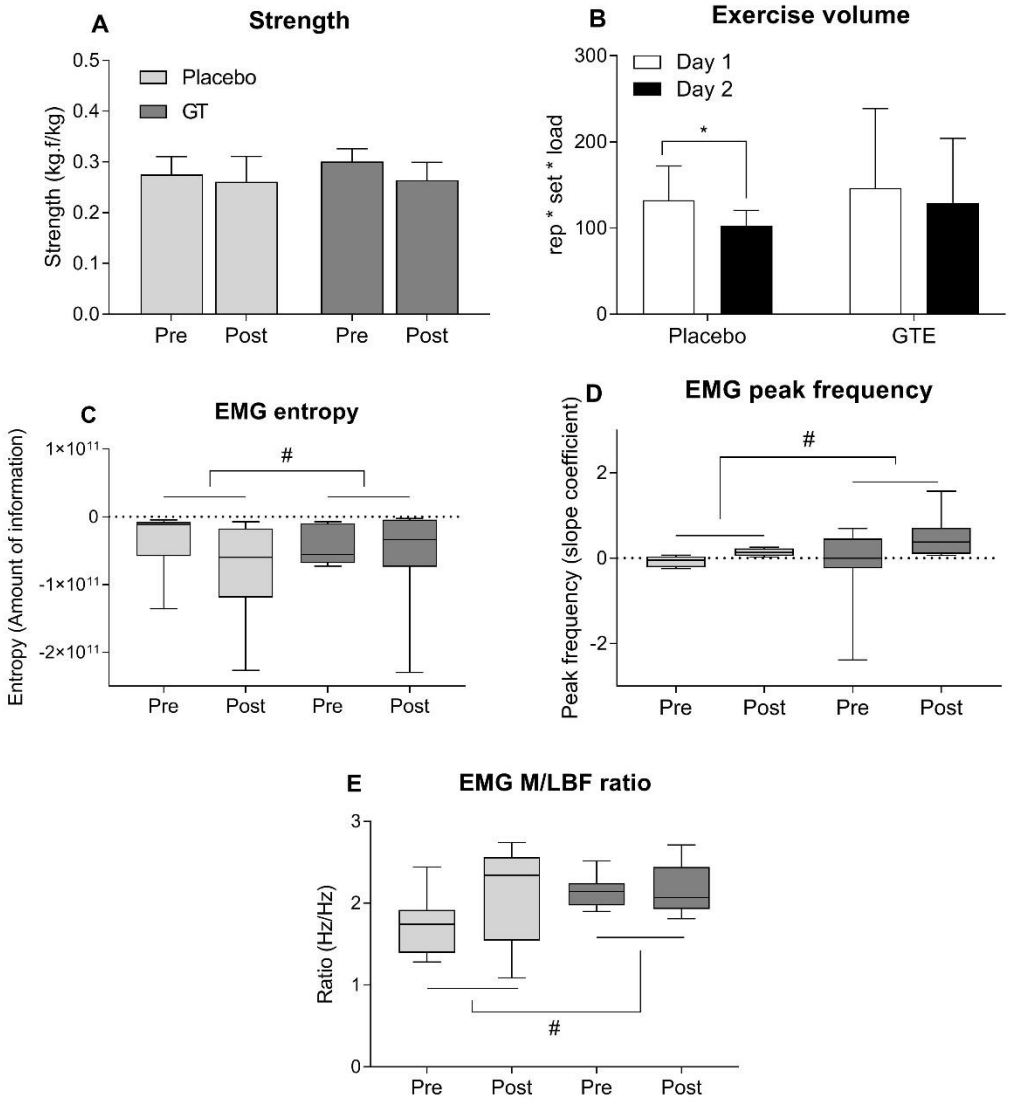

Figure 2. Strength and EMG results. A) Strength for placebo and GTE group; B) Work volume (repetitions * sets * load) from both days of fatigue for each group; C) Entropy of EMG signals for each group; D) Slope frequency for each group; and E) Electromyography (EMG) median to low band frequency ratio (M/LBF ratio) for each group. All results in percentage are expressed as the variation from basal measure (without fatigue). * means pre and post different intragroup, # means different percentage between groups $P < 0.05$.

6.4.2 Biochemical assays

The GTE **[Fig. 3A**, $t_{(1)}$ = 3.385; P = 0.011] and placebo groups [**Fig. 3A**, $t_{(1)}$ = 7.997; P < 0.001] experienced similar increase in CK levels with fatigue [P = 0.798]. Placebo group showed an increase in DCFH in fatigue [**Fig. 3B**, $t_{(1)}$ = 4.177; P = 0.004], which did not happen in the GTE group [**Fig. 3B**, $t_{(1)}$ = 1.769; P = 0.120]. TBARS increased in the placebo group [**Fig. 3C**, P = 0.039] but not in the GTE group [**Fig. 3C**, $t_{(1)}$ = 1.901; P = 0.099], and pre/post delta was higher in the placebo group [**Fig. 3C**, P = 0.014; *d* = 1.08]. Also, the delta in GSH activity was smaller for the placebo group [**Fig. 3D**, $t_{(1)}$ = 2.557; P = 0.029; *d* = 1.27].

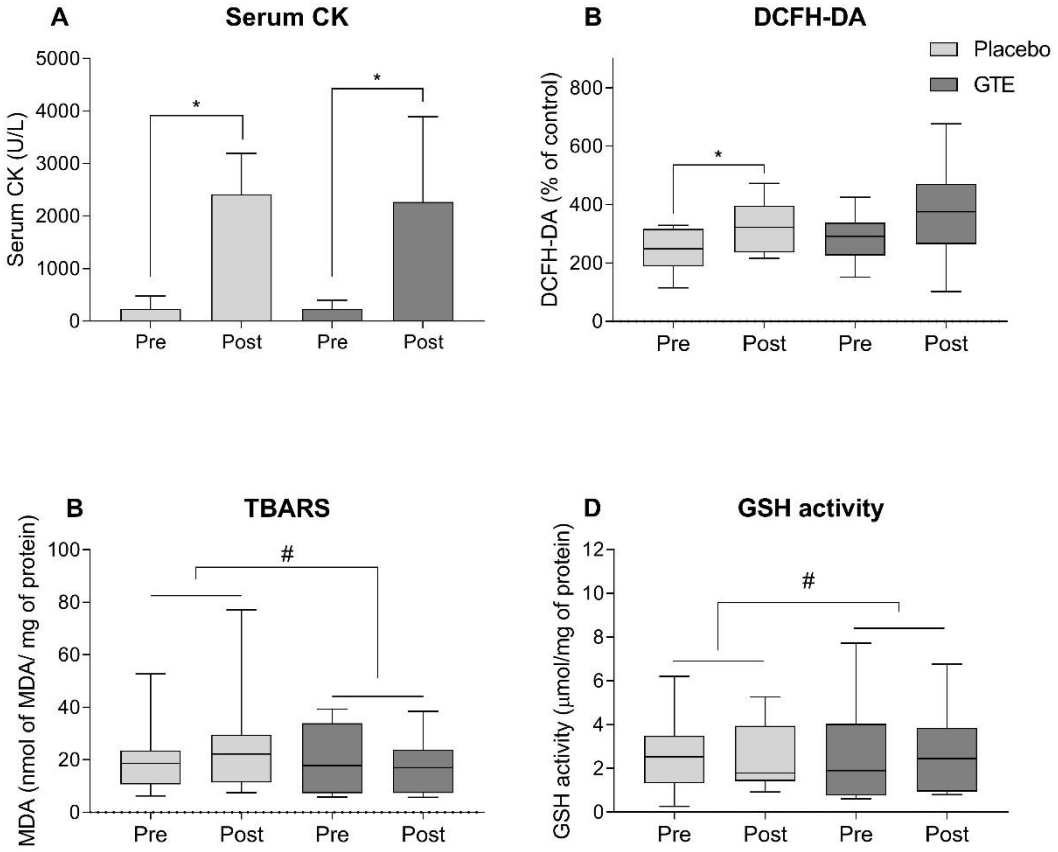

Figure 3. Results of biochemical analysis. A) Plasma creatine kinase (CK) levels variation for each group; B) Reactive oxygen species (ROS) production evaluated by

dichloro-dihydro-fluorescein diacetate (DFCH-DA) increasing; C) Plasma lipid peroxidation variation measured by thiobarbituric acid reactive substances (TBARS) and; D) Glutathione (GSH) content variation for each group. All results in percentage are expressed as the variation from basal measure (without fatigue). * means pre and post different intragroup, # means different percentage between groups $P < 0.05$.

6.5 Discussion

Here we aimed to describe the cumulative fatigue and observe the potential of GTE in preventing or reducing the effects of cumulative fatigue on neuromechanical outcomes related to strength production and biochemical markers of exercise-induced muscle damage. The hypothesis that GTE supplementation would avoid muscle damage was rejected, but supplementation with GTE was confirmed as beneficial for oxidative status and preserved neuromechanical activity and exercise volume under a condition of cumulative fatigue.

We performed the isometric MVC before and after exercise to attest to the presence of fatigue as widely reported [1]. We found that fatigue induced two consecutive days before MVC does not cause loss of strength. Still, our neuromechanical and biochemical measurements indicate that changes resulting from late and cumulative fatigue would not be verified only by assessing MVC. The group that received the GTE supplementation was able to sustain the exercise volume under fatigue, which may be understood as better resistance to fatigue, and may have important practical applicability (e.g., exercise sustained for a longer time).

We found different electrical manifestations of fatigue between the groups. The cumulated fatigue resulted in a shifting of the peak frequency to the left for the placebo group, which suggests that this group was more susceptible to fatigue than the GTE group. This left shift of the spectrum indicates that the task has become more costly for the placebo and helps to explain its lower exercise volume [33].

Furthermore, to determine which frequencies changed during the MVC under fatigue, we assessed the M/LBF ratio of the EMG frequency spectrum, suggested by Karthick and Ramakrishnan [27]. The placebo group demonstrated a behavior towards increasing the M/LBF ratio, different from the GTE group that showed a tendency to shift in the opposite direction. The difference in the behavior of the M/LBF ratio while holding the 100% of MVC between the groups reinforces that fatigue affects the recruitment of muscle fibers over time and suggests that the GTE can prevent or delay this change [1].

The increased entropy in the GTE group means a larger probability of arranging the electrical information of the electromyography signals (RMS) amplitude. In physiological terms, it may refer to changes in the train of action potentials. A lower capacity to arrange information, as found in the placebo group, has been previously defined as signals with lower complexity. This could be summarized as a poor neuromuscular capacity to adapt to cumulative fatigue [34]. We interpret the neuromuscular activation entropy varying in opposite directions for each group as an indicator of better neuromuscular strategy in the GTE than the placebo.

Despite these pieces of evidence, the question is, what mechanism explains the protective effect of GTE supplementation against cumulative fatigue

in these participants? Since the GTE constitution is privileged concerning the number and positions of the hydroxyl groups in the rings, its antioxidant capacity is pronounced, and this characteristic helps explain our results [35]. First, our biochemical analyses revealed that cumulative fatigue induced similar levels of muscle damage in both groups. GTE supplementation could not minimize the effects of cumulative exercise on serum CK levels, different from previous studies also considering GTE supplementation and responses to a single bout of exercise [36]. It may indicate that the exercise protocol was too severe for untrained men. We hypothesize that the muscle damage triggered inflammatory processes, which produced high levels of ROS verified by DCFH-DA measurement, generating a state of oxidative stress that could delay the restoration of tissue homeostasis or even reinforce muscle damage [6]. The GTE seemed to avoid the exacerbation and persistence of ROS production and helped preserve the exercise volume.

Also, we found increased GSH levels in the GTE group. We hypothesize that GTE enabled the biosynthesis of GSH, probably by transactivation of the gamma-glutamylcysteine synthetase [37]. In obese people with metabolic syndrome, GTE demonstrated increasing GSH availability [38]. This result indicates that in addition to the action of catechins, supplementation with GTE favors the endogenous antioxidant activity.

ROS production was higher in the placebo group after cumulative fatigue, and GTE was able to reduce oxidative stress. A study conducted by Vezzoli et al. [39] found a correlation between endurance performance in strenuous exercise and oxidative stress in runners. Likewise, Gravier [40] found no significant correlation between muscle fatigue and oxidative stress in sedentary

individuals subjected to exhaustion in cycling. The increase in oxidative stress was accompanied by changes in the frequency domain of electromyography, as found in our study. Once again, the antioxidant capacity of GTE seems to bring benefits in exercise, minimizing the disturbances caused by cumulative muscle fatigue in electromyography.

Jówko et al. [11] demonstrated that although GTE supplementation modifies oxygen and fat consumption in athletes, this food supplement is not able to confirm in humans the performance benefits verified in the animal model. By shifting the applicability to delay fatigue trying to speed recovery over a sequence of exercise days, we observed that the GTE antioxidant capacity appears to have a potential benefit in the exercise context. It may influence neuromuscular performance and improve fatigue resistance, resulting in a higher exercise volume. Therefore, we suggest that GTE supplementation benefits endurance performance in the participants. Our study also provides evidence of a GTE dose that may be safe and effective for individuals starting an exercise program.

We are aware that our study has some limitations, and our results claim for further validation in subjects of different characteristics and exercise backgrounds. The dropouts and the conditions of public health limited our sample. Although we used other techniques to confirm oxidative status, our oxidative stress marker was TBARS which, although more accessible, is not a first-choice technique. Finally, we were unable to perform biopsies to quantify the muscle damage.

Our study offers as a practical application the possibility of using a natural product as a dietary supplement with relatively easy access to a wide population to minimize oxidative stress deleterious consequences for workload in physical

exercise, indicating a potential benefit of GTE supplementation for endurance performance.

In summary, the GTE supplementation did not affect the magnitude of muscle damage after cumulative fatigue. On the other hand, GTE supplementation helps preserve neuromuscular performance and maintain exercise volume by minimizing oxidative stress resultant of cumulative fatigue in untrained men.

6.6 References

1 Enoka RM, Duchateau J. Muscle fatigue: what, why and how it influences muscle function. J Physiol 2007/08/19 ed. 2008; 586:11–23.

2 Pizzino G, Irrera N, Cucinotta M, Pallio G, Mannino F, Arcoraci V, et al. Oxidative Stress: Harms and Benefits for Human Health. Oxid Med Cell Longev 2017; 2017:8416763.

3 Proske U, Morgan DL. Muscle damage from eccentric exercise: mechanism, mechanical signs, adaptation and clinical applications. J Physiol 2001; 537:333–45.

4 Steinbacher P, Eckl P. Impact of oxidative stress on exercising skeletal muscle. Biomolecules 2015/04/14 ed. 2015; 5:356–77.

5 Shing CM, Peake JM, Ahern SM, Strobel NA, Wilson G, Jenkins DG, et al. The effect of consecutive days of exercise on markers of oxidative stress. Appl Physiol Nutr Metab 2007/07/12 ed. 2007; 32:677–85.

6 Biswas SK. Does the Interdependence between Oxidative Stress and Inflammation Explain the Antioxidant Paradox? Oxid Med Cell Longev 2016; 2016:5698931.

7 Machado AS, da Silva W, Souza MA, Carpes FP. Green Tea Extract Preserves Neuromuscular Activation and Muscle Damage Markers in Athletes Under Cumulative Fatigue. Front Physiol 2018/09/04 ed. 2018; 9:9.

8 da Silva W, Machado AS, Souza MA, Mello-Carpes PB, Carpes FP. Effect of green tea extract supplementation on exercise-induced delayed onset muscle soreness and muscular damage. Physiol Behav 2018/05/11 ed. 2018; 194:5.

9 Parker L, McGuckin TA, Leicht AS. Influence of exercise intensity on systemic oxidative stress and antioxidant capacity. Clin Physiol Funct Imaging 2014; 34:377–83.

10 de Sousa CV, Sales MM, Rosa TS, Lewis JE, de Andrade RV, Simões HG. The Antioxidant Effect of Exercise: A Systematic Review and Meta-Analysis. Sports Med Auckl NZ 2017; 47:277–93.

11 Jówko E. Green Tea Catechins and Sport Performance. In: Lamprecht M, editor. Antioxidants in Sport Nutrition 2015; Boca Raton (FL): CRC Press/Taylor & Francis; 2015.

12 Chow H-HS, Cai Y, Hakim IA, Crowell JA, Shahi F, Brooks CA, et al. Pharmacokinetics and safety of green tea polyphenols after multiple-dose administration of epigallocatechin gallate and polyphenon E in healthy individuals. Clin Cancer Res Off J Am Assoc Cancer Res 2003; 9:3312–9.

13 Borges RB, Mancuso ACB, Camey SA, Leotti VB, Hirakata VN, Azambuja GS, et al. Power and Sample Size for Health Researchers: uma ferramenta para cálculo de tamanho amostral e poder do teste voltado a

pesquisadores da área da saúde [Internet]. 2021st-04–13th ed. Vol. 40, Clinical & Biomedical Research. 2021; 2021.

14 Potvin JR, Bent LR. A validation of techniques using surface EMG signals from dynamic contractions to quantify muscle fatigue during repetitive tasks. J Electromyogr Kinesiol 1997/06/01 ed. 1997; 7:131–9.

15 Priego-Quesada JI, De la Fuente C, Kunzler MR, Perez-Soriano P, Hervás-Marín D, Carpes FP. Relationship between Skin Temperature, Electrical Manifestations of Muscle Fatigue, and Exercise-Induced Delayed Onset Muscle Soreness for Dynamic Contractions: A Preliminary Study. Int J Environ Res Public Health 2020; 17:E6817.

16 Dostal AM, Samavat H, Bedell S, Torkelson C, Wang R, Swenson K, et al. The safety of green tea extract supplementation in postmenopausal women at risk for breast cancer: results of the Minnesota Green Tea Trial. Food Chem Toxicol 2015; 83:26–35.

17 Martin BJ, Tan RB, Gillen JB, Percival ME, Gibala MJ. No effect of short-term green tea extract supplementation on metabolism at rest or during exercise in the fed state. Int J Sport Nutr Exerc Metab 2014; 24:656–64.

18 Samavat H, Wu AH, Ursin G, Torkelson CJ, Wang R, Yu MC, et al. Green Tea Catechin Extract Supplementation Does Not Influence Circulating Sex Hormones and Insulin-Like Growth Factor Axis Proteins in a Randomized Controlled Trial of Postmenopausal Women at High Risk of Breast Cancer. J Nutr 2019; 149:619–27.

19 Harasym J, Oledzki R. Effect of fruit and vegetable antioxidants on total antioxidant capacity of blood plasma. Nutr Burbank Los Angel Cty Calif 2014; 30:511–7.

20 Naumovski N, Blades BL, Roach PD. Food Inhibits the Oral Bioavailability of the Major Green Tea Antioxidant Epigallocatechin Gallate in Humans. Antioxid Basel Switz 2015; 4:373–93.

21 Sugita M, Kapoor MP, Nishimura A, Okubo T. Influence of green tea catechins on oxidative stress metabolites at rest and during exercise in healthy humans. Nutrition 2015/12/24 ed. 2016; 32:321–31.

22 Oliveira LF, Matta TT, Alves DS, Garcia MA, Vieira TM. Effect of the shoulder position on the biceps brachii emg in different dumbbell curls. J Sports Sci Med 2009/01/01 ed. 2009; 8:24–9.

23 Hermens HJ, Freriks B, Disselhorst-Klug C, Rau G. Development of recommendations for SEMG sensors and sensor placement procedures. J Electromyogr Kinesiol 2000/10/06 ed. 2000; 10:361–74.

24 Guzman-Venegas RA, Biotti Picand JL, de la Rosa FJ. Functional compartmentalization of the human superficial masseter muscle. PLoS One 2015/02/19 ed. 2015; 10:10.

25 Zhang X, Zhou P. Sample entropy analysis of surface EMG for improved muscle activity onset detection against spurious background spikes. J Electromyogr Kinesiol 2012/07/18 ed. 2012; 22:901–7.

26 Marri K, Swaminathan R. Analyzing the influence of curl speed in fatiguing biceps brachii muscles using sEMG signals and multifractal detrended moving average algorithm. In 2016; 2016. p. 3658–61.

27 Karthick PA, Ramakrishnan S. Muscle fatigue analysis using surface EMG signals and time–frequency based medium-to-low band power ratio. In: Electronics Letters 2016; Orlando, USA: IEEE; 2016. p. 185–6.

28 Baird MF, Graham SM, Baker JS, Bickerstaff GF. Creatine-kinase and exercise-related muscle damage implications for muscle performance and recovery. J Nutr Metab 2012/01/31 ed. 2012; 2012:13.

29 Ohkawa H, Ohishi N, Yagi K. Assay for lipid peroxides in animal tissues by thiobarbituric acid reaction. Anal Biochem 1979/06/01 ed. 1979; 95:351–8.

30 Hissin PJ, Hilf R. A fluorometric method for determination of oxidized and reduced glutathione in tissues. Anal Biochem 1976/07/01 ed. 1976; 74:214–26.

31 Silveira LR. Considerações críticas e metodológicas na determinação de espécies reativas de oxigênio e nitrogênio em células musculares durante contrações. Arq Bras Endocrinol Metabol 2004; 48:812–22.

32 Sullivan GM, Feinn R. Using Effect Size-or Why the P Value Is Not Enough. J Grad Med Educ 2013/09/03 ed. 2012; 4:279–82.

33 Cifrek M, Medved V, Tonkovic S, Ostojic S. Surface EMG based muscle fatigue evaluation in biomechanics. Clin Biomech 2009/03/17 ed. 2009; 24:327–40.

34 Cashaback JG, Cluff T, Potvin JR. Muscle fatigue and contraction intensity modulates the complexity of surface electromyography. J Electromyogr Kinesiol 2012/09/11 ed. 2013; 23:78–83.

35 Peluso I, Serafini M. Antioxidants from black and green tea: from dietary modulation of oxidative stress to pharmacological mechanisms. Br J Pharmacol 2017; 174:1195–208.

36 Herrlinger KA, Chirouzes DM, Ceddia MA. Supplementation with a polyphenolic blend improves post-exercise strength recovery and muscle soreness. Food Nutr Res 2015/12/23 ed. 2015; 59:10.

37 Myhrstad MC, Carlsen H, Nordstrom O, Blomhoff R, Moskaug JO. Flavonoids increase the intracellular glutathione level by transactivation of the gamma-glutamylcysteine synthetase catalytical subunit promoter. Free Radic Biol Med 2002/02/28 ed. 2002; 32:386–93.

38 Basu A, Betts NM, Mulugeta A, Tong C, Newman E, Lyons TJ. Green tea supplementation increases glutathione and plasma antioxidant capacity in adults with the metabolic syndrome. Nutr Res 2013/03/20 ed. 2013; 33:180–7.

39 Vezzoli A, Dellanoce C, Mrakic-Sposta S, Montorsi M, Moretti S, Tonini A, et al. Oxidative Stress Assessment in Response to Ultraendurance Exercise: Thiols Redox Status and ROS Production according to Duration of a Competitive Race. Oxid Med Cell Longev 2016/08/10 ed. 2016; 2016:6439037.

40 Gravier G, Steinberg JG, Lejeune PJ, Delliaux S, Guieu R, Jammes Y. Exercise-induced oxidative stress influences the motor control during maximal incremental cycling exercise in healthy humans. Respir Physiol Neurobiol 2013; 186:265–72.

CAPÍTULO VII

7.1 DISCUSSÃO

Nessa tese discutimos o conceito de fadiga acumulada, bem como estratégias para sua quantificação e análise. Também investigamos como uma intervenção baseada em um composto natural pode repercutir para a prevenção de condições que de fadiga acumulada acarretem redução na capacidade física e recuperação.

No primeiro estudo, nosso interesse era demonstrar que a fadiga acumulada é um problema real na prática esportiva, tendo em vista que a condição de fadiga desafia o treinamento e o desempenho em competição (Wan et al., 2017). Por meio de um banco de dados de uma equipe de ciclismo profissional, pudemos explorar os dados de desempenho de 12 atletas em duas edições do Giro d'Itália. Os resultados encontrados são similares aos encontrados na Vuelta a España e Tour de France (El Helou et al., 2010), o que significa que esse projeto tem aplicabilidade nas maiores competições de ciclismo do mundo.

Nesse artigo, além de prover uma detalhada descrição da prova, o que tem ampla aplicabilidade para treinadores e atletas, verificamos que conforme os estágios progridem, a capacidade de permanecer pedalando em intensidades mais altas é prejudicada. O dia de descanso interrompe esse ciclo, permitindo o retorno às zonas de pedalada mais intensas, mas a prova mais uma vez avança e a fadiga volta a prejudicar o desempenho. Assim, reiteramos que respeitar a temporalidade da regeneração muscular é necessário para manter o desempenho (Morán-Navarro et al., 2017), mas também acrescentamos que a

persistente interrupção do ciclo de recuperação gera intensificação da perda de desempenho. Esse tipo de avaliação emprega dados que geralmente são monitorados pelas equipes de ciclismo, seja no contexto profissional ou amador, e permitem inferências para o treinamento para vários níveis de intensidade Destacamos, portanto, a importância de explorar bancos de dados gerados por equipes e treinadores do ciclismo.

Devido a necessidade de estudar a fadiga acumulada em outros contextos, principalmente utilizando intervenções para prevenção da fadiga que nem sempre serão arriscadas em competições, entendemos que a fadiga acumulada deve ser reproduzida e avaliada em laboratório. Para isso, preparamos um conjunto de avaliações bioquímicas e biomecânicas, mesclando medidas amplamente consolidadas como a dinamometria, eletromiografia e a avaliação de níveis de espécies reativas de oxigênio e CK no sangue (Baird et al., 2012; Enoka & Duchateau, 2016; Shing et al., 2007) com uma técnica de imagem que vem ganhando muita popularidade na análise do movimento humano, e a qual nos colocamos como exploradores do seu potencial: a termografia infravermelha (IRT).

A IRT é bem consolidada enquanto tecnologia da avaliação de temperatura de superfícies no geral, inclusive nas ciências da saúde (Priego Quesada, 2017), mas é relativamente nova no monitoramento de desempenho esportivo. Seja para doenças como o câncer, seja para lesões macroscópicas do sistema musculoesquelético, a técnica de avaliação da IRT envolve muitas vezes a comparação da simetria das temperaturas entre um local potencialmente injuriado e um local controle (Vardasca et al., 2012). Por exemplo, para o câncer de mama comparam-se os padrões térmicos de um seio com o outro, ou ainda

para lesão muscular, uma coxa com a outra, e assim por diante (Priego Quesada, 2017).

Porém, antes de trazer esse tipo de avaliação para o contexto da fadiga acumulada, precisávamos garantir que nosso equipamento era adequado, e padronizar a forma de coletar e processar os dados para obter resultados fidedignos. Por isso, avaliamos a capacidade de diferentes câmeras termográficas infravermelhas de detectar assimetrias térmicas em diferentes distâncias de amostras artificiais. Além de prover a outros pesquisadores diretrizes sobre a acurácia de tais câmeras, vimos que nosso equipamento tem resultados próximos a um dos modelos mais sofisticados entre as câmeras termográficas. No mesmo sentido, verificamos que os termogramas devem ser registrados o mais perto possível da região de interesse, corroborando um estudo anterior (Kirimtat et al., 2020), o que restringe, por exemplo, as avaliações a segmentos menores em detrimento a fotos de um membro de cada vez ou a fotos de corpo inteiro. Ainda com o objetivo de atestar a fiabilidade do diagnóstico de fadiga muscular por meio da IRT, avaliamos os resultados extraídos dos termogramas por diferentes pesquisadores, e notamos que há consistência dos resultados entre avaliadores, que é recomendável que para cada estudo uma única câmera seja utilizada e, por fim, que a temperatura média é a variável mais confiável.

Uma vez que padronizamos o uso da IRT, o próximo passo foi recrutar participantes para a indução da fadiga acumulada em laboratório. Protocolos de fadiga acumulada envolvem pelo menos três dias de exposição ao exercício, sendo dois para executar a fadiga em dias consecutivos e um terceiro momento para avaliar as consequências do protocolo (Kataoka et al., 2022; Tosovic et al.,

2016). Executando esse protocolo, vimos que a fadiga acumulada imposta sobre o bíceps braquial do membro não preferido gerou perda de força no terceiro dia, o que coincidiu com um aumento de temperatura média da pele em comparação aos valores basais, e em comparação ao membro controle. Esse aumento da temperatura provavelmente ocorreu em consequência de um processo inflamatório local como resposta ao dano muscular típico desse tipo de protocolo (da Silva, Machado, Souza, Kunzler, et al., 2018; Machado et al., 2018). Vimos, portanto, que é possível simular uma situação de fadiga acumulada em laboratório e que é possível provocá-la em músculo isolado. A IRT parece não ser capaz de atestar a fadiga em tempo real (Bartuzi et al., 2012), mas tem potencial para o avaliação pós dias consecutivos de exercícios (Priego Quesada et al., 2015).

Finalmente, nos propusemos a avaliar o extrato de chá verde (ECV) como alternativa para evitar ou minimizar os efeitos negativos da fadiga acumulada sobre aspectos do desempenho. Nesse estudo utilizamos como medida biomecânica a eletromiografia, uma técnica com protocolos padronizados e com maior capacidade de explorar os eventos da contração muscular (Cifrek et al., 2009). Essa escolha se mostrou adequada, uma vez que o protocolo de indução de fadiga acumulada não gerou perda de força muscular no terceiro dia, mas algumas das variáveis eletromiográficas estavam alteradas. Isso reforça a tese que o sistema neuromuscular tem componentes de redundância, e portanto, executar uma tarefa de produção de força mesmo sob fadiga (P. W. Marshall et al., 2021). Nas medidas bioquímicas vimos com nitidez o efeito da fadiga acumulada, principalmente pela alta presença de CK ao fim do protocolo e pelas variáveis que atestam o status oxidativo.

Em resumo, apesar de nenhum grupo apresentar variação de força com o protocolo, apenas o grupo que recebeu ECV foi capaz de preservar o volume de trabalho no segundo dia de indução de fadiga, bem como apresentou resultados preservados nas variáveis eletromiográficas. No mesmo sentido, o nível de dano muscular foi aumentado em ambos os grupos, mas a produção de radicais livres foi reduzida nesse grupo, o que produziu menor estresse oxidativo e maior atividade da enzima glutationa GSH, provavelmente estimulada pelo próprio extrato de chá verde. Em conjunto, esses dados indicam que o ECV tem potencial para preservar o volume de trabalho e a contratilidade muscular de homens submetidos a fadiga acumulada.

7.2 CONCLUSÃO

Com base em nossos resultados, podemos concluir que:

1. É possível verificar a fadiga acumulada por meio de dados de volume e zona de potência em dias consecutivos de competição como durante um *grand tour*. Os dias de descanso favoreceram a recuperação do desempenho, o que reforça o fato de que a perda do desempenho se deve à interrupção do processo de recuperação da homeostase muscular.
2. Câmeras com características de hardware mais baixas são mais propensas a apresentar maiores taxas de erro. Além disso, a distância mais próxima entre a câmera e a região de interesse foi um fator

determinante para a precisão dos resultados. Em conjunto, esses resultados também indicam que a padronização dos protocolos de medição é um fator determinante para a validade da análise das assimetrias de temperatura.

3. Encontramos maior correlação intraclasse entre câmeras e interexaminadores na variável temperatura média, mas quando são considerados os efeitos do exercício físico, a variabilidade dos dados aumenta. É recomendável utilizar sempre o mesmo modelo de câmera para cada projeto, sendo a temperatura média a variável mais confiável.
4. A termografia infravermelha é capaz de detectar o aquecimento da pele devido à fadiga acumulada. As medidas de temperatura mínima e média da pele se mostram relacionadas com redução da força muscular quando a fadiga acumulada é induzida por dois dias consecutivos de exercício. A relação entre a temperatura da pele e as perdas de força parece promissora para ajudar a ajustar os programas de exercícios e otimizar a performance.
5. A utilização de um produto natural de relativamente fácil acesso a população (extrato de chá verde) como suplemento alimentar ajuda a minimizar as consequências deletérias do estresse oxidativo para a carga de trabalho no exercício físico, indicando um potencial benefício desse produto para o desempenho de resistência.
6. A suplementação de extrato de chá verde não afetou a magnitude do dano muscular após a fadiga cumulativa. Por outro lado, ajuda a preservar o desempenho neuromuscular e manter o volume de

exercício, minimizando os efeitos da fadiga cumulativa em homens não treinados.

7.3 PERSPECTIVAS FUTURAS

1. Determinar se a fadiga acumulada tem características específicas para pessoas do sexo masculino e feminino, e o impacto do ciclo hormonal das mulheres na avaliação dos seus efeitos;
2. Investigar se as variáveis eletromiográficas afetadas pela fadiga acumulada se relacionam com as variações da temperatura da pele;
3. Explorar se o nível de condicionamento físico influencia na capacidade de o extrato de chá verde produzir seus efeitos antioxidantes;
4. Entender se fatores comportamentais como motivação, estresse, humor, etc. podem contribuir para a fadiga acumulada;
5. Desenvolver ferramentas de análise de dados que possam combinar diferentes informações e gerar índices que não se baseiem apenas na variação da perda de força para atestar a fadiga acumulada.

8 REFERÊNCIAS

Accattato, F., Greco, M., Pullano, S. A., Carè, I., Fiorillo, A. S., Pujia, A., Montalcini, T., Foti, D. P., Brunetti, A., & Gulletta, E. (2017). Effects of acute physical exercise on oxidative stress and inflammatory status in young, sedentary obese subjects. *PLOS ONE*, *12*(6), e0178900. https://doi.org/10.1371/journal.pone.0178900

Albert, W. J., Wrigley, A. T., McLean, R. B., & Sleivert, G. G. (2006). Sex differences in the rate of fatigue development and recovery. *Dynamic Medicine: DM*, *5*, 2. https://doi.org/10.1186/1476-5918-5-2

Albertus-Kajee, Y., Tucker, R., Derman, W., & Lambert, M. (2010). Alternative methods of normalising EMG during cycling. *Journal of Electromyography and Kinesiology*, *20*(6), 1036–1043. https://doi.org/10.1016/j.jelekin.2010.07.011

Allen, D. G., & Westerblad, H. (2001). Role of phosphate and calcium stores in muscle fatigue. *The Journal of Physiology*, *536*(Pt 3), 657–665. https://doi.org/10.1111/j.1469-7793.2001.t01-1-00657.x

Armstrong, R. B., Warren, G. L., & Warren, J. A. (1991). Mechanisms of Exercise-Induced Muscle Fibre Injury: *Sports Medicine*, *12*(3), 184–207. https://doi.org/10.2165/00007256-199112030-00004

Astokorki, A. H. Y., & Mauger, A. R. (2017). Transcutaneous electrical nerve stimulation reduces exercise-induced perceived pain and improves endurance exercise performance. *European Journal of Applied Physiology*, *117*(3), 483–492. https://doi.org/10.1007/s00421-016-3532-6

Baird, M. F., Graham, S. M., Baker, J. S., & Bickerstaff, G. F. (2012). Creatine-kinase and exercise-related muscle damage implications for muscle

performance and recovery. *J Nutr Metab*, *2012*(1), 13. https://doi.org/10.1155/2012/960363

Banfi, G., Melegati, G., Barassi, A., Dogliotti, G., Melzi d'Eril, G., Dugué, B., & Corsi, M. M. (2009). Effects of whole-body cryotherapy on serum mediators of inflammation and serum muscle enzymes in athletes. *Journal of Thermal Biology*, *34*(2), 55–59. https://doi.org/10.1016/j.jtherbio.2008.10.003

Barbieri, E., & Sestili, P. (2012). Reactive Oxygen Species in Skeletal Muscle Signaling. *Journal of Signal Transduction*, *2012*, 1–17. https://doi.org/10.1155/2012/982794

Bartuzi, P., Roman-Liu, D., & Wiśniewski, T. (2012). The Influence of Fatigue on Muscle Temperature. *International Journal of Occupational Safety and Ergonomics*, *18*(2), 233–243. https://doi.org/10.1080/10803548.2012.11076931

Baumert, P., Temple, S., Stanley, J. M., Cocks, M., Strauss, J. A., Shepherd, S. O., Drust, B., Lake, M. J., Stewart, C. E., & Erskine, R. M. (2021). Neuromuscular fatigue and recovery after strenuous exercise depends on skeletal muscle size and stem cell characteristics. *Scientific Reports*, *11*(1), 7733. https://doi.org/10.1038/s41598-021-87195-x

Beckhauser, T. F., Francis-Oliveira, J., & De Pasquale, R. (2016). Reactive Oxygen Species: Physiological and Physiopathological Effects on Synaptic Plasticity: Supplementary Issue: Brain Plasticity and Repair. *Journal of Experimental Neuroscience*, *10s1*, JEN.S39887. https://doi.org/10.4137/JEN.S39887

Bedrood, Z., Rameshrad, M., & Hosseinzadeh, H. (2018). Toxicological effects of *Camellia sinensis* (green tea): A review. *Phytotherapy Research*, *32*(7), 1163–1180. https://doi.org/10.1002/ptr.6063

Bernatoniene, J., & Kopustinskiene, D. M. (2018). The Role of Catechins in Cellular Responses to Oxidative Stress. *Molecules (Basel, Switzerland)*, *23*(4), E965. https://doi.org/10.3390/molecules23040965

Bigland-Ritchie, B., Jones, D. A., Hosking, G. P., & Edwards, R. H. (1978). Central and peripheral fatigue in sustained maximum voluntary contractions of human quadriceps muscle. *Clinical Science and Molecular Medicine*, *54*(6), 609–614. https://doi.org/10.1042/cs0540609

Bilodeau, M., Schindler-Ivens, S., Williams, D. M., Chandran, R., & Sharma, S. S. (2003). EMG frequency content changes with increasing force and during fatigue in the quadriceps femoris muscle of men and women. *Journal of Electromyography and Kinesiology: Official Journal of the International Society of Electrophysiological Kinesiology*, *13*(1), 83–92. https://doi.org/10.1016/s1050-6411(02)00050-0

Birben, E., Sahiner, U. M., Sackesen, C., Erzurum, S., & Kalayci, O. (2012). Oxidative Stress and Antioxidant Defense. *World Allergy Organization Journal*, *5*(1), 9–19. https://doi.org/10.1097/WOX.0b013e3182439613

Boe, S. G., Rice, C. L., & Doherty, T. J. (2008). Estimating Contraction Level Using Root Mean Square Amplitude in Control Subjects and Patients With Neuromuscular Disorders. *Archives of Physical Medicine and Rehabilitation*, *89*(4), 711–718. https://doi.org/10.1016/j.apmr.2007.09.047

Bouzigon, R., Dupuy, O., Tiemessen, I., De Nardi, M., Bernard, J.-P., Mihailovic, T., Theurot, D., Miller, E. D., Lombardi, G., & Dugué, B. M. (2021). Cryostimulation for Post-exercise Recovery in Athletes: A Consensus and Position Paper. *Frontiers in Sports and Active Living*, *3*, 688828. https://doi.org/10.3389/fspor.2021.688828

Braicu, C., Ladomery, M. R., Chedea, V. S., Irimie, A., & Berindan-Neagoe, I. (2013). The relationship between the structure and biological actions of green tea catechins. *Food Chemistry*, *141*(3), 3282–3289. https://doi.org/10.1016/j.foodchem.2013.05.122

Cè, E., Longo, S., Limonta, E., Coratella, G., Rampichini, S., & Esposito, F. (2020). Peripheral fatigue: New mechanistic insights from recent technologies. *European Journal of Applied Physiology*, *120*(1), 17–39. https://doi.org/10.1007/s00421-019-04264-w

Charkoudian, N. (2003). Skin Blood Flow in Adult Human Thermoregulation: How It Works, When It Does Not, and Why. *Mayo Clinic Proceedings*, *78*(5), 603–612. https://doi.org/10.4065/78.5.603

Chen, L., Deng, H., Cui, H., Fang, J., Zuo, Z., Deng, J., Li, Y., Wang, X., & Zhao, L. (2018). Inflammatory responses and inflammation-associated diseases in organs. *Oncotarget*, *9*(6), 7204–7218. https://doi.org/10.18632/oncotarget.23208

Cifrek, M., Medved, V., Tonkovic, S., & Ostojic, S. (2009). Surface EMG based muscle fatigue evaluation in biomechanics. *Clin Biomech (Bristol, Avon)*, *24*(4), 327–340. https://doi.org/10.1016/j.clinbiomech.2009.01.010

Clarke, H. H., Shay, C. T., & Mathews, D. K. (1955). Strength decrement index: A new test of muscle fatigue. *Archives of Physical Medicine and Rehabilitation*, *36*(6), 376–378.

Clarkson, P. M., & Hubal, M. J. (2002). Exercise-Induced Muscle Damage in Humans: *American Journal of Physical Medicine & Rehabilitation*, *81*(Supplement), S52–S69. https://doi.org/10.1097/00002060-200211001-00007

Couto, N., Wood, J., & Barber, J. (2016). The role of glutathione reductase and related enzymes on cellular redox homoeostasis network. *Free Radical Biology and Medicine*, *95*, 27–42. https://doi.org/10.1016/j.freeradbiomed.2016.02.028

da Silva, W., Machado, Á. S., Souza, M. A., Kunzler, M. R., Priego-Quesada, J. I., & Carpes, F. P. (2018). Can exercise-induced muscle damage be related to changes in skin temperature? *Physiological Measurement*, *39*(10), 104007. https://doi.org/10.1088/1361-6579/aae6df

da Silva, W., Machado, A. S., Souza, M. A., Mello-Carpes, P. B., & Carpes, F. P. (2018). Effect of green tea extract supplementation on exercise-induced delayed onset muscle soreness and muscular damage. *Physiol Behav*, *194*(1), 5. https://doi.org/10.1016/j.physbeh.2018.05.006

Dahlstedt, A. J., Katz, A., Wieringa, B., & Westerblad, H. (2000). Is creatine kinase responsible for fatigue? Studies of isolated skeletal muscle deficient in creatine kinase. *The FASEB Journal*, *14*(7), 982–990. https://doi.org/10.1096/fasebj.14.7.982

Davis, H. L., Alabed, S., & Chico, T. J. A. (2020). Effect of sports massage on performance and recovery: A systematic review and meta-analysis. *BMJ*

Open Sport & Exercise Medicine, *6*(1), e000614. https://doi.org/10.1136/bmjsem-2019-000614

Dekkers, J. C., van Doornen, L. J. P., & Kemper, H. C. G. (1996). The Role of Antioxidant Vitamins and Enzymes in the Prevention of Exercise-Induced Muscle Damage: *Sports Medicine*, *21*(3), 213–238. https://doi.org/10.2165/00007256-199621030-00005

D'Emanuele, S., Maffiuletti, N. A., Tarperi, C., Rainoldi, A., Schena, F., & Boccia, G. (2021). Rate of Force Development as an Indicator of Neuromuscular Fatigue: A Scoping Review. *Frontiers in Human Neuroscience*, *15*, 701916. https://doi.org/10.3389/fnhum.2021.701916

El Helou, N., Berthelot, G., Thibault, V., Tafflet, M., Nassif, H., Campion, F., Hermine, O., & Toussaint, J.-F. (2010). Tour de France, Giro, Vuelta, and classic European races show a unique progression of road cycling speed in the last 20 years. *Journal of Sports Sciences*, *28*(7), 789–796. https://doi.org/10.1080/02640411003739654

Enoka, R. M., & Duchateau, J. (2008). Muscle fatigue: What, why and how it influences muscle function. *J Physiol*, *586*(1), 11–23. https://doi.org/10.1113/jphysiol.2007.139477

Enoka, R. M., & Duchateau, J. (2016). Translating Fatigue to Human Performance. *Medicine & Science in Sports & Exercise*, *48*(11), 2228–2238. https://doi.org/10.1249/MSS.0000000000000929

Fatouros, I., & Jamurtas, A. (2016). Insights into the molecular etiology of exercise-induced inflammation: Opportunities for optimizing performance. *Journal of Inflammation Research*, *Volume 9*, 175–186. https://doi.org/10.2147/JIR.S114635

Fernandes, A. de A., Amorim, P. R. dos S., Brito, C. J., de Moura, A. G., Moreira, D. G., Costa, C. M. A., Sillero-Quintana, M., & Marins, J. C. B. (2014). Measuring skin temperature before, during and after exercise: A comparison of thermocouples and infrared thermography. *Physiological Measurement*, *35*(2), 189–203. https://doi.org/10.1088/0967-3334/35/2/189

Fernandes, J., Lamb, K., & Twist, C. (2019). Exercise-Induced Muscle Damage and Recovery in Young and Middle-Aged Males with Different Resistance Training Experience. *Sports*, *7*(6), 132. https://doi.org/10.3390/sports7060132

Fernández-Lázaro, D., Mielgo-Ayuso, J., Seco Calvo, J., Córdova Martínez, A., Caballero García, A., & Fernandez-Lazaro, C. (2020). Modulation of Exercise-Induced Muscle Damage, Inflammation, and Oxidative Markers by Curcumin Supplementation in a Physically Active Population: A Systematic Review. *Nutrients*, *12*(2), 501. https://doi.org/10.3390/nu12020501

Flôres, M. F., Martins, A., Schimidt, H. L., Santos, F. W., Izquierdo, I., Mello-Carpes, P. B., & Carpes, F. P. (2014). Effects of green tea and physical exercise on memory impairments associated with aging. *Neurochemistry International*, *78*, 53–60. https://doi.org/10.1016/j.neuint.2014.08.008

Folland, J. P., & Williams, A. G. (2007). The Adaptations to Strength Training: Morphological and Neurological Contributions to Increased Strength. *Sports Medicine*, *37*(2), 145–168. https://doi.org/10.2165/00007256-200737020-00004

Formenti, D., Ludwig, N., Gargano, M., Gondola, M., Dellerma, N., Caumo, A., & Alberti, G. (2013). Thermal Imaging of Exercise-Associated Skin Temperature Changes in Trained and Untrained Female Subjects. *Annals of Biomedical Engineering*, *41*(4), 863–871. https://doi.org/10.1007/s10439-012-0718-x

Fraga, C. G., Galleano, M., Verstraeten, S. V., & Oteiza, P. I. (2010). Basic biochemical mechanisms behind the health benefits of polyphenols. *Molecular Aspects of Medicine*, *31*(6), 435–445. https://doi.org/10.1016/j.mam.2010.09.006

Fukai, T., & Ushio-Fukai, M. (2011). Superoxide dismutases: Role in redox signaling, vascular function, and diseases. *Antioxidants & Redox Signaling*, *15*(6), 1583–1606. https://doi.org/10.1089/ars.2011.3999

Gomes, M., Santos, P., Correia, P., Pezarat-Correia, P., & Mendonca, G. V. (2021). Sex differences in muscle fatigue following isokinetic muscle contractions. *Scientific Reports*, *11*(1), 8141. https://doi.org/10.1038/s41598-021-87443-0

González-Izal, M., Malanda, A., Gorostiaga, E., & Izquierdo, M. (2012). Electromyographic models to assess muscle fatigue. *Journal of Electromyography and Kinesiology*, *22*(4), 501–512. https://doi.org/10.1016/j.jelekin.2012.02.019

Goodall, S., Charlton, K., Howatson, G., & Thomas, K. (2015). Neuromuscular Fatigability during Repeated-Sprint Exercise in Male Athletes. *Medicine & Science in Sports & Exercise*, *47*(3), 528–536. https://doi.org/10.1249/MSS.0000000000000443

Goodall, S., Thomas, K., Harper, L. D., Hunter, R., Parker, P., Stevenson, E., West, D., Russell, M., & Howatson, G. (2017). The assessment of neuromuscular fatigue during 120 min of simulated soccer exercise. *European Journal of Applied Physiology*, *117*(4), 687–697. https://doi.org/10.1007/s00421-017-3561-9

Goyal, M. M., & Basak, A. (2010). Human catalase: Looking for complete identity. *Protein & Cell*, *1*(10), 888–897. https://doi.org/10.1007/s13238-010-0113-z

Greenberg, D. B. (2002). Clinical Dimensions of Fatigue. *The Primary Care Companion to The Journal of Clinical Psychiatry*, *04*(03), 90–93. https://doi.org/10.4088/PCC.v04n0301

Hadžić, V., Širok, B., Malneršič, A., & Čoh, M. (2019). Can infrared thermography be used to monitor fatigue during exercise? A case study. *Journal of Sport and Health Science*, *8*(1), 89–92. https://doi.org/10.1016/j.jshs.2015.08.002

Häkkinen, K. (1995). Neuromuscular fatigue and recovery in women at different ages during heavy resistance loading. *Electromyography and Clinical Neurophysiology*, *35*(7), 403–413.

Halperin, I., Chapman, D. W., & Behm, D. G. (2015). Non-local muscle fatigue: Effects and possible mechanisms. *European Journal of Applied Physiology*, *115*(10), 2031–2048. https://doi.org/10.1007/s00421-015-3249-y

Hargreaves, M., & Spriet, L. L. (2020). Skeletal muscle energy metabolism during exercise. *Nature Metabolism*, *2*(9), 817–828. https://doi.org/10.1038/s42255-020-0251-4

Hernández, A., Cheng, A., & Westerblad, H. (2012). Antioxidants and Skeletal Muscle Performance: “Common Knowledge” vs. Experimental Evidence. *Frontiers in Physiology*, *3*. https://doi.org/10.3389/fphys.2012.00046

Hou, X., Liu, J., Weng, K., Griffin, L., Rice, L. A., & Jan, Y.-K. (2021). Effects of Various Physical Interventions on Reducing Neuromuscular Fatigue Assessed by Electromyography: A Systematic Review and Meta-Analysis. *Frontiers in Bioengineering and Biotechnology*, *9*, 659138. https://doi.org/10.3389/fbioe.2021.659138

Hunter, S. K. (2018). Performance Fatigability: Mechanisms and Task Specificity. *Cold Spring Harbor Perspectives in Medicine*, *8*(7), a029728. https://doi.org/10.1101/cshperspect.a029728

Hunter, S. K., Critchlow, A., & Enoka, R. M. (2005). Muscle endurance is greater for old men compared with strength-matched young men. *Journal of Applied Physiology*, *99*(3), 890–897. https://doi.org/10.1152/japplphysiol.00243.2005

Jo, E., Juache, G., Saralegui, D., Weng, D., & Falatoonzadeh, S. (2018). The Acute Effects of Foam Rolling on Fatigue-Related Impairments of Muscular Performance. *Sports*, *6*(4), 112. https://doi.org/10.3390/sports6040112

Jówko, E. (2015). Green Tea Catechins and Sport Performance. In M. Lamprecht (Ed.), *Antioxidants in Sport Nutrition*. CRC Press/Taylor & Francis. http://www.ncbi.nlm.nih.gov/books/NBK299060/

Karlsson, J. (1979). Localized muscular fatigue: Role of muscle metabolism and substrate depletion. *Exercise and Sport Sciences Reviews*, *7*(1), 1???42. https://doi.org/10.1249/00003677-197900070-00003

Karp, G. (2010). *Cell and molecular biology: Concepts and experiments* (6th ed). John Wiley.

Karthick, P. A., & Ramakrishnan, S. (2016). Muscle fatigue analysis using surface EMG signals and time–frequency based medium-to-low band power ratio. *Electronics Letters*, *52*, 185–186. https://doi.org/10.1049/el.2015.3460

Kataoka, R., Vasenina, E., Hammert, W. B., Ibrahim, A. H., Dankel, S. J., & Buckner, S. L. (2022). Is there Evidence for the Suggestion that Fatigue Accumulates Following Resistance Exercise? *Sports Medicine*, *52*(1), 25–36. https://doi.org/10.1007/s40279-021-01572-0

Khaitin, V., Bezuglov, E., Lazarev, A., Matveev, S., Ivanova, O., Maffulli, N., & Achkasov, E. (2021). Markers of muscle damage and strength performance in professional football (soccer) players during the competitive period. *Annals of Translational Medicine*, *9*(2), 113. https://doi.org/10.21037/atm-20-2923

Khan, N., & Mukhtar, H. (2013). Tea and Health: Studies in Humans. *Current Pharmaceutical Design*, *19*(34), 6141–6147. https://doi.org/10.2174/1381612811319340008

Kirimtat, A., Krejcar, O., Selamat, A., & Herrera-Viedma, E. (2020). FLIR vs SEEK thermal cameras in biomedicine: Comparative diagnosis through infrared thermography. *BMC Bioinformatics*, *21*(Suppl 2), 88. https://doi.org/10.1186/s12859-020-3355-7

Kuipers, H. (1994). Exercise-Induced Muscle Damage. *International Journal of Sports Medicine*, *15*(03), 132–135. https://doi.org/10.1055/s-2007-1021034

Lai, N., Gladden, L. B., Carlier, P. G., & Cabrera, M. E. (2008). Models of muscle contraction and energetics. *Drug Discovery Today. Disease Models*, *5*(4), 273–288. https://doi.org/10.1016/j.ddmod.2009.07.001

Lamprecht, M. (Ed.). (2015). *Antioxidants in sport nutrition*. CRC Press, Taylor & Francis Group.

Lanferdini, F. J., Bini, R. R., Baroni, B. M., Klein, K. D., Carpes, F. P., & Vaz, M. A. (2018). Improvement of Performance and Reduction of Fatigue With Low-Level Laser Therapy in Competitive Cyclists. *International Journal of Sports Physiology and Performance*, *13*(1), 14–22. https://doi.org/10.1123/ijspp.2016-0187

Lattier, G., Millet, G. Y., Martin, A., & Martin, V. (2004). Fatigue and Recovery After High-Intensity Exercise Part II: Recovery Interventions. *International Journal of Sports Medicine*, *25*(7), 509–515. https://doi.org/10.1055/s-2004-820946

Linnamo, V., Häkkinen, K., & Komi, P. V. (1997). Neuromuscular fatigue and recovery in maximal compared to explosive strength loading. *European Journal of Applied Physiology and Occupational Physiology*, *77*(1–2), 176–181. https://doi.org/10.1007/s004210050317

Lobo, V., Patil, A., Phatak, A., & Chandra, N. (2010). Free radicals, antioxidants and functional foods: Impact on human health. *Pharmacognosy Reviews*, *4*(8), 118. https://doi.org/10.4103/0973-7847.70902

Lubos, E., Loscalzo, J., & Handy, D. E. (2011). Glutathione peroxidase-1 in health and disease: From molecular mechanisms to therapeutic opportunities. *Antioxidants & Redox Signaling*, *15*(7), 1957–1997. https://doi.org/10.1089/ars.2010.3586

Machado, A. S., da Silva, W., Souza, M. A., & Carpes, F. P. (2018). Green Tea Extract Preserves Neuromuscular Activation and Muscle Damage Markers in Athletes Under Cumulative Fatigue. *Front Physiol*, *9*(1), 9. https://doi.org/10.3389/fphys.2018.01137

Mair, S. D., Seaber, A. V., Glisson, R. R., & Garrett, W. E. (1996). The Role of Fatigue in Susceptibility to Acute Muscle Strain Injury. *The American Journal of Sports Medicine*, *24*(2), 137–143. https://doi.org/10.1177/036354659602400203

Marshall, P. W. M., Cross, R., & Haynes, M. (2018). The fatigue of a full body resistance exercise session in trained men. *Journal of Science and Medicine in Sport*, *21*(4), 422–426. https://doi.org/10.1016/j.jsams.2017.06.020

Marshall, P. W., Melville, G. W., Cross, R., Marquez, J., Harrison, I., & Enoka, R. M. (2021). Fatigue, pain, and the recovery of neuromuscular function after consecutive days of full-body resistance exercise in trained men. *European Journal of Applied Physiology*, *121*(11), 3103–3116. https://doi.org/10.1007/s00421-021-04777-3

Marx, R. (1933). Muscular Fatigue, Muscle Strain and Muscle Cramps. *California and Western Medicine*, *38*(2), 96–97.

Mendez-Villanueva, A., Edge, J., Suriano, R., Hamer, P., & Bishop, D. (2012). The Recovery of Repeated-Sprint Exercise Is Associated with PCr Resynthesis, while Muscle pH and EMG Amplitude Remain Depressed. *PLoS ONE*, *7*(12), e51977. https://doi.org/10.1371/journal.pone.0051977

Miller, B. F., Gruben, K. G., & Morgan, B. J. (2000). Circulatory responses to voluntary and electrically induced muscle contractions in humans. *Physical Therapy*, *80*(1), 53–60.

Mittal, M., Siddiqui, M. R., Tran, K., Reddy, S. P., & Malik, A. B. (2014). Reactive oxygen species in inflammation and tissue injury. *Antioxidants & Redox Signaling*, *20*(7), 1126–1167. https://doi.org/10.1089/ars.2012.5149

Montgomery, P. G., Pyne, D. B., Hopkins, W. G., Dorman, J. C., Cook, K., & Minahan, C. L. (2008). The effect of recovery strategies on physical performance and cumulative fatigue in competitive basketball. *Journal of Sports Sciences*, *26*(11), 1135–1145. https://doi.org/10.1080/02640410802104912

Morán-Navarro, R., Pérez, C. E., Mora-Rodríguez, R., de la Cruz-Sánchez, E., González-Badillo, J. J., Sánchez-Medina, L., & Pallarés, J. G. (2017). Time course of recovery following resistance training leading or not to failure. *European Journal of Applied Physiology*, *117*(12), 2387–2399. https://doi.org/10.1007/s00421-017-3725-7

Murase, T., Haramizu, S., Shimotoyodome, A., Nagasawa, A., & Tokimitsu, I. (2005). Green tea extract improves endurance capacity and increases muscle lipid oxidation in mice. *American Journal of Physiology. Regulatory, Integrative and Comparative Physiology*, *288*(3), R708-715. https://doi.org/10.1152/ajpregu.00693.2004

Murase, T., Haramizu, S., Shimotoyodome, A., Tokimitsu, I., & Hase, T. (2006). Green tea extract improves running endurance in mice by stimulating lipid utilization during exercise. *American Journal of Physiology. Regulatory,*

Integrative and Comparative Physiology, *290*(6), R1550-1556. https://doi.org/10.1152/ajpregu.00752.2005

Ørtenblad, N., Westerblad, H., & Nielsen, J. (2013). Muscle glycogen stores and fatigue: Muscle glycogen and fatigue. *The Journal of Physiology*, *591*(18), 4405–4413. https://doi.org/10.1113/jphysiol.2013.251629

Ortiz, R. O., Sinclair Elder, A. J., Elder, C. L., & Dawes, J. J. (2019). A Systematic Review on the Effectiveness of Active Recovery Interventions on Athletic Performance of Professional-, Collegiate-, and Competitive-Level Adult Athletes: *Journal of Strength and Conditioning Research*, *33*(8), 2275–2287. https://doi.org/10.1519/JSC.0000000000002589

Panche, A. N., Diwan, A. D., & Chandra, S. R. (2016). Flavonoids: An overview. *Journal of Nutritional Science*, *5*, e47. https://doi.org/10.1017/jns.2016.41

Peake, J. M., Neubauer, O., Della Gatta, P. A., & Nosaka, K. (2017). Muscle damage and inflammation during recovery from exercise. *Journal of Applied Physiology*, *122*(3), 559–570. https://doi.org/10.1152/japplphysiol.00971.2016

Peters, R. A. (1913). The heat production of fatigue and its relation to the production of lactic acid in amphibian muscle. *The Journal of Physiology*, *47*(3), 243–271. https://doi.org/10.1113/jphysiol.1913.sp001622

Piponnier, E., Martin, V., Bourdier, P., Biancarelli, B., Kluka, V., Garcia-Vicencio, S., Jegu, A.-G., Cardenoux, C., Morio, C., Coudeyre, E., & Ratel, S. (2019). Maturation-related changes in the development and etiology of neuromuscular fatigue. *European Journal of Applied Physiology*, *119*(11–12), 2545–2555. https://doi.org/10.1007/s00421-019-04233-3

Powers, S. K., & Jackson, M. J. (2008). Exercise-induced oxidative stress: Cellular mechanisms and impact on muscle force production. *Physiological Reviews*, *88*(4), 1243–1276. https://doi.org/10.1152/physrev.00031.2007

Priego Quesada, J. I. (Ed.). (2017). *Application of Infrared Thermography in Sports Science* (1st ed. 2017). Springer International Publishing : Imprint: Springer. https://doi.org/10.1007/978-3-319-47410-6

Priego Quesada, J. I., Carpes, F. P., Bini, R. R., Salvador Palmer, R., Pérez-Soriano, P., & Cibrián Ortiz de Anda, R. M. (2015). Relationship between skin temperature and muscle activation during incremental cycle exercise. *Journal of Thermal Biology*, *48*, 28–35. https://doi.org/10.1016/j.jtherbio.2014.12.005

Prochniewicz, E., Spakowicz, D., & Thomas, D. D. (2008). Changes in actin structural transitions associated with oxidative inhibition of muscle contraction. *Biochemistry*, *47*(45), 11811–11817. https://doi.org/10.1021/bi801080x

Rahman, T., Hosen, I., Islam, T., & Shekhar, H. (2012). Oxidative stress and human health. *Advances in Bioscience and Biotechnology*, *03*, 997–1019. https://doi.org/10.4236/abb.2012.327123

Ribeiro, A. S., Avelar, A., Schoenfeld, B. J., Trindade, M. C. C., Ritti-Dias, R. M., Altimari, L. R., & Cyrino, E. S. (2014). Effect of 16 Weeks of Resistance Training on Fatigue Resistance in Men and Women. *Journal of Human Kinetics*, *42*(1), 165–174. https://doi.org/10.2478/hukin-2014-0071

Ring, E. F. J. (2006). The historical development of thermometry and thermal imaging in medicine. *Journal of Medical Engineering & Technology*, *30*(4), 192–198. https://doi.org/10.1080/03091900600711332

Rosenthal, T. C., Majeroni, B. A., Pretorius, R., & Malik, K. (2008). Fatigue: An overview. *American Family Physician*, *78*(10), 1173–1179.

Sánchez-Migallón, V., López-Samanes, Á., Del Coso, J., Navandar, A., Aagaard, P., & Moreno-Pérez, V. (2022). Effects of consecutive days of matchplay on maximal hip abductor and adductor strength in female field hockey players. *BMC Sports Science, Medicine and Rehabilitation*, *14*(1), 3. https://doi.org/10.1186/s13102-021-00394-x

Schimidt, H. L., Garcia, A., Martins, A., Mello-Carpes, P. B., & Carpes, F. P. (2017). Green tea supplementation produces better neuroprotective effects than red and black tea in Alzheimer-like rat model. *Food Research International*, *100*, 442–448. https://doi.org/10.1016/j.foodres.2017.07.026

Schimidt, H. L., Vieira, A., Altermann, C., Martins, A., Sosa, P., Santos, F. W., Mello-Carpes, P. B., Izquierdo, I., & Carpes, F. P. (2014). Memory deficits and oxidative stress in cerebral ischemia–reperfusion: Neuroprotective role of physical exercise and green tea supplementation. *Neurobiology of Learning and Memory*, *114*, 242–250. https://doi.org/10.1016/j.nlm.2014.07.005

Schoenfeld, B. J., Ogborn, D., & Krieger, J. W. (2016). Effects of Resistance Training Frequency on Measures of Muscle Hypertrophy: A Systematic Review and Meta-Analysis. *Sports Medicine*, *46*(11), 1689–1697. https://doi.org/10.1007/s40279-016-0543-8

Seifried, H. E., Anderson, D. E., Fisher, E. I., & Milner, J. A. (2007). A review of the interaction among dietary antioxidants and reactive oxygen species. *The Journal of Nutritional Biochemistry*, *18*(9), 567–579. https://doi.org/10.1016/j.jnutbio.2006.10.007

Shing, C. M., Peake, J. M., Ahern, S. M., Strobel, N. A., Wilson, G., Jenkins, D. G., & Coombes, J. S. (2007). The effect of consecutive days of exercise on markers of oxidative stress. *Appl Physiol Nutr Metab*, *32*(4), 677–685. https://doi.org/10.1139/H07-051

Simmons, G. H., Wong, B. J., Holowatz, L. A., & Kenney, W. L. (2011). Changes in the control of skin blood flow with exercise training: Where do cutaneous vascular adaptations fit in? *Experimental Physiology*, *96*(9), 822–828. https://doi.org/10.1113/expphysiol.2010.056176

Steinbacher, P., & Eckl, P. (2015). Impact of oxidative stress on exercising skeletal muscle. *Biomolecules*, *5*(2), 356–377. https://doi.org/10.3390/biom5020356

Stewart, R. D., Duhamel, T. A., Rich, S., Tupling, A. R., & Green, H. J. (2008). Effects of Consecutive Days of Exercise and Recovery on Muscle Mechanical Function. *Medicine & Science in Sports & Exercise*, *40*(2), 316–325. https://doi.org/10.1249/mss.0b013e31815adf02

Sundstrup, E., Jakobsen, M. D., Brandt, M., Jay, K., Aagaard, P., & Andersen, L. L. (2016). Strength Training Improves Fatigue Resistance and Self-Rated Health in Workers with Chronic Pain: A Randomized Controlled Trial. *BioMed Research International*, *2016*, 1–11. https://doi.org/10.1155/2016/4137918

Suzuki, T., Pervin, M., Goto, S., Isemura, M., & Nakamura, Y. (2016). Beneficial Effects of Tea and the Green Tea Catechin Epigallocatechin-3-gallate on Obesity. *Molecules*, *21*(10), 1305. https://doi.org/10.3390/molecules21101305

Taylor, J. L., Amann, M., Duchateau, J., Meeusen, R., & Rice, C. L. (2016). Neural Contributions to Muscle Fatigue: From the Brain to the Muscle and Back Again. *Medicine & Science in Sports & Exercise*, *48*(11), 2294–2306. https://doi.org/10.1249/MSS.0000000000000923

Tibana, R. A., de Almeida, L. M., Frade de Sousa, N. M., Nascimento, D. da C., Neto, I. V. de S., de Almeida, J. A., de Souza, V. C., Lopes, M. de F. T. P. L., Nobrega, O. de T., Vieira, D. C. L., Navalta, J. W., & Prestes, J. (2016). Two Consecutive Days of Extreme Conditioning Program Training Affects Pro and Anti-inflammatory Cytokines and Osteoprotegerin without Impairments in Muscle Power. *Frontiers in Physiology*, *7*, 260. https://doi.org/10.3389/fphys.2016.00260

Tosovic, D., Than, C., & Brown, J. M. M. (2016). The effects of accumulated muscle fatigue on the mechanomyographic waveform: Implications for injury prediction. *European Journal of Applied Physiology*, *116*(8), 1485–1494. https://doi.org/10.1007/s00421-016-3398-7

Vardasca, R., Ring, E. F. J., Plassmann, P., & Jones, C. (2012). Termal symmetry of the upper and lower extremities in healthy subjects. *Thermology International*, *22*, 53–60.

Vieira, W., Goes, R., Costa, F., Parizotto, N., Perez, S., Baldissera, V., Munin, F., & Schwantes, M. (2006). Adaptação enzimática da LDH em ratos submetidos a treinamento aeróbio em esteira e laser de baixa intensidade.

Revista Brasileira de Fisioterapia, *10*(2). https://doi.org/10.1590/S1413-35552006000200011

Wadley, A. J., Veldhuijzen van Zanten, J. J. C. S., & Aldred, S. (2013). The interactions of oxidative stress and inflammation with vascular dysfunction in ageing: The vascular health triad. *AGE*, *35*(3), 705–718. https://doi.org/10.1007/s11357-012-9402-1

Wallimann, T., Wyss, M., Brdiczka, D., Nicolay, K., & Eppenberger, H. M. (1992). Intracellular compartmentation, structure and function of creatine kinase isoenzymes in tissues with high and fluctuating energy demands: The "phosphocreatine circuit" for cellular energy homeostasis. *The Biochemical Journal*, *281 (Pt 1)*, 21–40. https://doi.org/10.1042/bj2810021

Wan, J.-J., Qin, Z., Wang, P.-Y., Sun, Y., & Liu, X. (2017). Muscle fatigue: General understanding and treatment. *Experimental & Molecular Medicine*, *49*(10), e384. https://doi.org/10.1038/emm.2017.194

Wang, D., & Wang, X. (2019). Efficacy of laser therapy for exercise-induced fatigue: A meta-analysis. *Medicine*, *98*(38), e17201. https://doi.org/10.1097/MD.0000000000017201

Weerapong, P., Hume, P. A., & Kolt, G. S. (2005). The Mechanisms of Massage and Effects on Performance, Muscle Recovery and Injury Prevention: *Sports Medicine*, *35*(3), 235–256. https://doi.org/10.2165/00007256-200535030-00004

Yang, Y., Bay, P. B., Wang, Y. R., Huang, J., Teo, H. W. J., & Goh, J. (2018). Effects of Consecutive Versus Non-consecutive Days of Resistance

Training on Strength, Body Composition, and Red Blood Cells. *Frontiers in Physiology*, *9*, 725. https://doi.org/10.3389/fphys.2018.00725

Zarrouk, N., Rebai, H., Yahia, A., Souissi, N., Hug, F., & Dogui, M. (2011). Comparison of Recovery Strategies on Maximal Force-Generating Capacity and Electromyographic Activity Level of the Knee Extensor Muscles. *Journal of Athletic Training*, *46*(4), 386–394. https://doi.org/10.4085/1062-6050-46.4.386

Zhang, X., & Zhou, P. (2012). Sample entropy analysis of surface EMG for improved muscle activity onset detection against spurious background spikes. *J Electromyogr Kinesiol*, *22*(6), 901–907. https://doi.org/10.1016/j.jelekin.2012.06.005

ANEXO I – PRODUÇÕES RELACIONADAS COM A TESE

Cursos de curta duração ministrados:

1. I Seminário em Biomecânica da Faculdade SOGIPA, 2020 - Recuperação muscular após exercício: da biomecânica à bioquímica.

2. Mini Simpósio de Biomecânica - Desafios da locomoção, 2019 - Efeito da sensibilidade cutânea dos pés na pressão plantar.

Prêmios e distinções em eventos:

1. 2021 - Melhor trabalho apresentado na modalidade Poster, na categoria Locomoção e Postura, durante XIX CBB 2021, Congresso Brasileiro de Biomecânica - XIX CBB 2021 – Belo Horizonte, MG, Brasil.

2. 2020 - Best Poster, I International Congress on Application of Infrared Thermography in Sport Science – Valência, Espanha.

3. 2019 - Menção Honrosa de trabalho apresentado, II Simpósio de Fisiomecânica da Locomoção Terrestre – Florianópolis, SC, Brasil.

Artigos aceitos para publicação

1. **SOSA MACHADO, ÁLVARO**; SILVA, W.; ANDRADE, C.; FUENTE, C. I. L.; SOUZA, M. A.; CARPES, FELIPE P. Green tea supplementation favors exercise volume in untrained men under cumulative fatigue. Science & Sports. , 2022.

Artigos completos publicados em periódicos:

1. **MACHADO, ÁLVARO S**; PRIEGO-QUESADA, JOSE IGNACIO; JIMENEZ-PEREZ, IRENE; GIL-CALVO, MARINA; CARPES, FELIPE P; PEREZ-SORIANO, PEDRO. Effects of different hydration supports on stride kinematics, comfort, and impact accelerations during running. Gait & Posture. v.9, p.115 - , 2022.

2. MACHADO, MATHIAS S.; **MACHADO, ÁLVARO S**.; GUADAGNIN, ELIANE C.; SCHMIDT, DANIEL; GERMANO, ANDRESA M.C.; CARPES, FELIPE P. Effects of increasing temperature in different foot regions on foot sensitivity and postural control in young adults. Foot (Edinburgh). v.50, p.101887 - , 2022.

3. SILVA, W.; **SOSA MACHADO, ÁLVARO**; ROBERTO KUNZLER, MARCOS; JIMENEZ-PEREZ, I.; CALVO, M. G.; QUESADA, J. I. P.; CARPES, FELIPE P Reproducibility of skin temperature analyses by novice and experienced evaluators using infrared thermography. Journal of Thermal Biology. p.103345 - , 2022.

4. CARVALHO, J.; KUNZLER, M. R.; QUESADA, J. I. P.; APARICIO, I.; PEREZ-SORIANO, P.; **MACHADO, ÁLVARO S**.; CARPES, FELIPE P. Effects of 24 h Compression Interventions with Different Garments on Recovery Markers during Running. Life. v.11, p.905 - , 2021.

5. DA SILVA SOARES, JÉSSICA; CARPES, FELIPE P; DE FÁTIMA GERALDO, GISLAINE; BERTÚ MEDEIROS, FABÍOLA; ROBERTO KUNZLER, MARCOS; **SOSA MACHADO, ÁLVARO**; AUGUSTO PAOLUCCI, LEOPOLDO; GUSTAVO PEREIRA DE ANDRADE, ANDRÉ. Functional data analysis reveals

asymmetrical crank torque during cycling performed at different exercise intensities. Journal of Biomechanics. v.122, p.110478, 2021.

6. **MACHADO, ÁLVARO S**.; PRIEGO-QUESADA, JOSE IGNACIO; JIMENEZ-PEREZ, IRENE; GIL-CALVO, MARINA; CARPES, FELIPE PIVETTA; PEREZ-SORIANO, PEDRO. Influence of infrared camera model and evaluator reproducibility in the assessment of skin temperature responses to physical exercise. Journal of Thermal Biology, v.102913, p.102913 - , 2021.

7. DA SILVA, WILLIAN; **MACHADO, ÁLVARO SOSA**; LEMOS, ANDRESSA LEMES; DE ANDRADE, CAMILLA FERREIRA; PRIEGO-QUESADA, JOSE IGNACIO; CARPES, FELIPE P. Relationship between exercise-induced muscle soreness, pain thresholds, and skin temperature in men and women. Journal of Thermal Biology. v.100, p.103051, 2021.

8. QUESADA, J. I. P.; **MACHADO, ÁLVARO S.**; CALVO, M. G.; JIMENEZ-PEREZ, I.; CIBRIAN, R.; SALVADOR-PALMER, R.; PEREZ-SORIANO, P.
A methodology to assess the effect of sweat on infrared thermography data after running: preliminary study. Infrared Physics & Technology, p.103382 - , 2020.

9. SILVA, C. C.; **MACHADO, ÁLVARO S**.; SANTOS, G.; HELEN LIDIANE SCHIMIDT; KUNZLER, M. R.; CARPES, FELIPE P. Acute responses to barefoot 5 km treadmill running involve changes in landing kinematics and delayed onset muscle soreness. Gait & Posture. v.77, p.231 - 235, 2020.

10. DE MEDEIROS FIGUEIREDO, MARIANE; SILVELO FRANCO, PEDRO; FRAGA MORO, CRISTIANE; SOUZA DA ROCHA, EMMANUEL; **SOSA MACHADO, ALVARO**; PIVETTA CARPES, FELIPE. Uma única observação da pressão plantar representa a marcha de crianças em diferentes dias?. Revista Brasileira Ciências da Saúde. , v.24, p.161 - 170, 2020.

11. FUENTE, C. I. L.; **MACHADO, ÁLVARO S**.; KUNZLER, M. R.; CARPES, FELIPE P. Winter School on sEMG Signal Processing: An Initiative to Reduce Educational Gaps and to Promote the Engagement of Physiotherapists and Movement Scientists With Science. Frontiers in Neurology. , v.11, p.509 - , 2020.

Resumos publicados em anais de eventos

1. ZACHARIAS, L. M. S.; SILVA, W.; **SOSA MACHADO, ÁLVARO**; JIMENEZ-PEREZ, I.; CALVO, M. G.; QUESADA, J. I. P.; CARPES, FELIPE P
Concordância na análise da temperatura da pele entre avaliadores inexperientes e experientes usando termografia infravermelha In: XII Simpósio em Neuromecânica Aplicada: adaptação funcional no esporte, 2022, Taquara.
Anais do XII Simpósio em Neuromecânica Aplicada. , 2022.

2. PEREIRA, M. E. F.; **SOSA MACHADO, ÁLVARO**; SILVA, W.; MORAIS, A. C. L.; CARPES, FELIPE P
Efeito da dor muscular de início tardio induzida pelo exercício sobre o senso de posição articular In: XII Simpósio em Neuromecânica Aplicada: adaptação funcional no esporte, 2022
Anais do XII Simpósio em Neuromecânica Aplicada. , 2022.

3. PAZ, M. M.; MACHADO, MATHIAS S.; **SOSA MACHADO, ÁLVARO**; GUADAGNIN, E. C.; GERMANO, A. M. C.; CARPES, FELIPE P
Respostas sensoriais do pé e controle postural em idosos após o aquecimento passivo In: XII Simpósio em Neuromecânica Aplicada: adaptação funcional no esporte, 2022, Taquara.
Anais do XII Simpósio em Neuromecânica Aplicada. , 2022.

4. MORAIS, A. C. L.; **SOSA MACHADO, ALVARO**; SILVA, W.; CARPES, FELIPE P
Uso da termografia infravermelha para avaliar a fadiga acumulada In: XII

Simpósio em Neuromecânica Aplicada: adaptação funcional no esporte, 2022, Taquara.

Anais do XII Simpósio em Neuromecânica Aplicada. , 2022.

5. TULIUS, E. S.; SILVA, W.; **MACHADO, ÁLVARO S.**; KUNZLER, M. R.; JIMENEZ-PEREZ, I.; CALVO, M. G.; QUESADA, J. I. P.; CARPES, FELIPE P
Efeito do nível de experiência do avaliador na repetibilidade de medidas basais do quadríceps usando termografia infravermelha In: XIX Congresso Brasileiro de Biomecânica, 2021, Belo Horizonte.

Anais do XIX Congresso Brasileiro de Biomecânica. , 2021.

6. CARVALHO, J.; KUNZLER, M. R.; QUESADA, J. I. P.; APARICIO, I.; PEREZ-SORIANO, P.; **MACHADO, ÁLVARO S.**; Felipe P Carpes
Efeitos de meias compressivas sobre aspectos biomecânicos e fisiológicos da recuperação pós-exercício em corredores In: XIX Congresso Brasileiro de Biomecânica, 2021, Belo Horizonte.

Anais do XIX Congresso Brasileiro de Biomecânica. , 2021.

7. MACHADO, M. S.; **MACHADO, ÁLVARO S.**; GUADAGNIN, E. C.; SCHMIDT, D.; GERMANO, A. M. C.; Felipe P Carpes
Efeitos do aquecimento dos pés sobre o controle postural em idosos In: XIX Congresso Brasileiro de Biomecânica, 2021

Anais do XIX Congresso Brasileiro de Biomecânica. , 2021.

8. MORAIS, A. C. L.; PAZ, M. M.; **MACHADO, ÁLVARO S.**; SILVA, W.; JIMENEZ-PEREZ, I.; CALVO, M. G.; PEREZ-SORIANO, P.; QUESADA, J. I. P.; Felipe P Carpes
Influência do modelo de câmera infravermelha na determinação da temperatura da pele após exercício físico In: XIX Congresso Brasileiro de Biomecânica, 2021, Belo Horizonte.

Anais do XIX Congresso Brasileiro de Biomecânica. , 2021.

9. MACHADO, M. S.; **MACHADO, ÁLVARO S.**; GUADAGNIN, E. C.; SCHMIDT, D.; GERMANO, A. M. C.; Felipe P Carpes

O impacto de diferentes formas de aquecimentos da pele sobre a sensibilidade cutânea plantar em adultos jovens In: XIX Congresso Brasileiro de Biomecânica, 2021, Belo Horizonte.

Anais do XIX Congresso Brasileiro de Biomecânica. , 2021.

10. **MACHADO, ÁLVARO S.**; CANADA, M.; JIMENEZ-PEREZ, IRENE; CALVO, M. G.; Felipe P Carpes; PEREZ-SORIANO, P.; QUESADA, J. I. P.
Os recursos de desempenho junto com a distância afetam a detecção de assimetrias de temperatura com câmeras termográficas? In: XIX Congresso Brasileiro de Biomecânica, 2021, Belo Horizonte.

Anais do XIX Congresso Brasileiro de Biomecânica. , 2021.

11. PEREIRA, M. E. F.; Felipe P Carpes; SILVA, W.; **MACHADO, ÁLVARO S.**; PAZ, M. M.; PIRES, E. A. L. S.; PACHECO, M. R. V.; NICHELLE, G. B.
Percepção dos estudantes sobre o impacto da divulgação de uma tarefa das olimpíadas de biomecânica nas redes sociais In: XIX Congresso Brasileiro de Biomecânica, 2021, Belo Horizonte.

Anais do XIX Congresso Brasileiro de Biomecânica. , 2021.

12. SILVA, W.; **MACHADO, ÁLVARO S.**; LEMOS, A. L.; ANDRADE, C.; QUESADA, J. I. P.; Felipe P Carpes
Relationship between muscle soreness, pain and skin temperature in men and women In: XIX Congresso Brasileiro de Biomecânica, 2021, Belo Horizonte.

Anais do XIX Congresso Brasileiro de Biomecânica. , 2021.

13. PAZ, M. M.; SILVA, W.; **MACHADO, ÁLVARO S.**; KUNZLER, M. R.; JIMENEZ-PEREZ, I.; CALVO, M. G.; QUESADA, J. I. P.; Felipe P Carpes
Repetibilidade inter-examinador na avaliação da temperatura da pele da panturrilha pré e pós-exercício empregando termografia infravermelha In: XIX Congresso Brasileiro de Biomecânica, 2021, Belo Horizonte.

Anais do XIX Congresso Brasileiro de Biomecânica. , 2021.

14. KUNZLER, M. R.; CARVALHO, J.; QUESADA, J. I. P.; APARICIO, I.; PEREZ-SORIANO, P.; **MACHADO, ÁLVARO S.**; CARPES, FELIPE P

Effects of 24-h use of compression stockings with menthol and camphor on skin temperature following running In: I International Congress on Application of Infrared Thermography in Sport Science, 2020, Valencia.

Annals of the I International Congress on Application of Infrared Thermography in Sport Science. , 2020.

15. ANDRADE, C.; SILVA, W.; **MACHADO, ÁLVARO S.**; LEMOS, A. L.; QUESADA, J. I. P.; CARPES, FELIPE P

RELAÇÃO ENTRE DOR MUSCULAR INDUZIDA POR EXERCÍCIO E TEMPERATURA DA PELE EM HOMENS E MULHERES In: IV Simpósio Integrado dos PPGs da UNIPAMPA Uruguaiana, 2020, Uruguaiana.

Anais do IV Simpósio Integrado dos PPGs da UNIPAMPA Uruguaiana. , 2020.

16. SILVA, W.; **MACHADO, ÁLVARO S.**; LEMOS, A. L.; ANDRADE, C. F.; PRIEGO, J. I.; Felipe P Carpes

RELATIONSHIP BETWEEN EXERCISE-INDUCED MUSCLE SORENESS AND SKIN TEMPERATURE IN MEN AND WOMEN, In: Congresso Anual SBFIS OnLine, 2020, Ribeirão Preto.

Anais do Congresso Anual SBFIS OnLine. , 2020.

17. **MACHADO, ÁLVARO S.**; GIL-CALVO, M.; JIMENEZ-PEREZ, I.; ANDA, R. M. C. O.; SALVADOR-PALMER, R.; QUESADA, J. I. P.

The effect of sweat after running on skin temperature: infrared thermography vs thermal contact sensors In: I International Congress on Application of Infrared Thermography in Sport Science, 2020, Valencia.

Annals of the I International Congress on Application of Infrared Thermography in Sport Science. , 2020.

18. ANDRADE, C.; SILVA, W.; **MACHADO, ÁLVARO S.**; QUESADA, J. I. P.; Felipe P Carpes

A DOR MUSCULAR TARDIA INDUZIDA PELO EXERCÍCIO ESTÁ RELACIONADA COM MUDANÇAS NA TEMPERATURA DA PELE? In: Congresso Brasileiro de Biomecânica, 2019, Manaus.

Anais do Congresso Brasileiro de Biomecânica. , 2019.

19. ANDRADE, C.; **MACHADO, A. S.**; SILVA, W.; SOUZA, M. A.; CARPES, FELIPE P
Efeito da fadiga acumulada sobre os picos de torque no ciclismo In: X Simpósio em Neuromecânica Aplicada, 2019, Uruguaiana.
Anais do X Simpósio em Neuromecânica Aplicada. , 2019.

20. MACHADO, M. S.; GUADAGNIN, E. C.; **MACHADO, A. S.**; Felipe P Carpes
Efeito da manipulação na temperatura dos pés sobre a sensibilidade cutânea plantar In: X Simpósio em Neuromecânica Aplicada, 2019, Uruguaiana.
Anais do X Simpósio em Neuromecânica Aplicada. , 2019.

21. MACHADO, M. S.; Felipe P Carpes; **MACHADO, A. S.**; GUADAGNIN, E. C.
Efeitos da manipulação da temperatura de diferentes regiões dos pés sobre a sensibilidade cutânea plantar In: XI Salão Internacional de Ensino, Pesquisa e Extensão, 2019, Santana do Livramento.
Anais do XI Salão Internacional de Ensino, Pesquisa e Extensão. , 2019.

22. MARCELO, I. O.; CARPES, FELIPE P; SILVA, C. C.; KUNZLER, M. R.; **MACHADO, A. S.**; Felipe P Carpes; SANTOS, G.
Respostas a corrida descalça envolve mudanças cinemáticas de pouso e na dor muscular de iníciotardio In: XI Salão Internacional de Ensino, Pesquisa e Extensão, 2019, Santana do Livramento.
Anais do XI Salão Internacional de Ensino, Pesquisa e Extensão. , 2019.

23. MARCELO, I. O.; SILVA, C. C.; **MACHADO, ÁLVARO S.**; SANTOS, G.; KUNZLER, M. R.; Felipe P Carpes
Respostas agudas a corrida descalça envolvem mudanças na cinemática da aterissagem e na dor muscular de início tardio In: II Simpósio de Fisiomecânica da Locomoção Terrestre, 2019, Florianópolis.
Anais do II Simpósio de Fisiomecânica da Locomoção Terrestre. , 2019.

24. SILVA, C. C.; SANTOS, G.; **MACHADO, ÁLVARO S.**; Helen Lidiane

Schimidt; KUNZLER, M. R.; AZEVEDO, R. R.; Felipe P Carpes
RESPOSTAS AGUDAS A CORRIDA DESCALÇA: MUDANÇAS NA CINEMÁTICA E NA DOR MUSCULAR DE INÍCIO TARDIO In: Congresso Brasileiro de Biomecânica, 2019, Manaus.
Anais do Congresso Brasileiro de Biomecânica. , 2019.

25. MIGUENS, R. D.; **MACHADO, ÁLVARO S.**; CARVALHO, J.; KUNZLER, M. R.; Felipe P Carpes
Avaliação do ìndice tornozelo braquial em atletas amadores In: 10º Salão Internacional de Ensino, Pesquisa e Extensão, 2018, Santana do Livramento.
Anais do 10º Salão Internacional de Ensino, Pesquisa e Extensão. , 2018.

26. **MACHADO, A. S.**; SILVA, W.; SOUZA, M. A.; Felipe P Carpes
EFEITO DA SUPLEMENTAÇÃO COM CHÁ VERDE NO DESEMPENHO DE CICLISMO EM CONDIÇÃO DE FADIGA ACUMULADA In: IX Simpósio em Neuromecânica Aplicada, 2018, Santa Maria.
Anais do IX Simpósio em Neuromecânica Aplicada. , 2018.

27. ANDRADE, C. F.; Felipe P Carpes; **MACHADO, A. S.**
O EXERCÍCIO EM INTENSIDADE MODERADA PODE SER UTILIZADO COMO ESTRATÉGIA DE RECUPERAÇÃO ATIVA? In: 10º Salão Internacional de Ensino, Pesquisa e Extensão, 2018, Santana do Livramento.
Anais do 10º Salão Internacional de Ensino, Pesquisa e Extensão. , 2018.

28. SANTOS, M. A.; KUNZLER, M. R.; AZEVEDO, R. R.; **MACHADO, ÁLVARO S.**; Felipe P Carpes
Ouvir música enquanto realiza uma tarefa cognitiva pode atrasar a tomada de decisão em jovens? In: IX Simpósio em Neuromecânica Aplicada, 2018, Santa Maria.
Anais do IX Simpósio em Neuromecânica Aplicada. , 2018.